Composite Materials and Structures Program

Rensselaer Polytechnic Institute
Troy, N.Y. 12180-3590

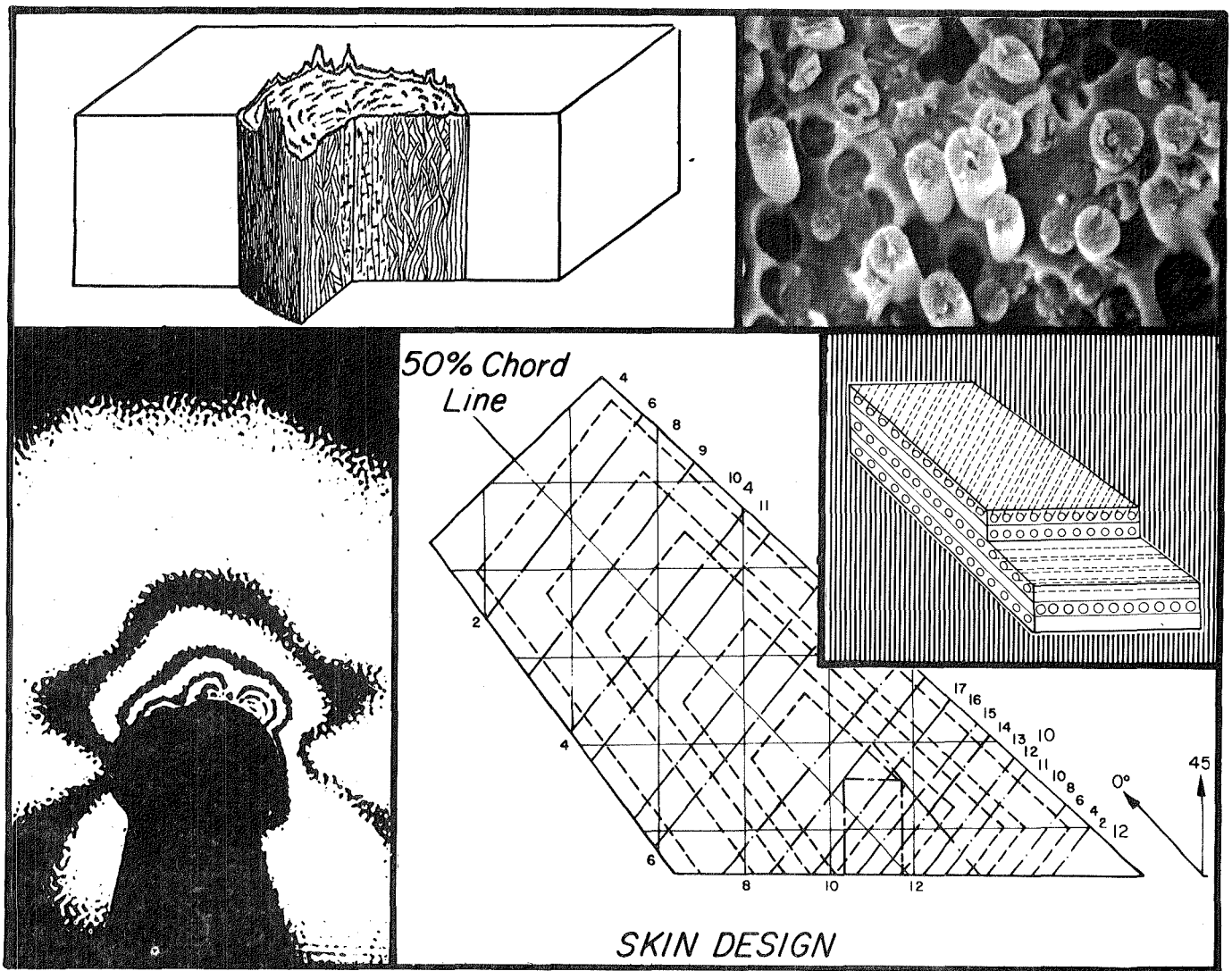

Sponsored by
NASA/AFOSR

Semi-Annual Progress Report

April 30, 1984 through September 30, 1984

COMPOSITE STRUCTURAL MATERIALS

Air Force Office of Scientific Research
and
National Aeronautics and Space Administration
Grant No. NGL 33-018-003

Co-Principal Investigators:

George S. Ansell
Dean, School of Engineering

Robert G. Loewy
Institute Professor

and

Stephen E. Wiberley
Professor of Chemistry

Rensselaer Polytechnic Institute
Troy, New York 12181

NASA Technical Officer

Michael A. Greenfield
Materials and Structures Division
NASA Headquarters

47th Semi-Annual Report December 1984

CONTENTS

LIST OF TABLES

LIST OF FIGURES

PART I

INTRODUCTION

INTRODUCTION

A resurgence of intense interest, research and applications mark the beginning of what may be considered the second generation of filamentary composite materials. Such interest and activity are as well-founded now as they were at the outset of the composites era more than twenty years ago. The possibility of using relatively brittle materials with high modulus, high strength, but low density in composites with good durability and high tolerance to damage and which, when they do fail, do so in a noncatastrophic manner, has been shown feasible, and the full potential is only just beginning to be realized.

The promise of substantially improved performance and potentially lower costs provides the driving force behind continued research into fiber reinforced composite materials for application in aerospace hardware.

Much progress has been achieved since the initial developments in the mid 1960's. Applications to primary structure have been rather limited on operational vehicles, mainly being utilized in a material-substitution mode on military aircraft. More extensive experiments, as a part of NASA's influential ACEE program, are currently underway on large airplanes in commercial passenger operation and in a few military developments, such as the AV-8B which has seen only limited service use and the X-29 which is in its initial flight testing program.

A strong technology base is required to fully exploit composites in sophisticated aerospace structures. NASA and AFOSR have supported expansion and strengthening of the technology base through programs which advance fundamental knowledge and the means by which this knowledge can be successfully applied in design and manufacture.

As the technology of composite materials and structures moves toward fuller adoption into aerospace structures, some of the problems of an earlier era are being solved, others which seemed important are being put into perspective as relatively minor, and still others unanticipated or put aside are emerging as of high priority. The purpose of the RPI program as funded by NASA and AFOSR has been to develop critical advanced technology in the areas of physical properties, structural concepts and analysis, manufacturing, reliability and life prediction.

Our approach to accomplishing these goals is through an interdisciplinary program, unusual in at least two important aspects for a university. First, the nature of the research is comprehensive - from fiber and matrix constituent properties research, through the integration of constiuents into composite materials and their characterization, the behavior of composites as they are used in generic structural components, their nondestructuve and proof testing and, where the state of the art will be advanced by doing so, extending the research effort into simulated service use so that the composite structure's long-term integrity under conditions

pertinent to such use can be assessed. Inherent in the RPI program is the motivation which basic research into the structural aspects provides for research at the materials level, and vice versa.

Second, interactions among faculty contributing to program objectives is on a day to day basis without regard to organizational lines. These contributors are a group wider than that supported under the project. Program management is largely at the working level, and administrative, scientific and technical decisions are made, for the most part, independent of considerations normally associated with academic departments. Depending on the flow of the research, this kind of involvement includes faculty, staff and students from chemistry, civil engineering, materials engineering, aeronautical engineering, mechanical engineering and mechanics.

A third aspect is a newly instituted initiative to increase involvement of NASA's Research Center scientists and engineers in the program at RPI, and vice versa. This has required, first, identification of individual researchers within NASA centers whose areas of interest, specialization and active investigation are in some way related to those of RPI faculty supported under the subject grant. Second, a program of active interchange has been encouraged and the means by which such interaction can be fostered is being sought. Important benefits envisioned from this increased communication include a clearer window to directions in academia for NASA researchers; opportunities to profit from NASA

experience, expertise and facilities for the faculty so involved and an additional channel for cross-fertilization across NASA Research Center missions through the campus program.

Overall program emphasis is on basic, long-term research in the following categories: (a) constituent materials, (b) composite materials, (c) generic structural elements, (d) processing science technology and (e) maintaining long-term structural integrity. Depending on the status of composite materials and structures research objectives, emphasis can be expected to shift from one time period to another among these areas. Progress in the program will be reported in the following pages under these headings. Those computer methodology developments are also undertaken which both support RPI projects in composite materials and structures research in the areas listed above and which also represent research with the potential of widely useful results in their own right.

In short, the NASA/AFOSR Composites Aircraft Program is a multi-faceted program planned and managed so that scientists and engineers in a number of pertinent disciplines at RPI will interact, both among themselves and with counterpart NASA Center researchers, to achieve its goals. Research in basic composition, characteristics and processing science of composite materials and their constituents is balanced against the mechanics, conceptual design, fabrication and testing of generic structural elements typical of aerospace vehicles so

as to encourage the discovery of unusual solutions to present and future problems. In the following sections, more detailed descriptions of the progress achieved in the various component parts of this comprehensive program are presented.

PART II

II-A MECHANICAL PROPERTIES OF HIGH PERFORMANCE CARBON FIBERS

II-A MECHANICAL PROPERTIES OF HIGH PERFORMANCE CARBON FIBERS

Senior Investigator: R. J. Diefendorf

1. Introduction

The studies of modulus distribution, strength distribution and residual stress measurement within a single fiber are of great interest. They may lead to the explanation of the anomalous behavior of modulus and strength with increasing heat-treatment temperature. Also, the results may hold the key to the realization of simultaneously developing high modulus and high strength fibers.

2. Status

Theoretical equations for predicting residual stresses in radial, hoop and longitudinal directions were derived from linear elasticity based on the perfect onion skin model and recorded in a recent semi-annual progress report[1]*. Residual stress measurements in high modulus, PAN-based carbon fiber, as well as modulus distribution in Type I, Type II and Type A PAN-based carbon fibers, were explored and reported[1,2,3]. Strength distributions within a single fiber of Type I, Type II and Type A PAN-based carbon fibers were established. Flaws on the fracture surface of a single fiber also were identified.

*Numbers in brackets in this section refer to the references which are listed on page 23.

3. Progress During Report Period

Hercules HMS, HTS, AS-4 and AS fibers and Union Carbide T-300 fiber were used in this study. The surface of the carbon fiber was removed by electrochemical etching[2,3]. The diameters of the fiber, both before and after etching, were measured by a laser diffraction technique[4]. The strength of single filaments was measured at a gauge length of 25.4mm under test conditions that allowed recovery of the primary fracture surfaces needed for identifying critical flaws.

The surface layer of carbon fiber has higher modulus[1,3] and, hence, will carry a higher fraction of load than the rest of the layers. Therefore, by removing the outside layer, the strength will also change. This strength distribution will vary among types of fiber and depends on the magnitude of local modulus, residual stress and flaw distribution.

The strength distributions of HMS, HTS, AS-4, AS and T-300 fibers are shown in Figures II-A-1a through II-A-1e and are based on the average value in each radius ratio group (via, group 1 for as-received fibers $r/r_o = 1$, group 2 for etched fibers with radius ratios ranging from 0.95 to 0.99, then r/r_o = 0.9-0.94 for group 3 and so on). By performing statistical analyses, such as Bartlett's test, ANOVA, Dunnett's test and the t-test[5], the group mean values were properly compared with each other. For HMS fibers, the mean strength of group 1 (as-received) is higher than those after etching.

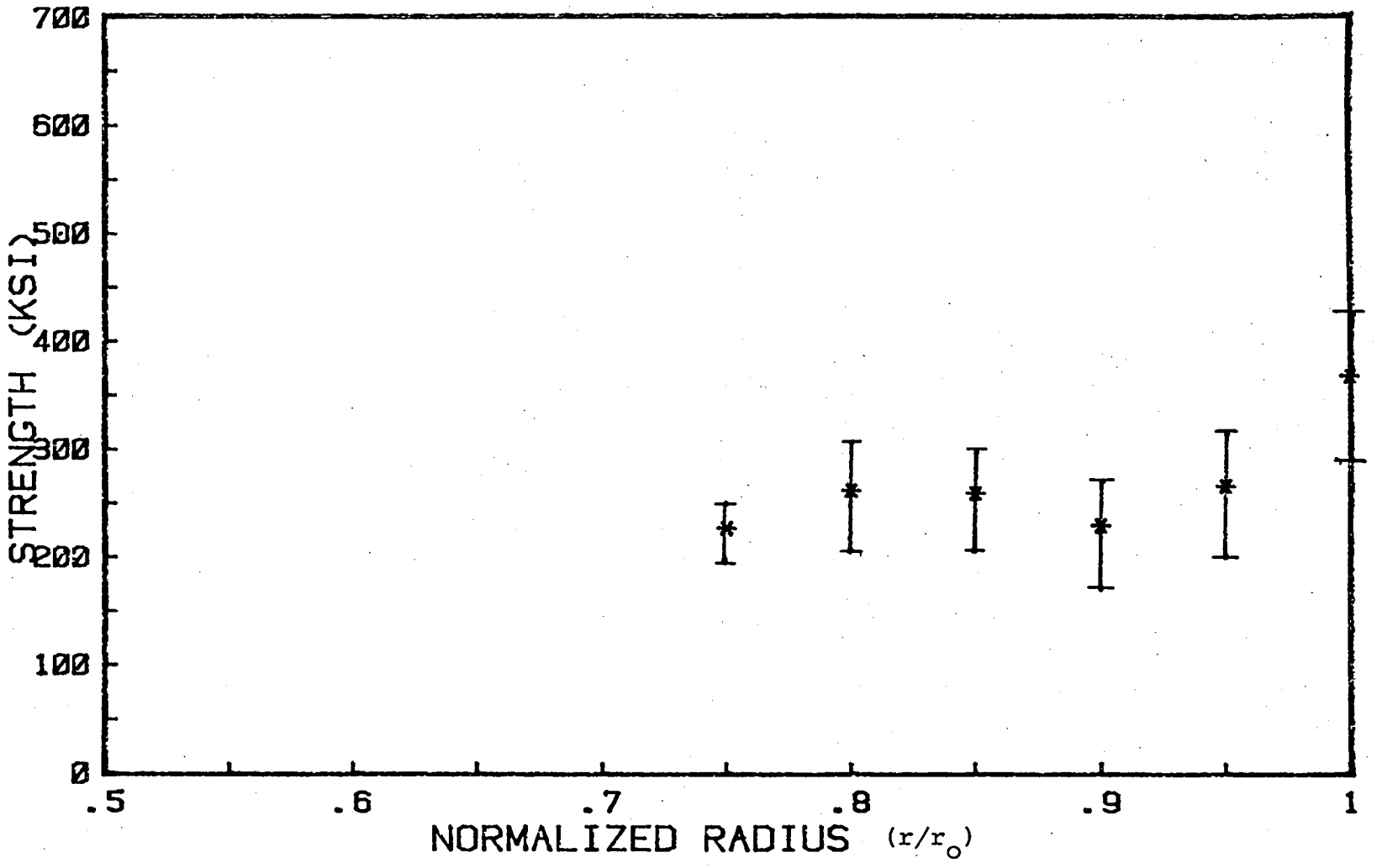

Figure II-A-1a. Strength Distribution as a Function of Normalized Fiber Radius for HMS Fibers.

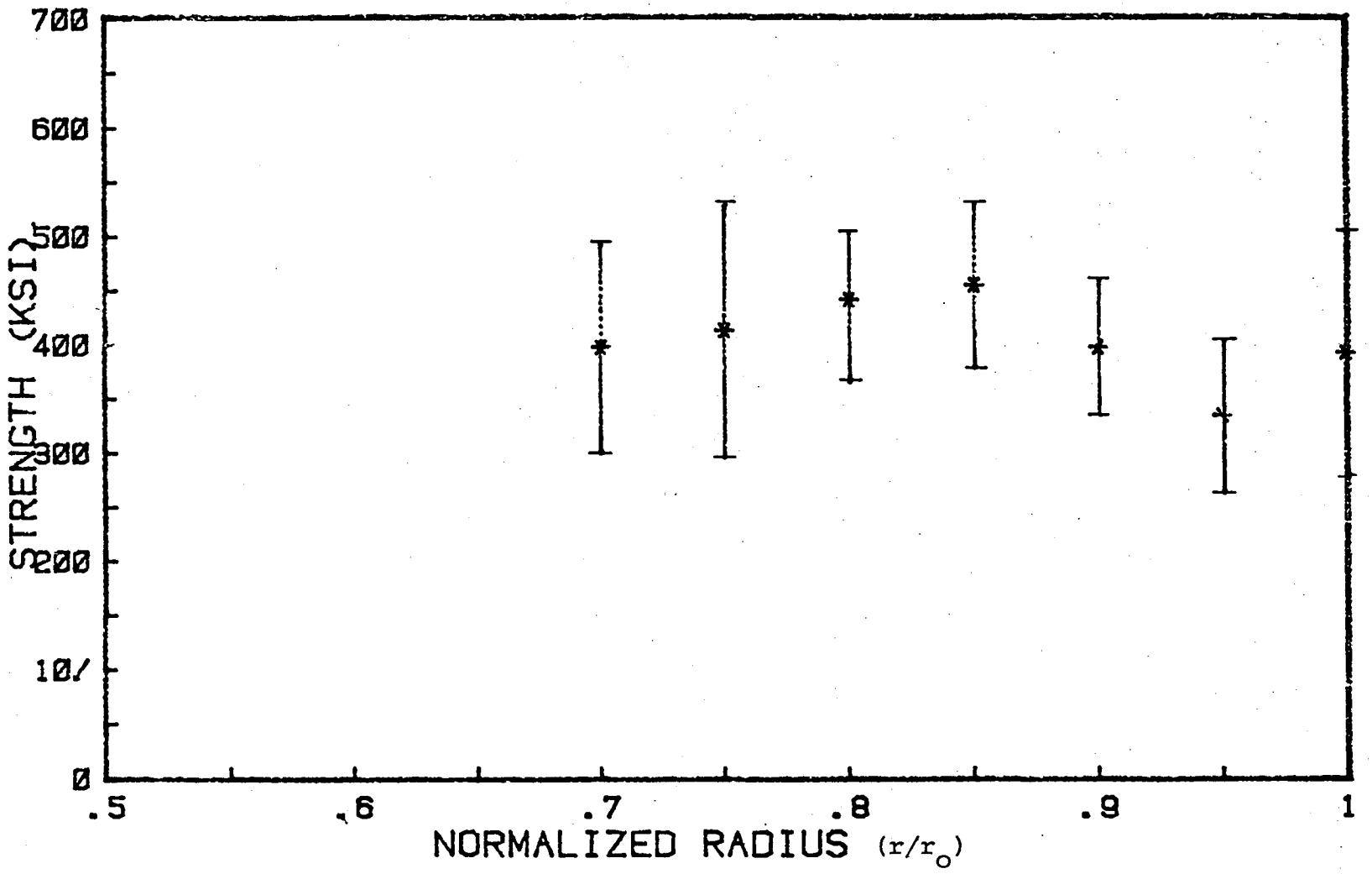

Figure II-A-1b. Strength Distribution as a Function of Normalized Fiber Radius for HTS Fibers.

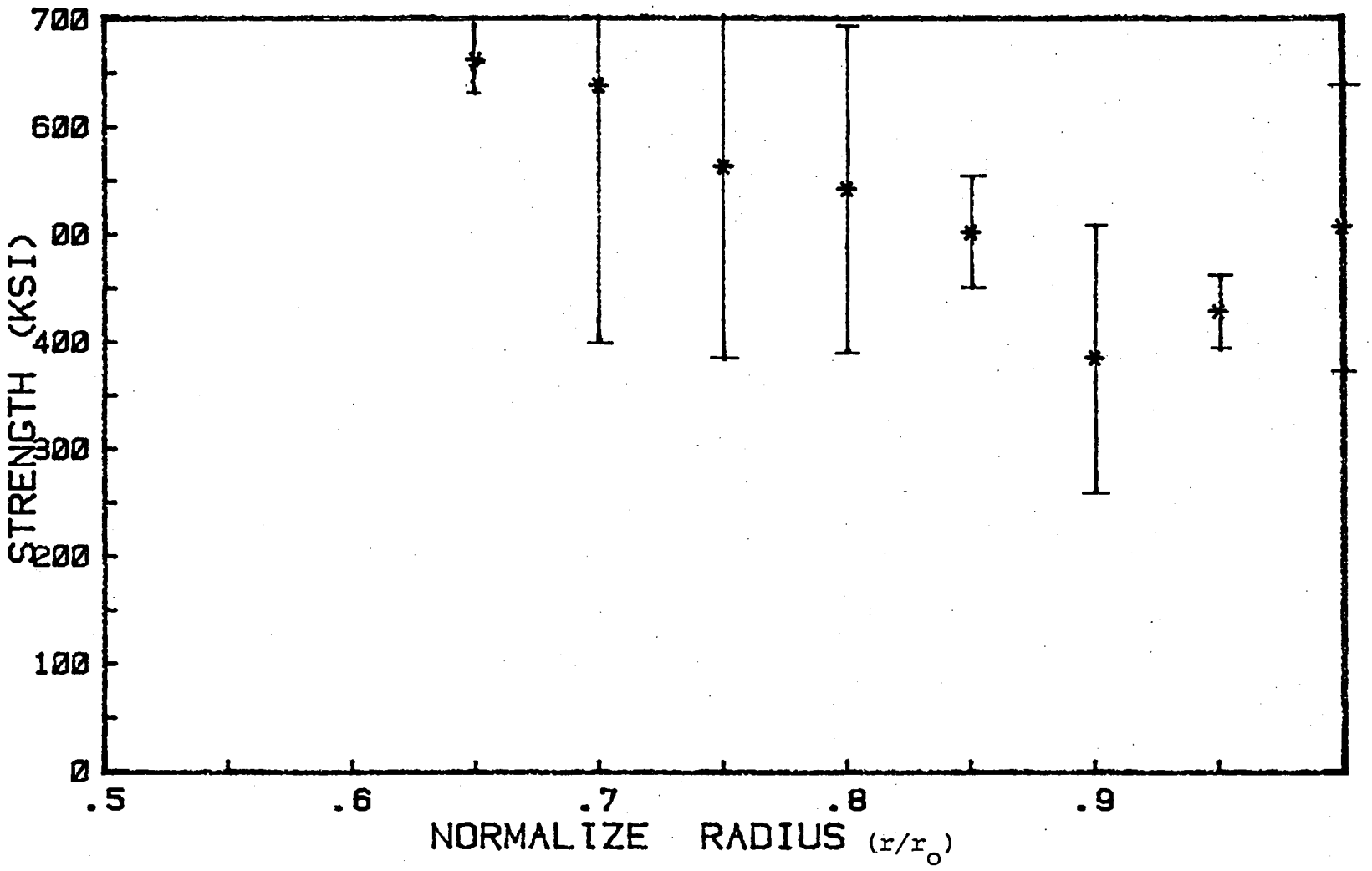

Figure II-A-1c. Strength Distribution as a Function of Normalized Fiber Radius for AS-4 Fibers.

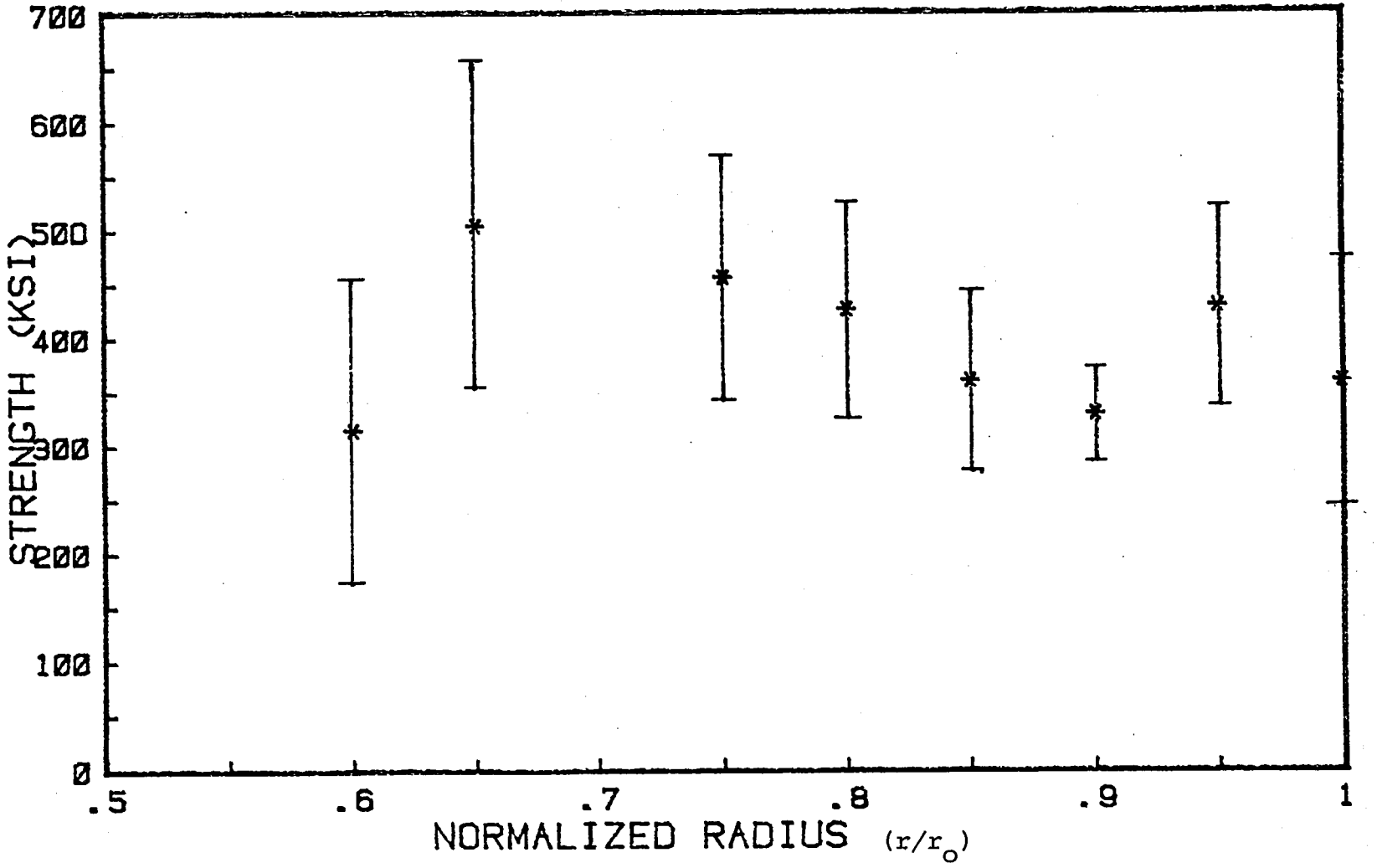

Figure II-A-1d. Strength Distribution as a Function of Normalized Fiber Radius for T-300 Fibers.

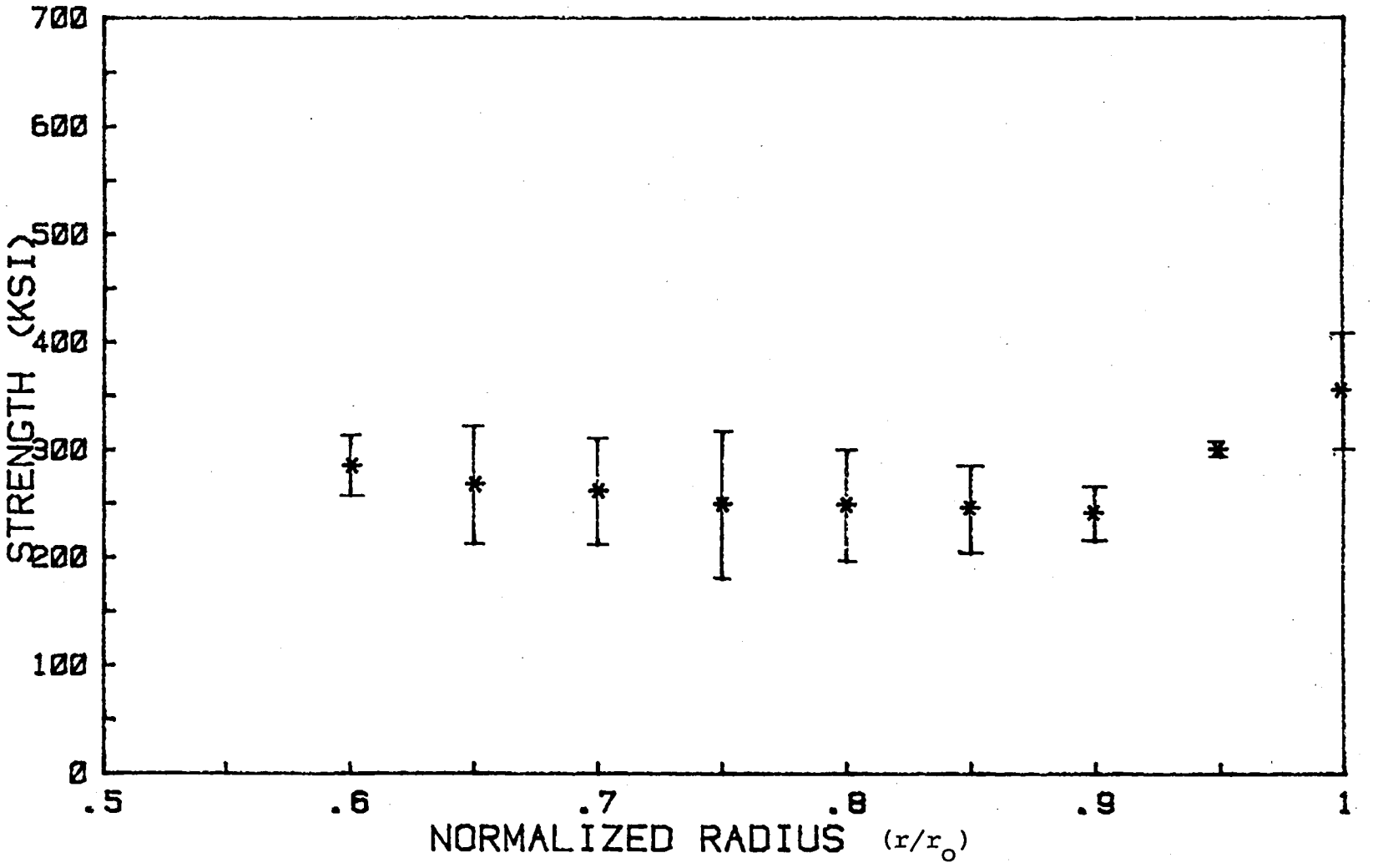

Figure II-A-1e. Strength Distribution as a Function of Normalized Fiber Radius for AS Fibers.

This finding is related to the structure of HMS fiber and the effect of residual stress distribution within the fiber. Because the layers of higher local modulus were etched away gradually, the average modulus of the remaining fiber became smaller and smaller. Simultaneously, the residual stress is relieved. Therefore, the surface compressive stress decreased. In terms of a flaw mechanism, most of the fracture surfaces of this high modulus species showed gross interior voids (see Figure II-A-2), and fracture is believed to originate from these voids. By removing the outer layer, the flaw originally in the interior was exposed as "surface" flaw (see Figure II-A-3). Also, less compressive stress protects this "surface" flaw from propagating, therefore, the strength drops. By comparing the mean strengths, the group pairs (2,3), (3,4), (4,5) and (5,6) showed that they share the same mean value. That is, the strength of HMS fiber dropped after the surface was removed and then stayed constant (as shown in Figure II-A-1a).

HTS carbon fibers, as shown before[1], have less of a modulus gradient and lower HTT than that of HMS fibers; therefore, less residual stress is expected. The strength distributions of HTS fibers are shown in Figure II-A-1b. Although the nominal mean values of strength in etched fiber groups are higher than those of as-received fibers, they are not significantly different statistically (see Figure II-A-1b). The fracture surfaces of HTS as-received fiber (Figure II-A-4) showed that failure initiated from a surface flaw. No serious

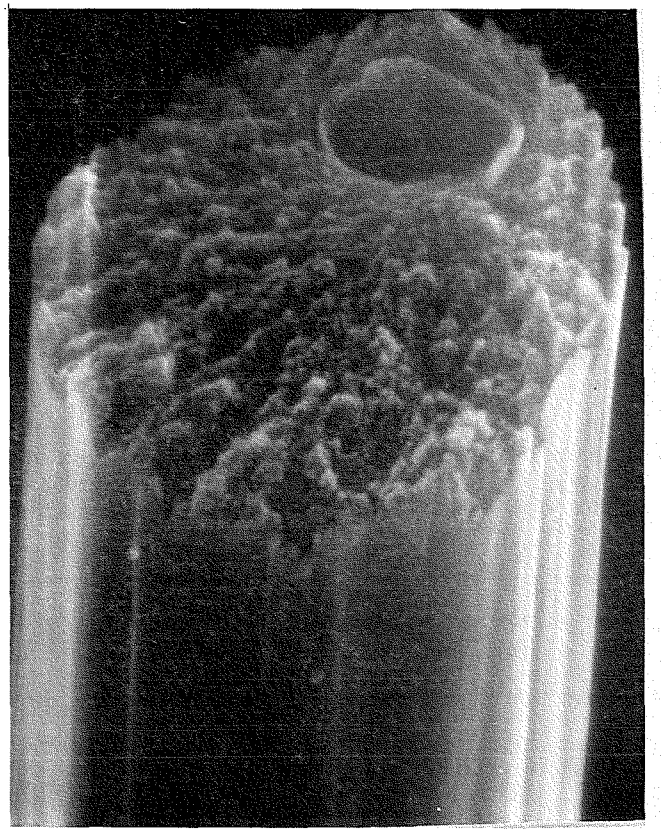

Figure II-A-2. SEM Fractography of HMS (As-Received) Carbon Fiber. (Shows interior flaw failure)

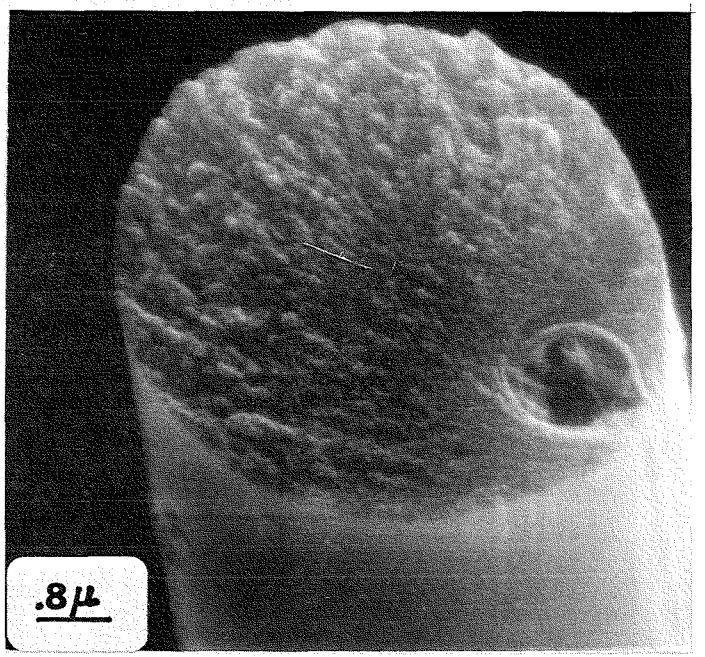

Figure II-A-3. SEM Fractography of HMS (Etched) Carbon Fiber. (Shows that the flaw originally in the interior was exposed as "surface" flaw)

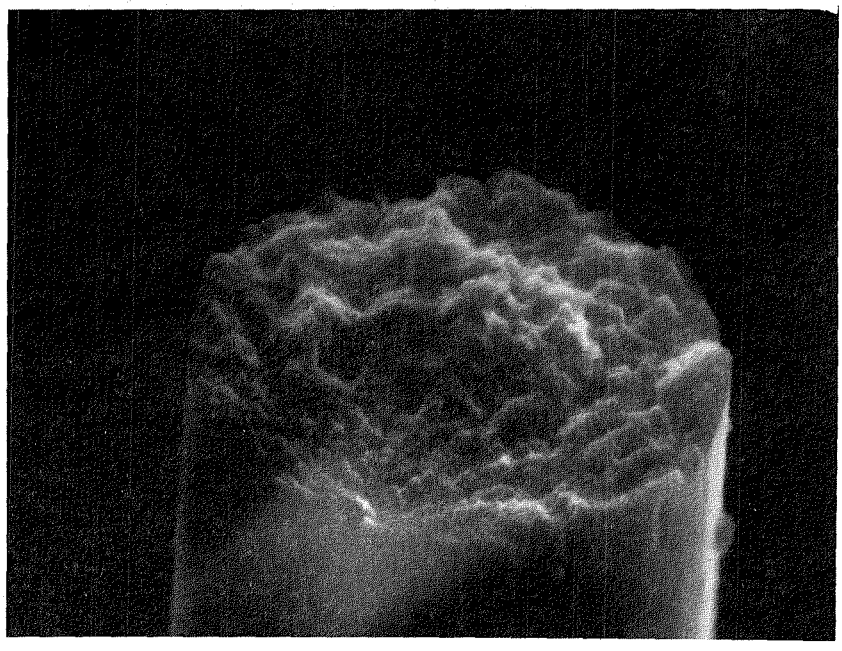

Figure II-A-4. The Failure Initiated from Surface Flaw for HTS (As-Received) Carbon Fibers.

interior voids, as in HMS fibers, are observed. This implies that less residual stress is present, otherwise, the surface compressive residual stress tends to inhibit the propagation of the crack from the surface. After the surface layers are removed, the average modulus is slightly decreased. Therefore, for constant strain the strength decreases only slightly. Since surface flaws may be removed when etching, the strength might be higher than, or stay at the same value, as group 1 fibers.

The past report[1] indicated that the modulus gradient of Type A (AS-4, AS and T-300) fibers is among the lowest of the carbon fiber types. Also, as the heat treatment temperature of Type A fibers is only 1100°C, the effect of residual stress is expected to be low. The group mean strength of AS-4 is all equal within the groups (as shown in Figure II-A-1c). The grand mean strength was 504 Ksi for a radius ratio down to .65 and with a pooled standard deviation of 150 Ksi.

The same results as with AS-4 fibers are found in T-300 fibers by using the Barlett's test and ANOVA (see Figure II-A-1d). However, the strength of AS fibers did not follow the same trend as other Type A fibers such as AS-4 and T-300 (see Figure II-A-1e). The mean strength of AS as-received fibers is only 355 Ksi, which is quite low compared to manufacturer's data (410 Ksi). Hence, the distribution could be due to scattering of data.

In general, there are two distinct types of distributions of strength among types of carbon fibers. Type I fibers have a strength gradient when etched, while Type II and Type A strength gradients were not observed. These strength distributions are related to the microstructure of the fibers. For Type I with a skin/core structure, the strength is higher at the surface; then it degrades toward the core, as the surface layer is removed. In addition, due to the relief of residual stress and the exposure of the interior flaws to the surface after etching, the strength of the etched fiber further decreases. Interior voids are found in Type I which are the main failure initiator for Type I. For Type II and Type A, no significant variations were observed in fiber strength as the surface was removed. Surface flaws are the main failure initiator for Type II and Type A fibers. Finally, no serious interior voids were found either in Type II or Type A fibers.

4. Plans for Upcoming Period

During the next reporting period, effort will concentrate on the following:

a) finding a suitable technique for uniformly etching pitch based carbon fiber as well as for residual stress measurement and

b) performing a fundamental study of the electrochemical etching mechanisms of carbon fiber by using a highly annealed pyrolytic graphite (HAPG) as the sample and methanol as the electrolyte.

5. References

1. 45th Semi-Annual Progress Report, Composite Structural Materials, Rensselaer Polytechnic Institute, Troy, NY, December 1983.

2. Chen, K. J. and R. J. Diefendorf, "Residual Stress in High Modulus Carbon Fibers", Progress in Science and Engineering of Composites, ICCM-IV, Tokyo, 1982, pp. 97-105.

3. Chen, K. J. and R. J. Diefendorf, "The Modulus Distributions in Carbon Fibers", 16th Biennial Conference on Carbon, July 1983, pp. 490-491.

4. Chen, K. J., "Mechanical Properties of High Performance Carbon Fibers", PhD. Thesis, Rensselaer Polytechnic Institute, Troy, NY, August 1984.

5. Walpol, R. E. and R. H. Myers, "Probability and Statistics for Engineering and Scientists", 2nd Ed., MacMillian Publishing Co., 1978, pp. 365-385.

6. Current Publications or Presentations by Professor Diefendorf on this Subject

"An Assessment of the Fundamental Understanding of Carbon Fiber and Matrix Materials for Carbon/Carbon Composites"

Presented at the Rocket Propulsion Laboratory Workshop of Carbon/Carbon Exit Cones, Aerospace Corp., El Segundo, CA, May 22-23, 1984.

"Pitch Solvent Interactions and Their Effects on Mesophase Formation", with J. G. Venner, p. 338.
"Characterization of Isotropic Phase and Mesophase Pitch Fractions", with S. H. Chen, p. 382.
"Effects of Lithium Reduction Techniques on the Determination of Pitch Molecular Weight", p. 384.

The preceeding 3 papers were published in Carbon 84 Conference Proceedings, July 1984 and along with
"Chemical Vapor Disposition of Carbon" an invited lecture, presented at the Carbon 84 Conference, University of Bordeaux, Bordeaux, France, July 2-6, 1984.

"Discotic Mesophase Formation in Pitches", with S. H. Chen and W. C. Stevens.

Published in 10th International Liquid Crystal Conference Proceedings, Paper 43, July, 1984 and, along with the paper

"Mesophase Formation in Polynuclear Aromatic Compounds"

Presented at the 10th International Liquid Crystal Conference, University of York, York, England, July 16-20, 1984.

"Materials Characterization of Carbon Fibers"

Presented at the Army Sagamore Conference, Lake Lucerne, NY, August 13-17, 1984.

PART III

COMPOSITE MATERIALS

III-A FATIGUE IN COMPOSITE MATERIALS

III-B EXPERIMENTAL AND THEORETICAL STUDIES OF MOISTURE AND TEMPERATURE EFFECTS ON THE MECHANICAL PROPERTIES OF GRAPHITE/EPOXY LAMINATES AND NEAT RESINS

III-C NUMERICAL INVESTIGATION OF THE MICROMECHANICS OF COMPOSITE FRACTURE

III-D DELAMINATION FAILURES OF COMPOSITE LAMINATES

III-A FATIGUE IN COMPOSITE MATERIALS

Senior Investigator: E. Krempl

1. Introduction

The deformation and failure behavior of graphite/epoxy tubes under biaxial (axial and torsion) loading is being investigated. The aim of this research is to increase basic understanding of and provide design information for the biaxial response of graphite/epoxy composites.

2. Status

In the previous progress report[1]* phenomenological damage laws based on residual strength or residual life were discussed, and a model was proposed from which various previously published models could be recovered by specialization. Specimen fabrication and tensile as well as fatigue testing of Gr/E $[\pm 45]_s$ tubes, in support of the theory, comprised most of the activity in the reporting period.

3. Progress During Report Period

The specimen design and the $[\pm 45]_s$ lay-up developed at Rensselaer Polytechnic Institute[2] were used to fabricate about fifty thin-walled tubes of graphite/epoxy. The details of this procedure are given in Reference [2] or in previous progress reports.

*Numbers in brackets in this section refer to the references which are listed on page 31.

Subsequently, static tests and fatigue tests were performed following the procedures of Reference [2] except that most of the tests were performed without extensometry.

The damage evolution equation proposed in Reference [1] is

$$\frac{dD}{dN} = g(D)f(s) \qquad (1)$$

where:

D is the dimensionless damage,
N is the number of cycles,
s is the dimensionless stress amplitude and
g and f are positive functions.

Equation (1) has no repository for mean stress and therefore cannot reproduce such effects. Accordingly, tests were run to check on the influence of mean stress. Figure III-A-1 shows that there is a small influence of mean stress for R values ($R = \sigma_{min}/\sigma_{max}$ where σ_{max} and σ_{min} are the maximum and minimum stresses of a cycle, respectively) ranging from R = -1 (completely reversed), R = 0- (fluctuating compression) to R = 0 (fluctuating tension). The normalizing factor of 145 MPa is the average tensile strength obtained with six specimens.

The following tests were all performed at R = 0 and a frequency of 5 Hz. First, the drop of residual strength with cycles was determined with the results given in Figure III-A-2. The circles indicate the residual strength after a fatigue test with s = 32% which was terminated at the indicated number of cycles. Subsequently, a tensile test was performed, and its result is plotted on the ordinate.

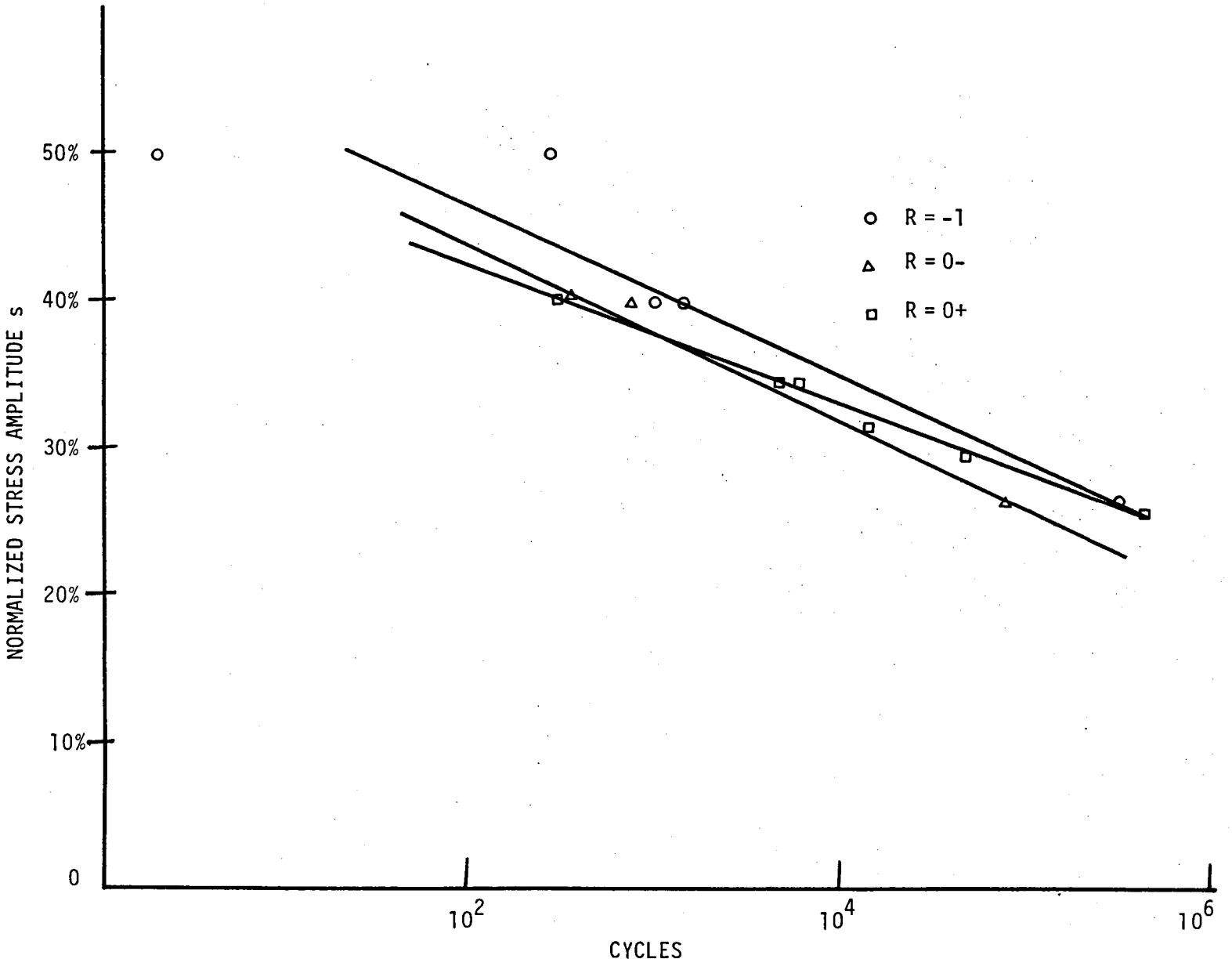

Figure III-A-1. The Influence of Mean Stress on the Axial Fatigue Behavior of $[\pm 45]_s$ Tubes. ($R = \sigma_{min}/\sigma_{max}$ where σ_{max} and σ_{min} are the maximum and minimum stress of a cycle, respectively. s = stress amplitude/145 MPa)

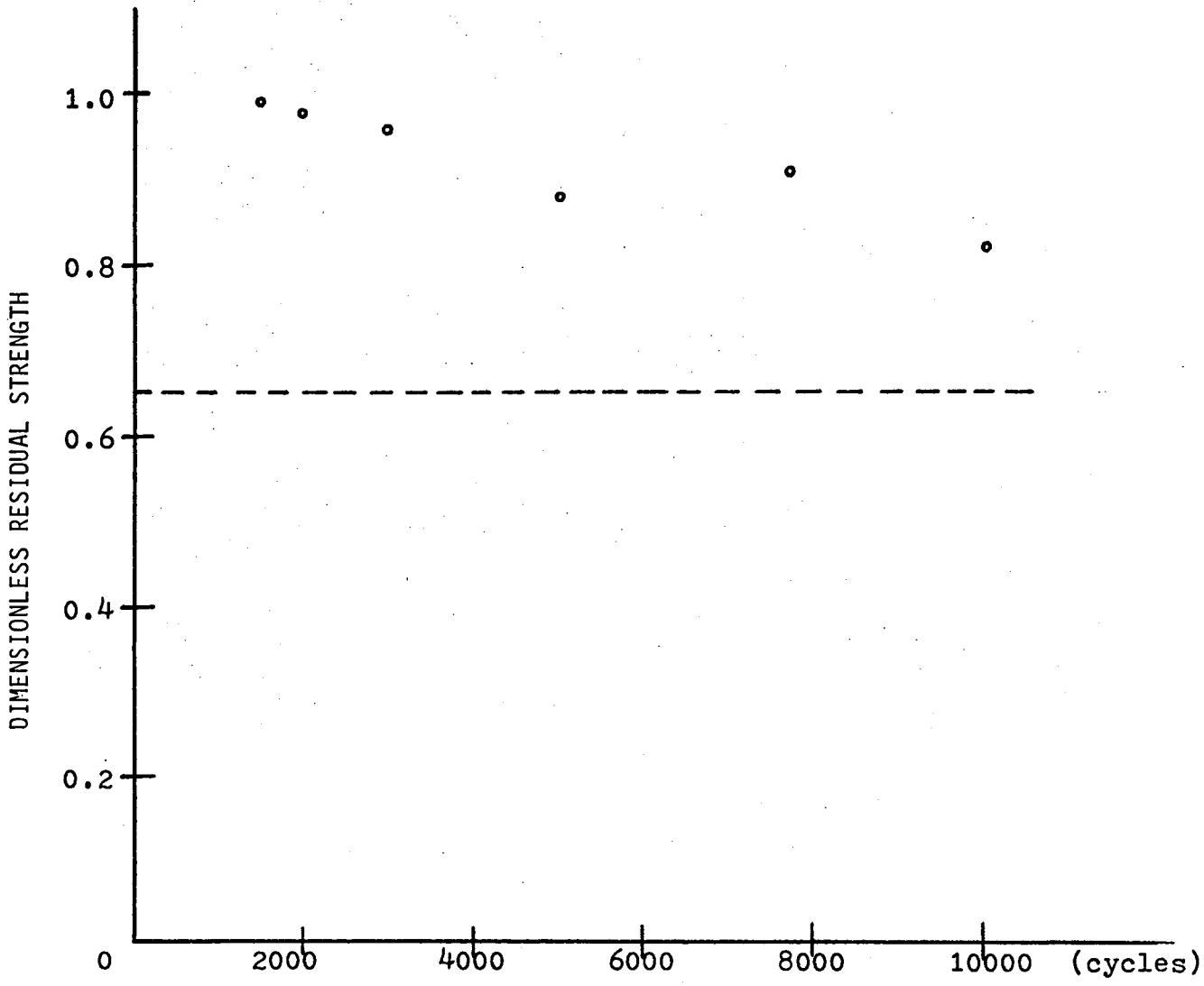

Figure III-A-2. Residual Strength (made dimensionless by dividing by 145 MPa) After Prior Uniaxial Fatigue Cycling at R = 0 with s = 32%. (Dashed line represents the maximum stress in a fatigue cycle.)

Figure III-A-2 shows the drop off of residual strength with cycles. The dashed line is the maximum fatigue stress of the fatigue test. At the cycles-to-failure corresponding to this maximum stress level, the residual strength is expected to be equal to it. The average life at an amplitude of 32% is 11,000 cycles. From this information and from the results shown in Figure III-A-2, it must be concluded that the residual strength decreases rapidly at the end of the life.

The results of Figure III-A-3 are obtained with specimens subjected to 5000 cycles at R = 0 with s = 32% and subsequent combined loading. The triangles represent the combined residual strength of the damaged specimens. The circles are results taken from [1] and represent the combined strength of virgin specimens.

It is tentatively concluded that the strength reduction due to uniaxial tension-tension fatigue cycling is uniform and affects the fracture strength in the first quadrant of the axial and shear stress space equally.

4. Plans for Upcoming Period

The experimental investigation outlined above will be continued using other test conditions.

5. References

1. 46th Semi-Annual Progress Report, Composite Structural Materials, Rensselaer Polytechnic Institute, Troy, NY, August 1984, pp. 29-33.

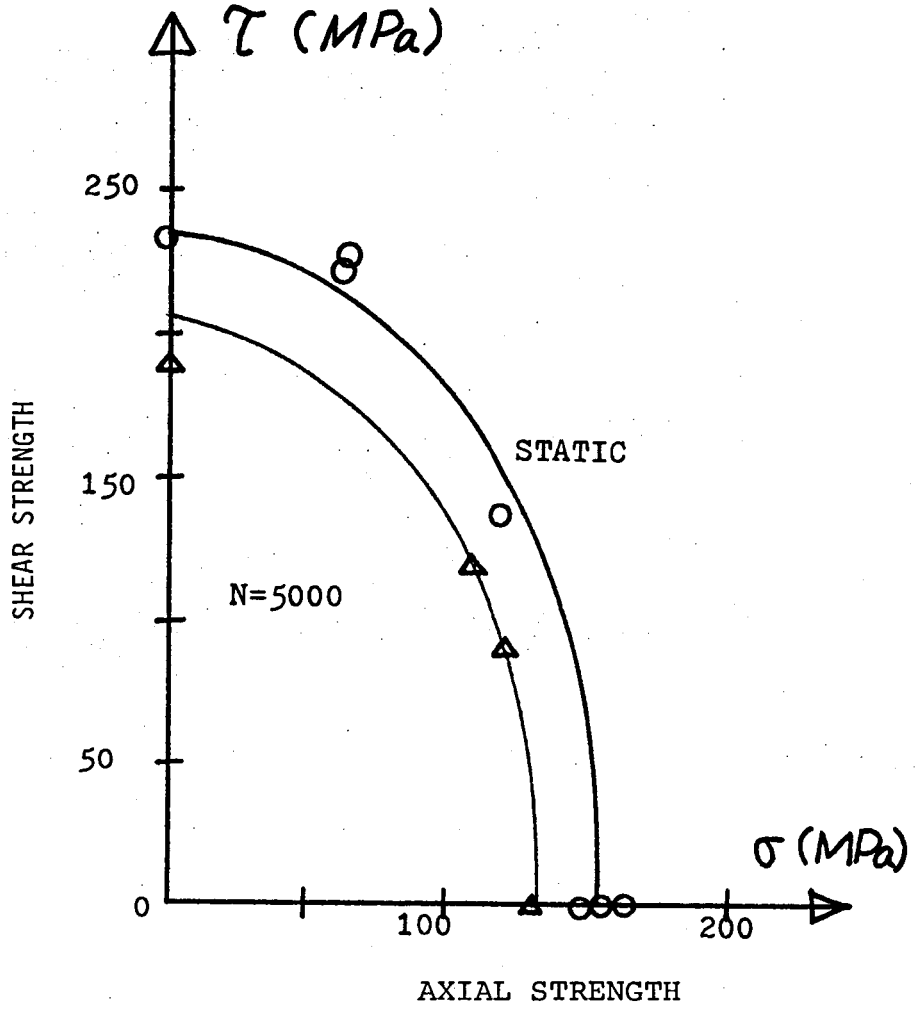

Figure III-A-3. Biaxial Fracture Strength of Virgin, O, and Predamaged, Δ, Specimens. (The damage was introduced during 5000 prior cycles at R = 0 and s = 32%. Results of virgin specimens are from [1]. σ ≡ axial stress, τ ≡ shear stress.)

2. T. M. Niu, "Biaxial Fatigue of Graphite/Epoxy $[\pm 45]_S$ Tubes", Dr.Eng. Thesis, Rensselaer Polytechnic Institute, Troy, NY, May 1983.

6. Current Publications or Presentations by Professor Krempl on this Subject

"Biaxial Fatigue Properties of Thin-Walled Composite Tubes", with D. M. Elzey, T. Ayar and R. G. Loewy.

To be presented at the Helicopter Fatigue Specialists' Meeting, American Helicopter Society Midwest Region, St. Louis, MO, October 16-18, 1984.

"Time-Dependent Deformation and Fatigue Behavior of $[\pm 45]_S$ Graphite-Epoxy Tubes under Combined Loading", with T.-M. Niu.

To be presented at the ASTM Symposium on Composite Materials: Fatigue and Fracture, Dallas/Ft. Worth, TX, October 24-25, 1984.

"Biaxial Fatigue and Damage Accumulation in Thin-Walled Graphite/Epoxy Tubes", with D. An.

To be presented at the IUTAM Symposium on the Mechanics of Damage and Fatigue, Technion-Israel Institute of Technology and Tel Aviv University, July 1-4, 1985.

III-B EXPERIMENTAL AND THEORETICAL STUDIES OF MOISTURE AND TEMPERATURE EFFECTS ON THE MECHANICAL PROPERTIES OF GRAPHITE/EPOXY LAMINATES AND NEAT RESINS

Senior Investigator: S. S. Sternstein

1. Introduction

During the present report period a new series of mechanical tests were initiated, as described herein.

Previous reports have described our small strain viscoelastic studies on carbon/epoxy laminates. Techniques such as stress relaxation, creep and dynamic mechanical spectroscopy were used to investigate the *in situ* behavior of the epoxy as a function of temperature and moisture history. One of our findings was that the so-called loss factor (i.e., tan δ) or ratio of out-of-phase modulus to in-phase modulus was sensitive to damage. For linear viscoelastic behavior it can be shown that loss factor is equal to the ratio of energy dissipation to energy storage per quarter cycle of sinewave.

For nonlinear viscoelastic behavior, or for dissipative processes which do not have fading memory or obey time-translation superposition, it is difficult or impossible to assign any specific meaning to the loss factor, as defined by phase angle measurements. How then does one characterize high load, large deformation, nonrecoverable dissipative phenomena?

One technique which directly measures energy dissipation is the cyclic hysteresis test. In this test, the sample is repeatedly loaded and unloaded between specified limits with continuous recording of load versus displacement. The area

inside the loop so formed is hysteresis or energy dissipated. The magnitude of the hysteresis is expected to vary with the number of cycles performed, the cycle limits and the previous history of the sample.

If the process being observed is linear viscoelastic, then the energy dissipation will vary as the square of the limit stress (or strain). On the other hand, phenomena such as crack formation in the matrix, fiber failure, fiber reorientation, interfacial failure, etc., are not viscoelastic (let alone linear viscoelastic). Thus, it is not clear as to how hysteresis should vary with the magnitude of stress or strain. However, one can anticipate that increasing damage will affect hysteresis and the rate of change of hysteresis with stress (or strain level).

2. Status

A preliminary set of experiments have been performed which appear to be quite promising. We have used the cyclic hysteresis method to measure energy dissipation on two distinctly different samples, one being a thermoset matrix composite (carbon-epoxy), the other a thermoplastic matrix (polysulfone-carbon) composite. Both sets of samples were prepared with a $[\pm 45]_{3S}$ stacking sequence and tested in tension. The approximate sample dimensions were: gage length = 1.4", width = 0.75", thickness = 0.065". The samples were tested using a constant crosshead speed of 0.2 cm/min. which gave a nominal strain rate of 5%/min. Compound limits were

used for this cycle, that is, the lower cycle point was set for zero load while the upper cycle point was set for a constant displacement. Cycling was performed for each sample until a stable (repetitive) hysteresis loop was obtained. A new sample specimen was then used for the next level of upper displacement limit.

3. Progress During Report Period

Typical results are shown in Figure III-B-1 for the thermoset matrix composite and in Figure III-B-2 for the thermoplastic matrix composite. The first cycle hysteresis loop is shown as well as the final repetitive (stable) hysteresis loop. After reaching the stable hysteresis loop condition, the samples were annealed in an oven at 100°C for twenty-four hours and retested. These data are shown in Figures III-B-1 and 2 as "recovery". It is interesting to note that the thermoplastic matrix composite (PS) shows a stiffening of the recovery curve relative to the original curve whereas the thermoset composite (Fiberite) shows a permanent softening.

The areas inside the hysteresis loops were measured and normalized by the volume of the sample, thereby obtaining energy dissipation per unit volume (in units of lb-in/in^3 or psi). The results are shown in Figure III-B-3 where energy dissipation is plotted versus the peak stress at the upper cycle point. It is interesting to note that the thermoset

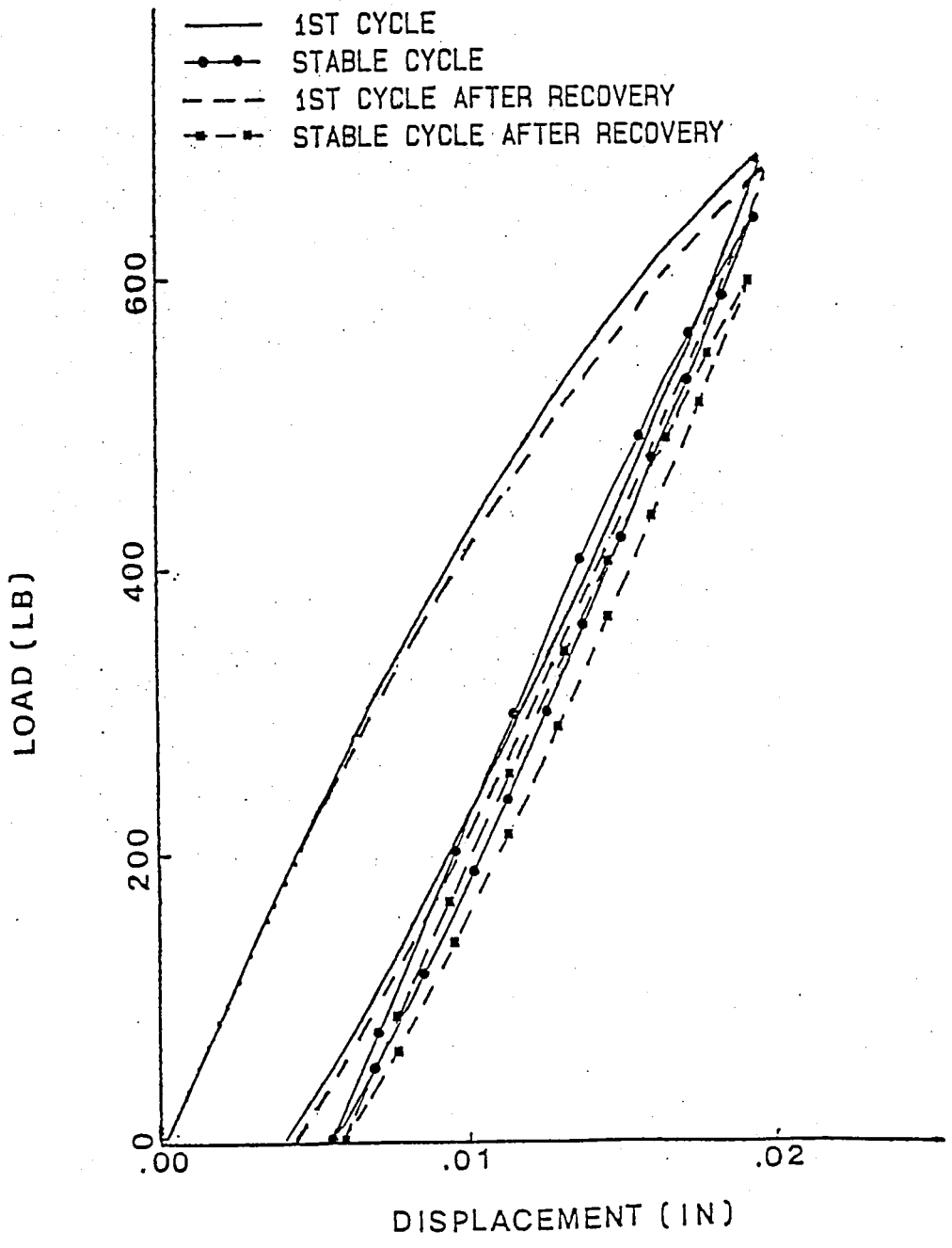

Figure III-B-1. Typical Hysteresis Loops Showing Load Versus Displacement for Fiberite, a Carbon-Epoxy (Thermoset) Laminate.

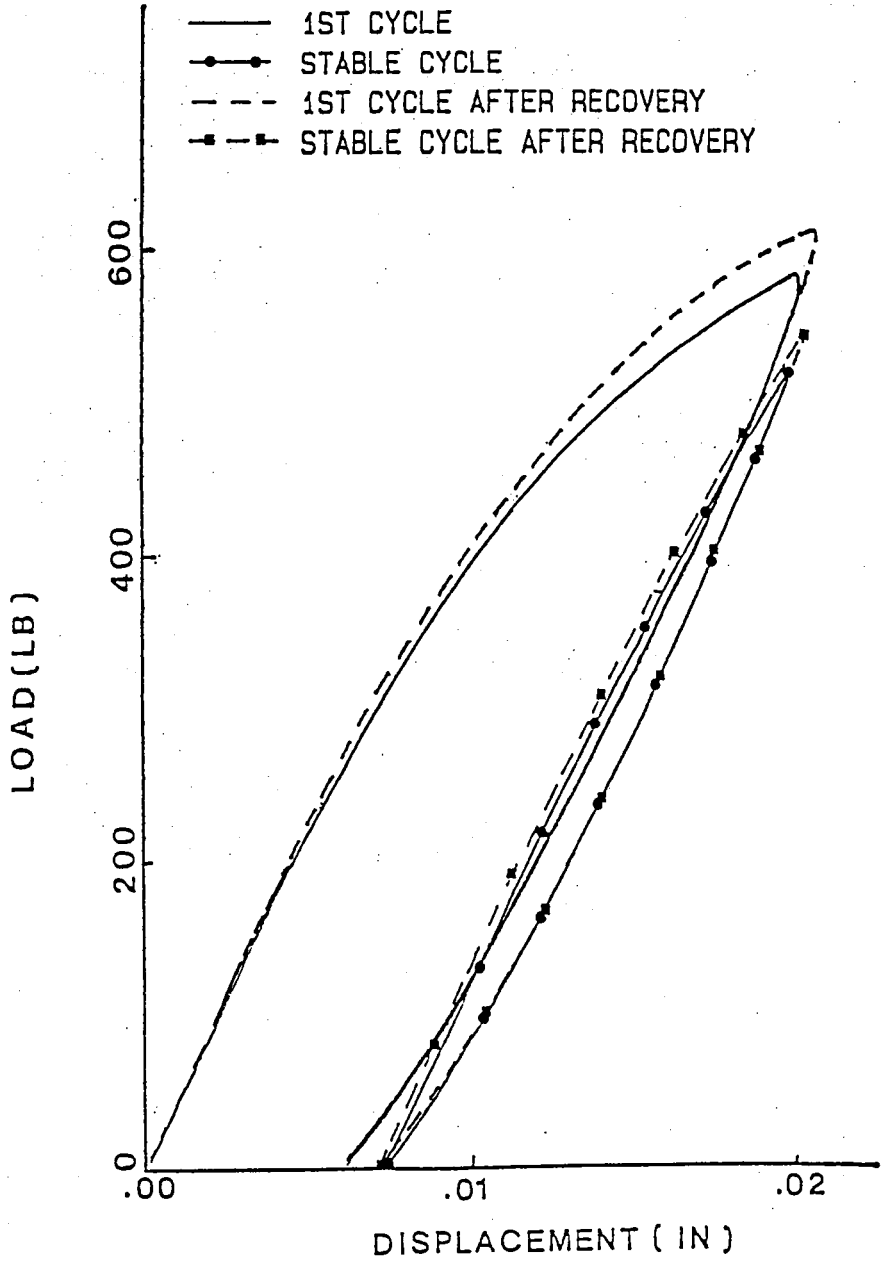

Figure III-B-2. Typical Hysteresis Loops Showing Load Versus Displacement for a Carbon-Polysulfone (Thermoplastic) Laminate.

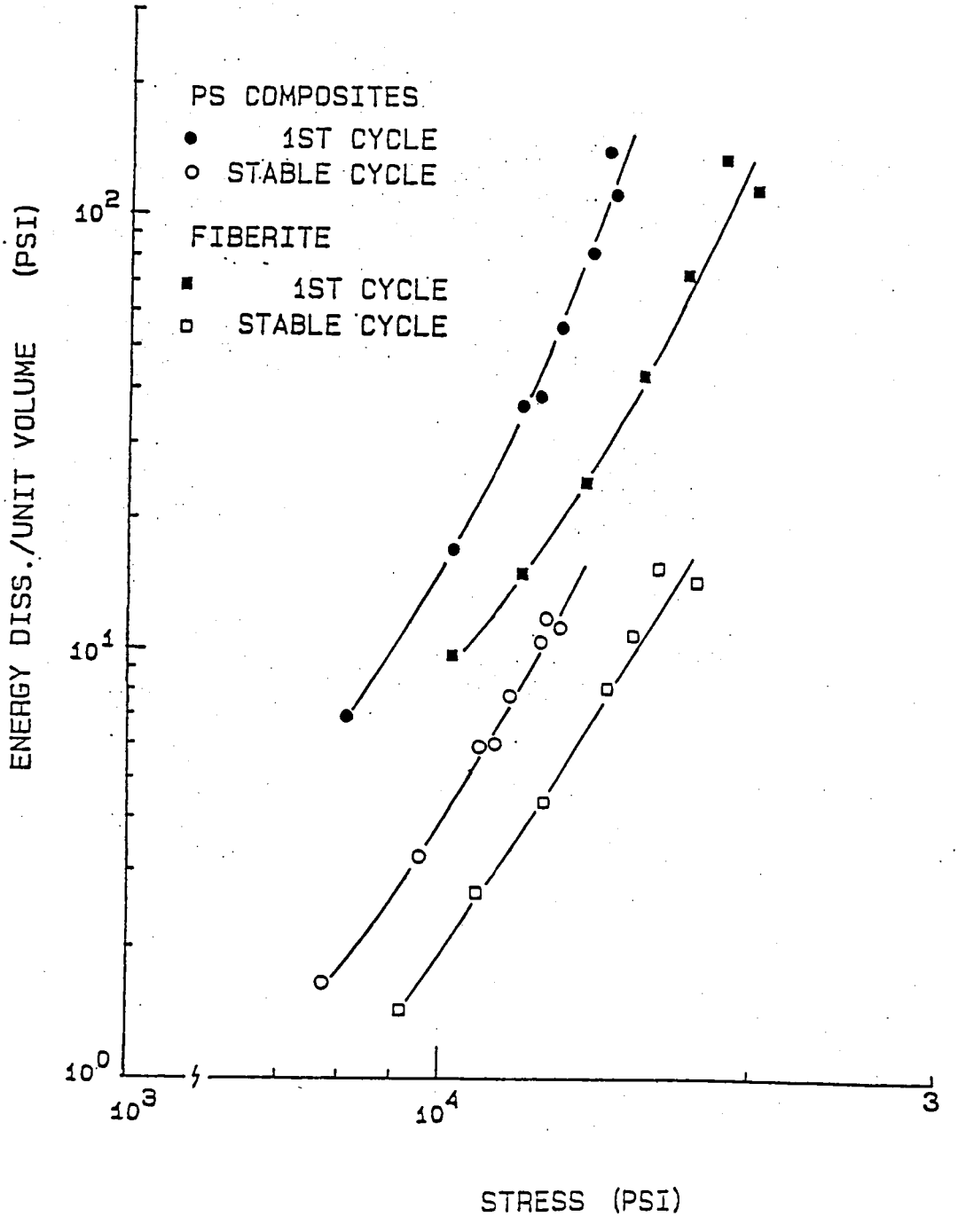

Figure III-B-3. Normalized Energy Dissipation Versus Peak Stress Level in the Cyclic Hysteresis Test.

(Fiberite) shows more nonlinearity with stress level than does the thermoplastic. It remains to be determined whether or not this represents an increased rate of damage production. Figure III-B-3 shows both the first cycle and stable cycle energy dissipation values.

The slopes of the curves in Figure III-B-3 are equal to or greater than four. Thus, energy dissipation is varying with the fourth power of stress. This is in marked contrast with the slope of two expected for linear behavior. We are currently continuing these tests at lower stress levels to determine if the curves of Figure III-B-3 bend over and approach a slope of two at lower stress values. If this happens, it may be possible to isolate the stress level at which damage processes initiate.

The energy dissipation is also shown versus upper cycle displacement (strain) in Figure III-B-4. Curiously, the thermoset and thermoplastic composites show surprisingly similar behavior when compared on a peak strain basis.

4. Plans for Upcoming Period

During the next period we plan to continue this work and extend it to several other thermoplastic matrix composites.

5. Current Publications or Presentations by Professor Sternstein on this Subject

"Mechanical Characterization of Composites"

Presented the invited lecture at Composites and Paper Technology Interchange, Stockholm, Sweden, June 25-29, 1984.

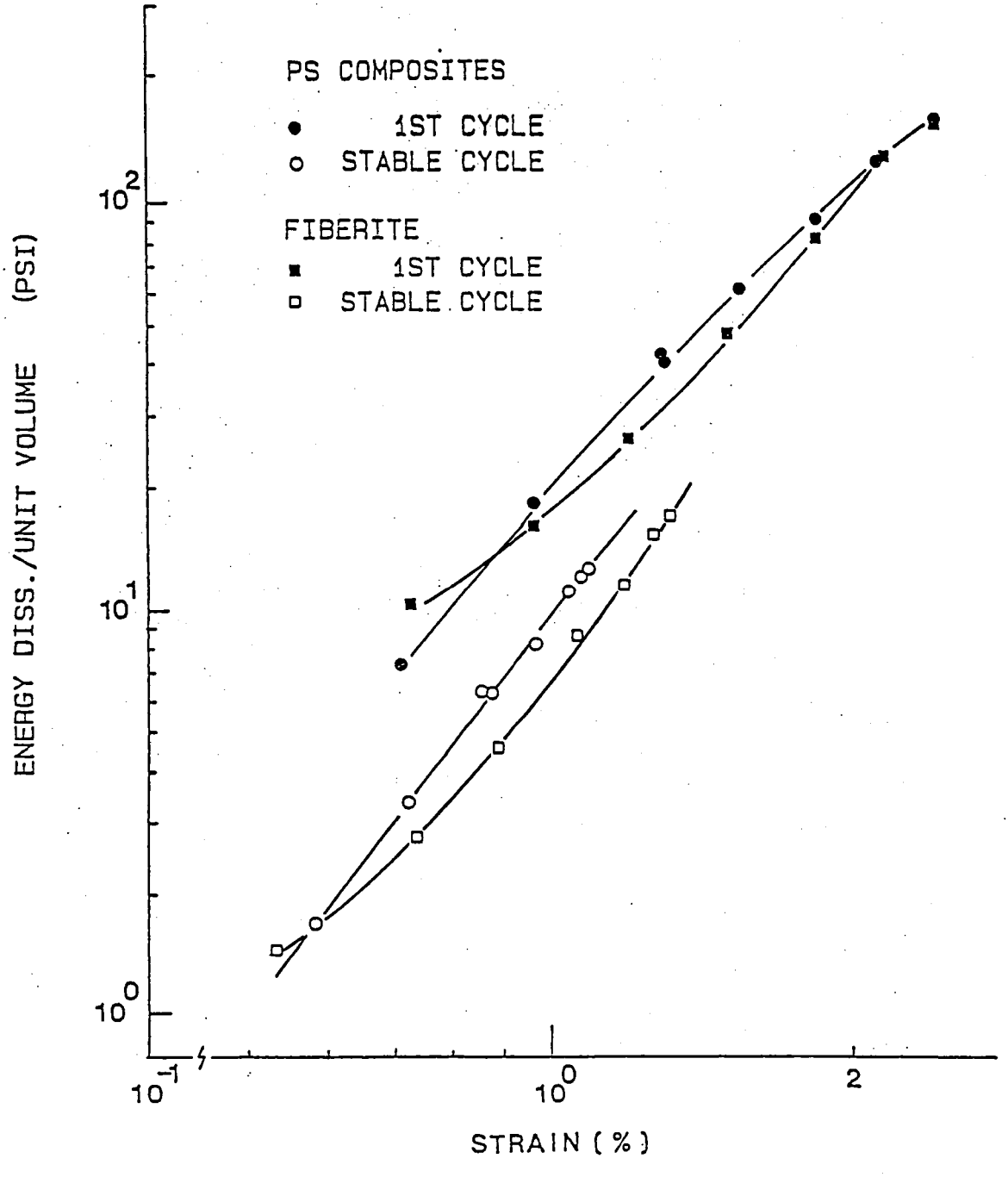

Figure III-B-4. Normalized Energy Dissipation Versus Peak Strain Level in the Cyclic Hysteresis Test.

"Mechanical Characterization and Failure of Composites"

Presented as an invited lecture at the Materials Research Council Meeting, La Jolla, CA, July 19-20, 1984.

"Viscoelastic Characterization of Composites"

Presented at the 188th National ACS Meeting, Philadelphia, PA, August 26-31, 1984.

III-C NUMERICAL INVESTIGATION OF THE MICROMECHANICS OF COMPOSITE FRACTURE

Senior Investigator: M. S. Shephard

1. Introduction

To understand mechanisms of failure in composites it is necessary to develop insight into their micromechanical behavior, including interactions between matrix and fibers as the load is increased from zero to that corresponding to failure. Investigation of these phenomena, either experimental or numerical, is difficult. The purpose of this project, carried out primarily by Nabil Yehia, is to develop a finite element program capable of performing the numerical investigations of two-dimensional micromechanical failure of composites.

2. Status

A generalized program for the two-dimensional analysis of static crack growth problems has been developed and tested. In addition to an examination and development of fracture criteria needed to track cracks in composites at the micromechanical level, the program employs fully automatic finite element mesh generation. This is an entirely new approach in program structure that was taken to allow for the automatic tracking of discrete crack growth.

3. Progress During Report Period

During the last reporting period, our effort concentrated on (a) completing the integration of the fully automatic mesh algorithms and (b) running of test cases to check the program's capabilities and to compare results.

a. Integration of Automatic Crack Tracking System

Previous progress reports have discussed the functions of the automatic crack tracking system which include:

1) a geometric based program control structure[1]*,
2) automatic mesh generation accounting for the presence of crack tips[1-3] and
3) finite element based fracture criteria[1].

The geometric based program control structure represents the link to the various parts of the program. It tells the mesh generator how and what to mesh and how to relate the loads, material properties and boundary conditions to that mesh. The analysis and propagation results are tied back to geometry which is updated using the geometry modification operators outlined in the last progress report. Because these operators must account for general geometric modifications, an efficient and flexible data structure must be employed.

Within the program geometry, entities are stored in linked list structures[1]. This data structure can account for geometric modification by simply adding data and shifting pointers within the list. For example, Figure III-C-1

*Numbers in brackets in this section refer to the references which are listed on page 65.

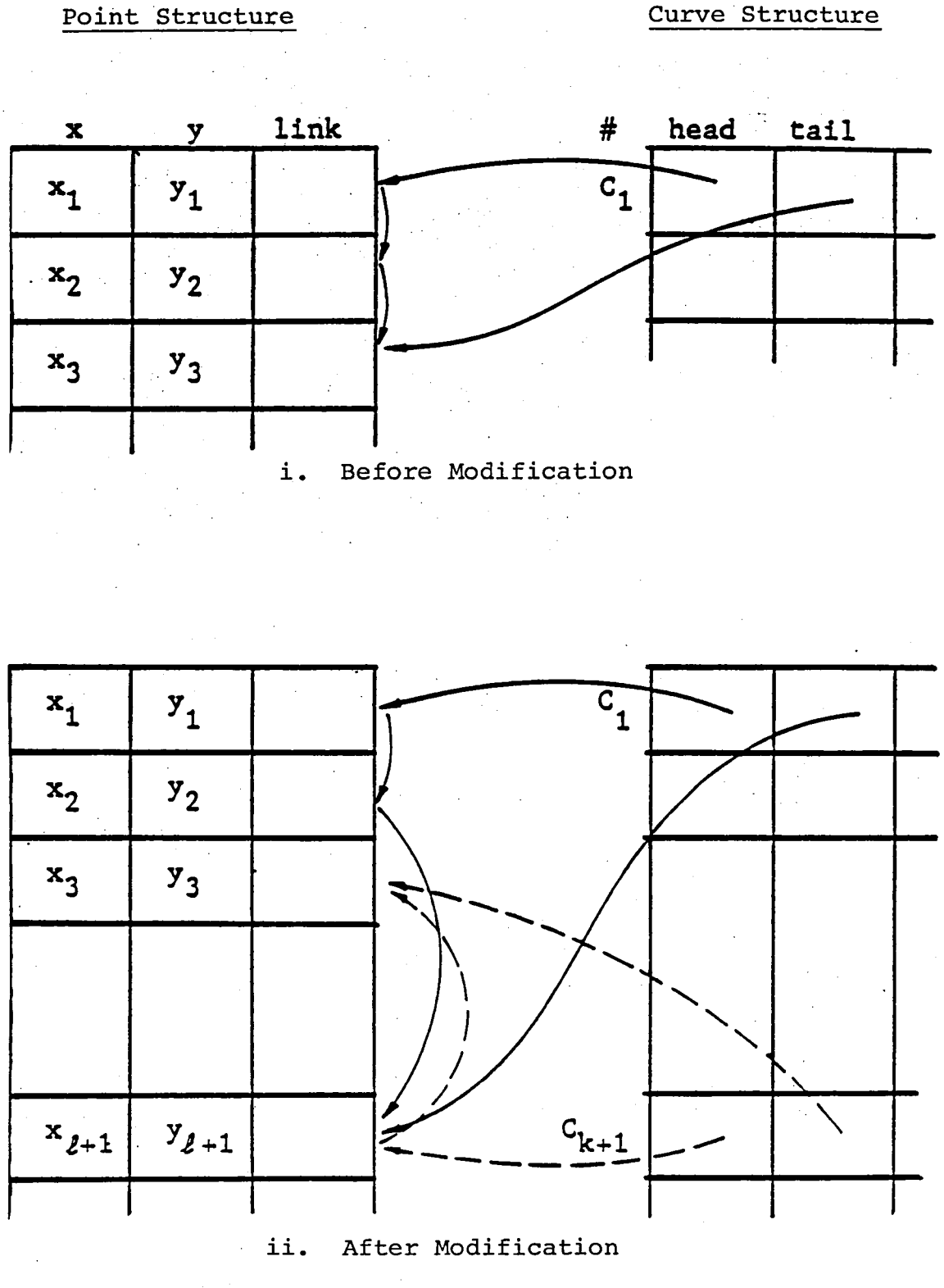

Figure III-C-1. Data Manipulation for Dividing a Curve into Two Curves.

demonstrates the changes to the point and curve data structure that occur when a curve is divided into curves. In this case, an entry is added to the curve list, and pointers in the point list are altered. No data needs to be shifted in this process.

In addition to the geometric operators needed to track crack propagation, features were needed to account for modifications to attribute (load, material property and boundary condition) information and to insure that a mesh would be generated properly for the given geometry[1]. Specific features included an ability to:

1) automatically change mesh size as a crack tip approaches a boundary,
2) eliminate any crack tip that hits an exteriod boundary and
3) split distributed loads and boundary conditions on curves cut by crack tips.

The final step in integrating the program was incorporating the crack nucleation and propagation algorithm that ties the finite element analysis and fracture prediction back to the geometry.

Once the user has defined the geometry of his problem and all the associated attributes related to geometry, the automated analysis is entered and proceeds as follows[1]:

Step 1:

- Read the problem definition and all attributes from the binary files to the COMMON blocks.

Step 2:

- Generate the finite element mesh and minimize the element wave front.

Step 3:

- Formulate the element stiffness matrices and solve them.

Step 4:

- Evaluate element stresses at the numerical integration points.

Step 5:

- If requested, enter the following crack nucleation routine:

  If maximum principal stress is less than the tensile strength, continue, else compute nucleation scaling factor $F = \sigma_t/\sigma_1$. If F is greater than the previous one, F_p, continue, else set $F = F_p$ then update the nucleation point coordinates and continue.

- Else continue.

Step 6:

- Set the nucleation scaling factor $F_{nu} = F$ and print out the nodal displacements and element stresses.

Step 7:

- If crack tips exist, enter the following crack propagation routine:

  a. Calculate the stress intensity factors at each crack tip.

  b. Calculate the crack propagation angle θ_o.

  c. Calculate the crack propagation increment $r_b(\theta_o)$ in the modified T-criterion and/or r in the S-criterion, in the predicted direction of propagation θ_o. Then, compare r_b or r with the material critical value, r_{cr}, and evaluate the propagation scaling factor, F, at each crack tip as;

     $-F = F\sqrt{r_{cr}/r_b}$ for the modified T-criterion or

     $-F = \sqrt{r_{cr}/r}$ for the S-criterion.

     Set the propatation scaling factor for the current iteration, F_{pr}, equal to the smallest F.

- Else continue.

Step 10:

Continue with Step 2.

b. Results of Examples

The previous progress report presented two example problems. Four additional example problems[1] are presented here.

Example 1:

In this example, the slant crack problem is considered under remote, uniform, uniaxial tension. The geometry considered has the dimensions 0.3*0.09*0.0015 in. which are the same as those of the specimens tested by Theocaris et al.[4] A crack with total length $2_{\alpha} = 0.016$ in., making an angle of 40 degrees with the load axis, is considered. Since no material properties for the test specimens have been reported by Theocaris et al., the following properties are assumed, E = 250 psi, $\sigma_y = 1$ psi, $K_{1c} = 1$ psi$\sqrt{\text{in}}$. and $\nu = 0.3$. The geometry and the finite element idealization of this problem are shown in Figure III-C-2. The initial crack propagation angle predicted by the modified T-criterion with the quarter point displacement technique is found to be -62.77° compared to 59° reported experimentally by Theocaris et al.[4] (i.e., 6% error). The S-criterion yields an angle of -51.48° (i.e., -12.7% error). With the modified T-criterion, the fracture load normalized with mode I fracture load is found to be 1.443 compared to 1.098 reported experimentally in Reference [4] (i.e., 31% error). The S-criterion yields a normalized fracture load of 1.548 (i.e., 41% error). The propagation was always unstable. Figure III-C-3

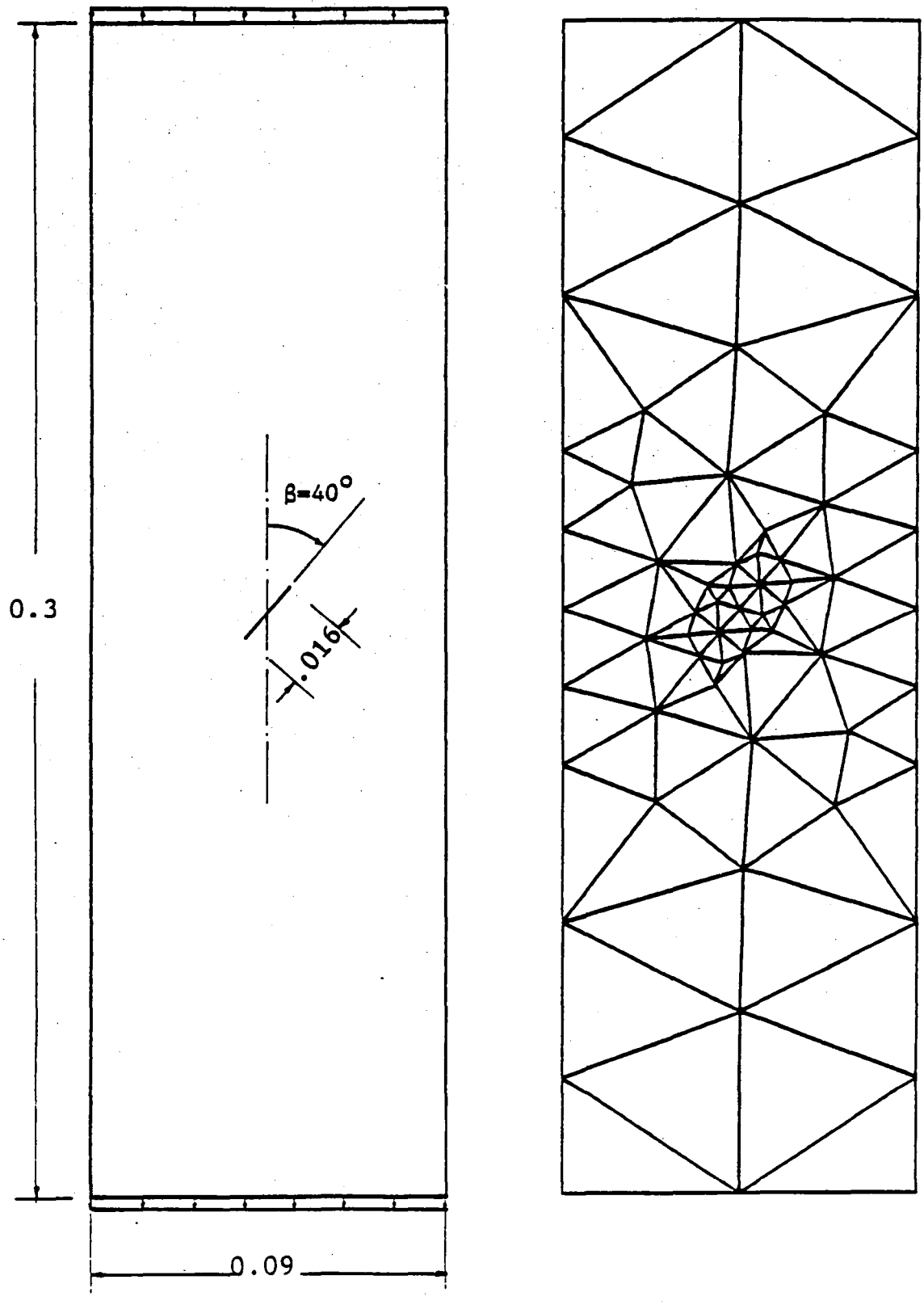

Figure III-C-2. Geometry and Finite Element Mesh of the 40° Slant Crack Geometry Tested by Theocaris et al.[4]

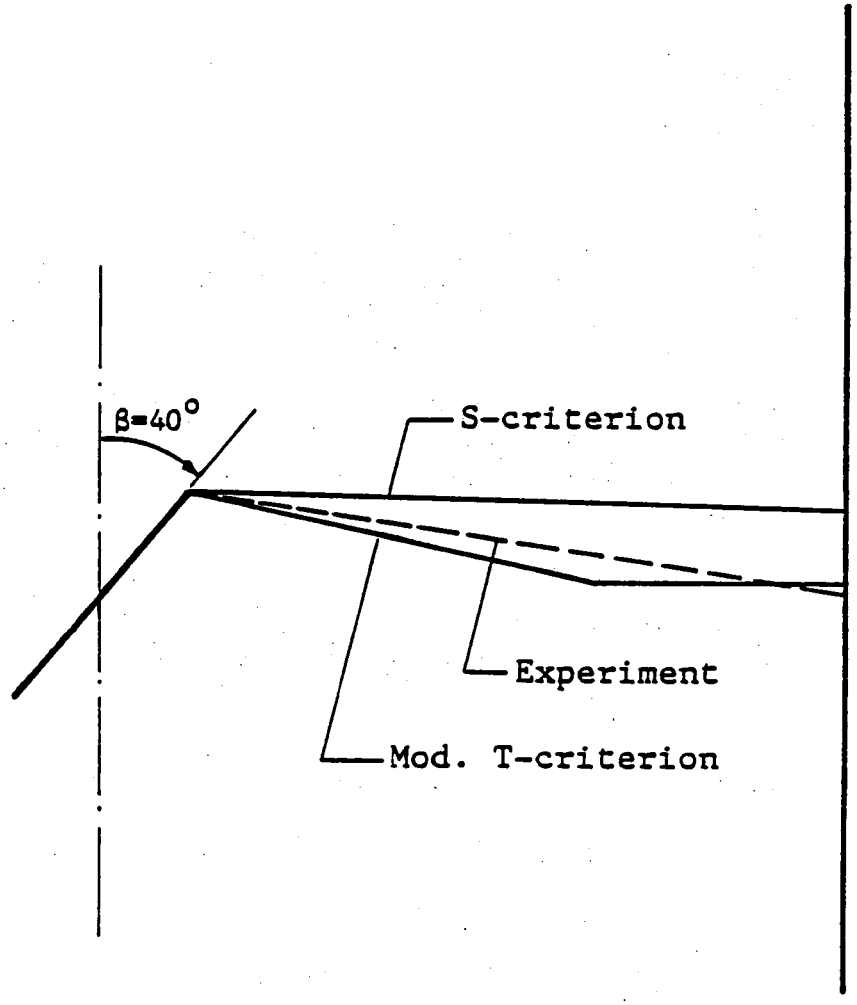

Figure III-C-3. Crack Propagation Path as Predicted by the Program CPFFEP in Comparison with the Path Experimentally Determined by Theocaris et al.

shows the propagation path predicted by both the modified T-criterion and the S-criterion and the approximate propagation path determined experimentally[4].

Example 2:

In this example, the slant crack geometry experimentally tested by Sih[5] is considered under plane stress conditions. The geometry is 18*9*0.1875 in. with a total crack length of $2\alpha = 2$ in. making a 40 degree angle with the load axis. The material properties are $E = 100$ ksi, $\sigma_y = 29.2$ ksi, $K_{1c} = 29.2$ ksi$\sqrt{\text{in.}}$ and $\nu = 0.333$. The geometry and finite element idealization of this problem are shown in Figure III-C-4. The initial crack propagation local angle predicted by the modified T-criterion using the quarter point displacement technique is found to be -62.83° compared to -55.6° reported experimentally by Sih[5] (i.e., +13% error). The S-criterion yields a normalized fracture load of 1.48 (i.e., +15.6% error). Note that better agreement between the numerical predictions and the experimental results is observed in this example. The propagation was always unstable. Figure III-C-5 shows the propagation path of the upper crack tip predicted by both the criteria and initial propagation path determined experimentally[5].

Example 3:

This example is the 1 in. thick plate with two holes as shown in Figure III-C-6. The starting mesh for this example is shown in Figure III-C-7. As indicated in Figure III-C-6, the plate is put into tension by a uniform load of 1 lb/in., and the circular hole has a small crack emanating from it. A plane stress condition is assumed with the following

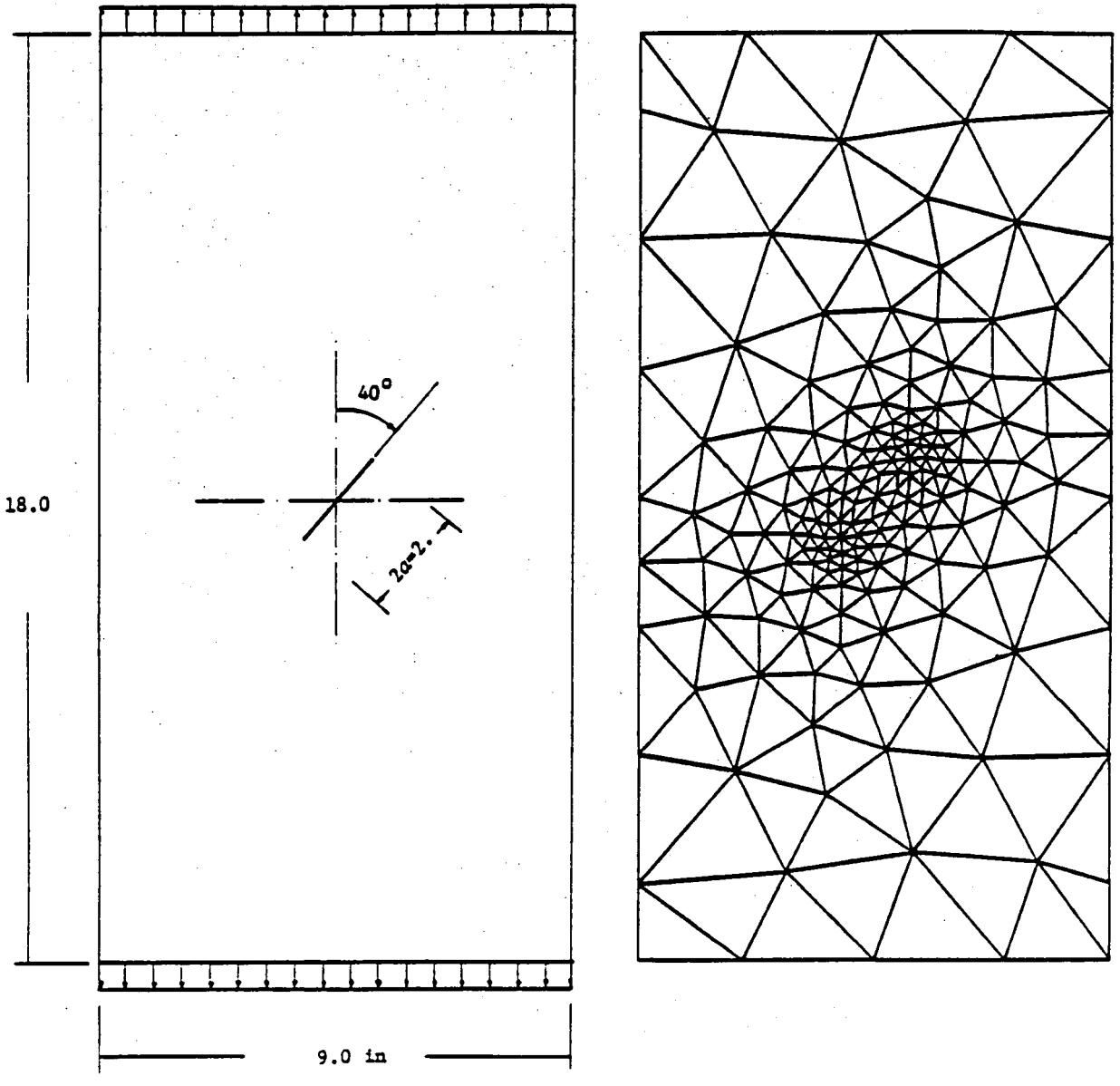

Figure III-C-4. Slant Crack Geometry Tested by Sih[5] and Its Finite Element Mesh.

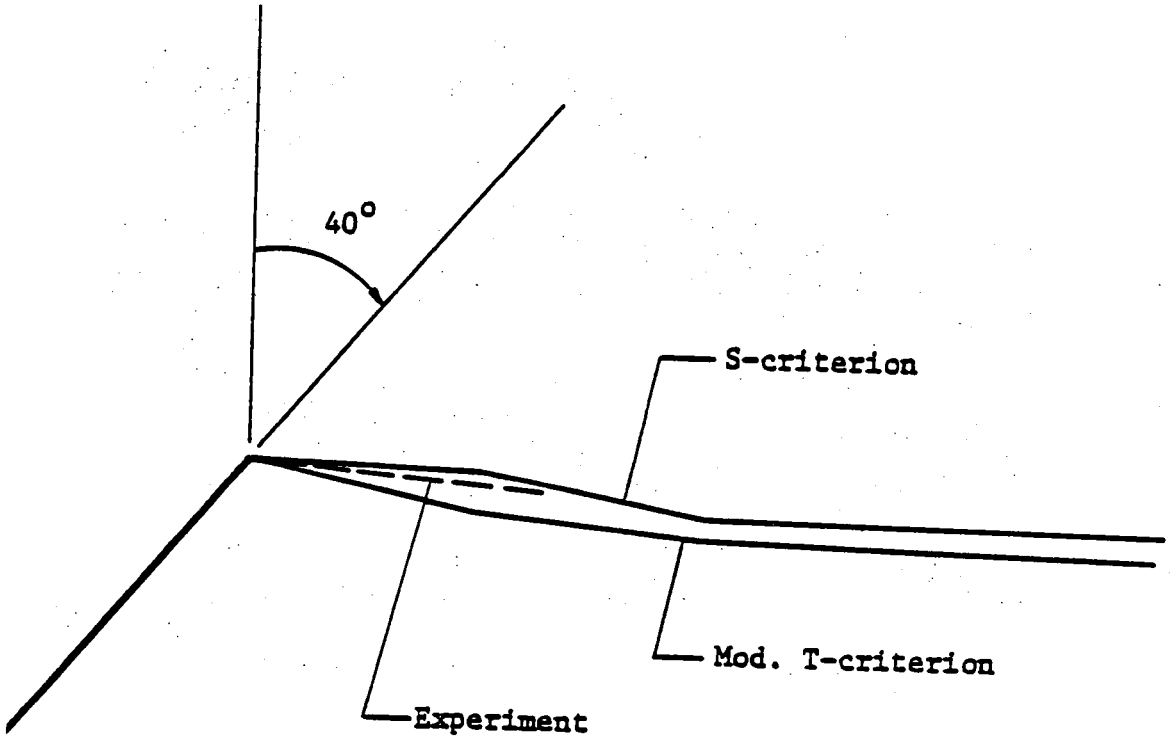

Figure III-C-5. Comparison of Crack Propagation Path Predicted by the S- and the Modified T-Criteria and the Initial Path Determined Experimentally.

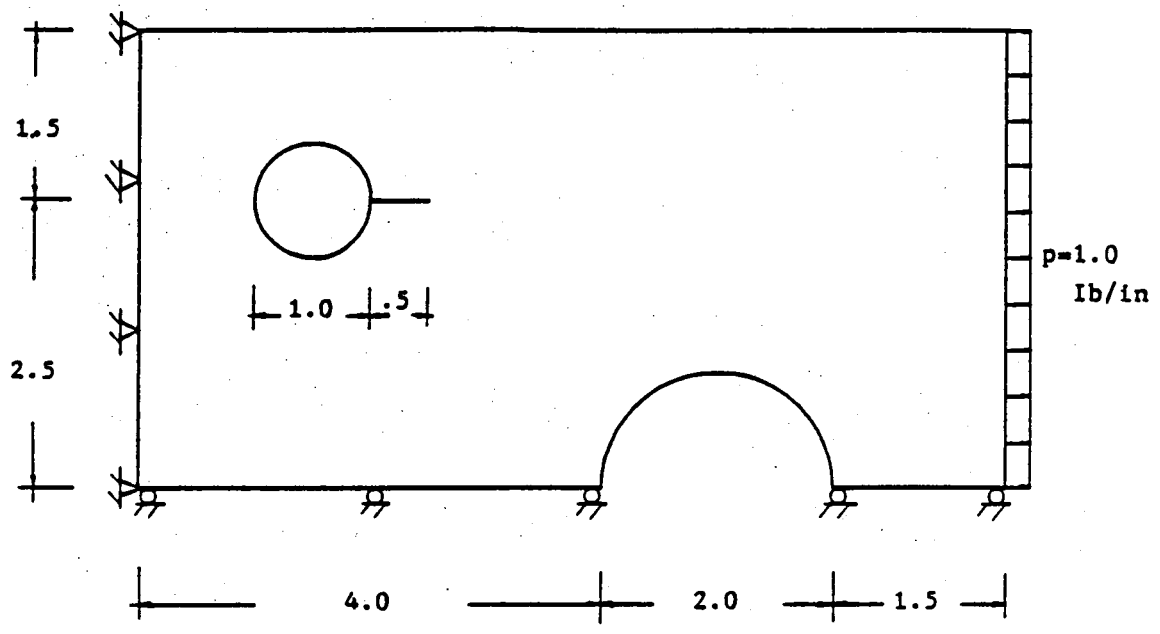

Figure III-C-6. Plate with Two Holes Under Tension.

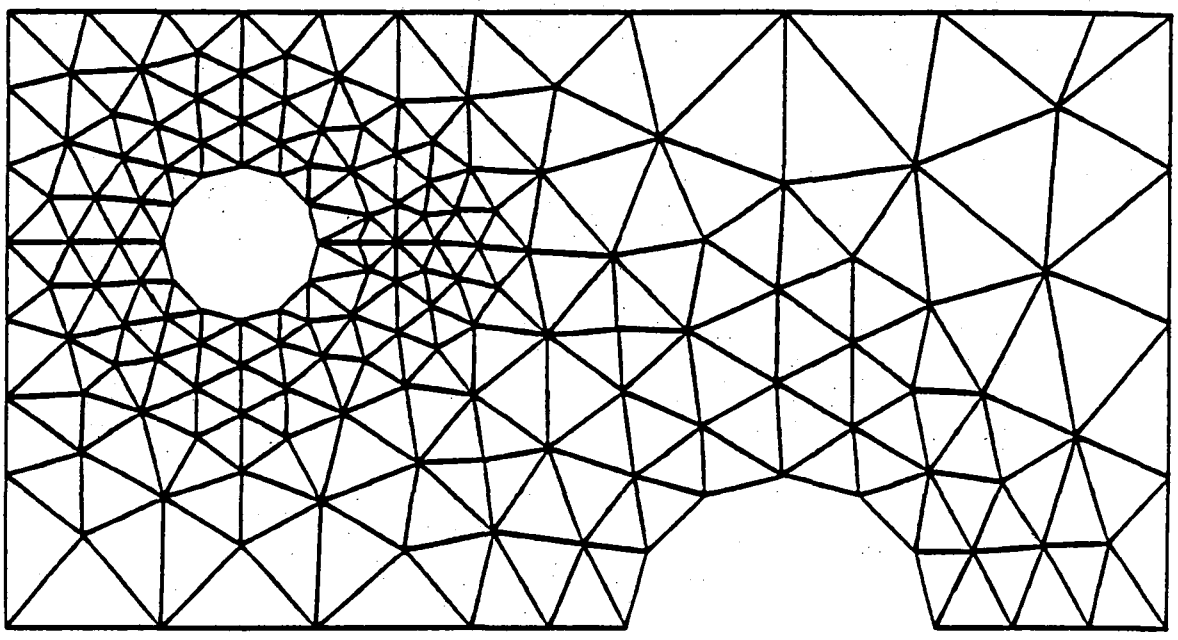

Figure III-C-7. The Starting Mesh for the Plate with Two Holes.

material properties, $E = \sigma_y = 1$ psi, $K_{1c} = 1$ psi$\sqrt{\text{in.}}$ and $\nu = 0.333$. The meshes for two steps of crack propagation are shown in Figure III-C-8. The fracture process, with a total of six propagation increments, as shown in Figure III-C-9, has been tracked using both the modified T-criterion (MT) and the S-criterion (S) with stress intensity factors calculated using the quarter point displacement technique. The predicted fracture loads for the next propagation increment are found to be p = 7.23, 9.66, 4.59, 1.27, 0.66 and 0.49 lb/in. Thus, the crack growth is stable for the first two increments, as indicated by positive load increments predicted for the next propagation. The rest of the propagation increments are unstable as indicated by the negative load increments. For this example, the crack propagation load and path predicted by the modified T-criterion are very close to the ones predicted by the S-criterion. However, when employing the assumption of [5] for choosing the positive angle of θ_o for cracks under compression (i.e., negative K_I and K_{II}), the first increment predicted by the S-criterion is found to occur at a local tip angle of 179° (i.e., the crack reverses its direction). This is 180° different from the propagation angle predicted by the modified T-criterion. This difference vanishes if the restriction of [5] is removed, which yields the propagation path predicted by both criteria (see Figure III-C-9).

Example 4:

In this example, a single fiber-matrix composite model is considered. It consists of a 2 in. diameter fiber embedded in an annular sheath of a 4 in. thick matrix with a 2 in. interface crack and loaded in the

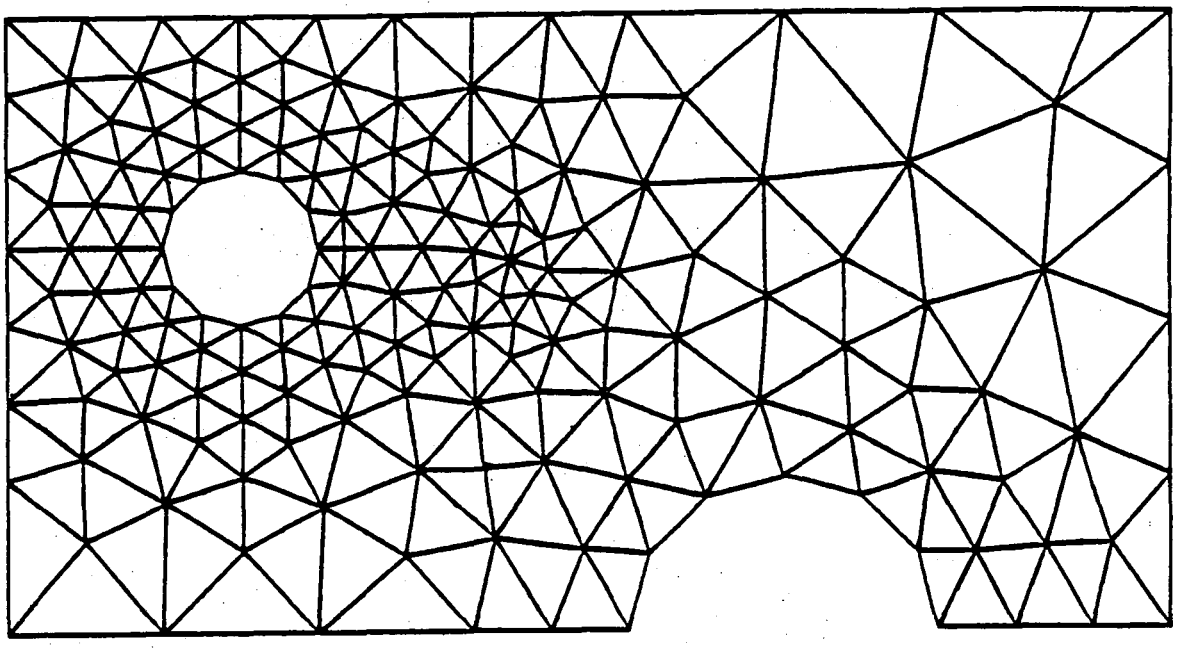

a) Second Propagation Increment

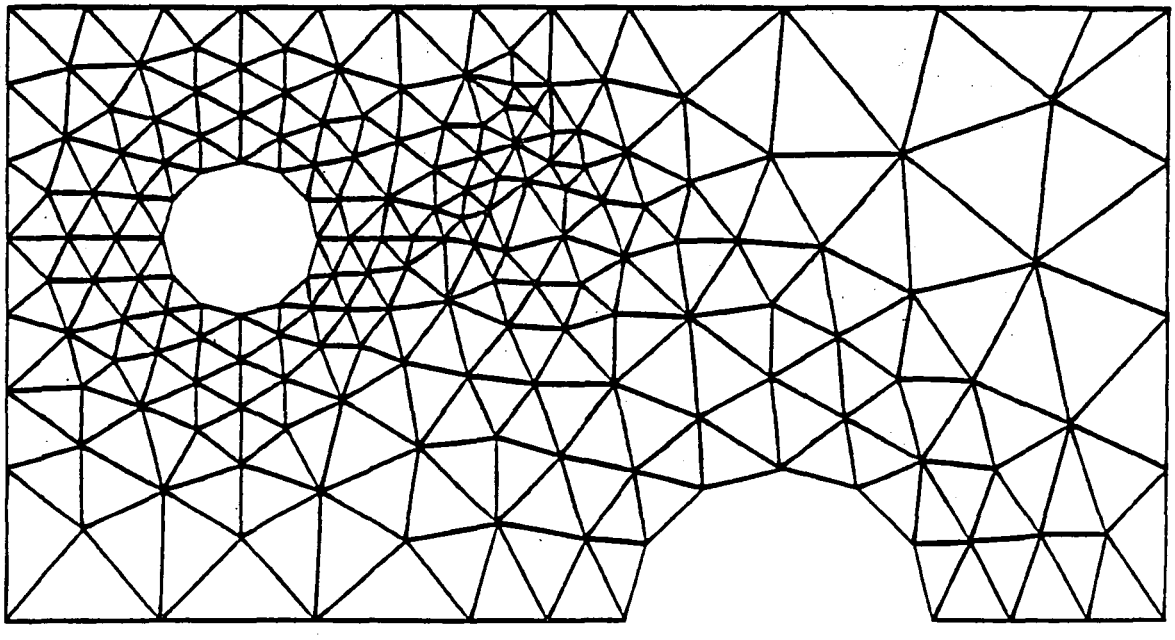

b) Fourth Propagation Increment

Figure III-C-8. Finite Element Mesh of the Plate.

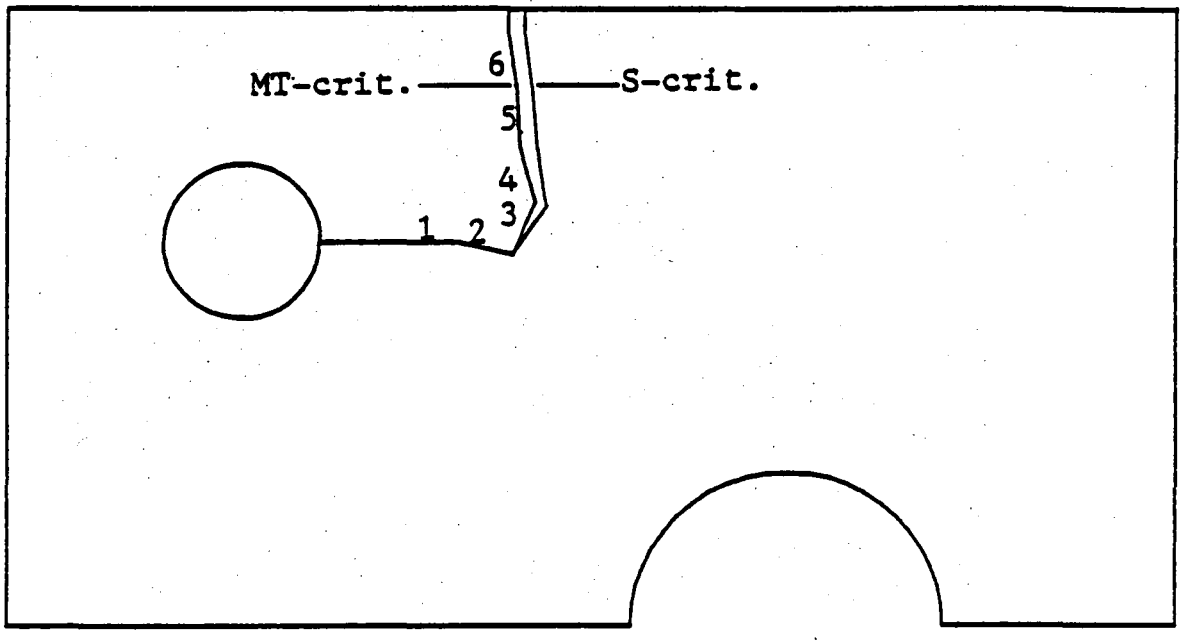

Figure III-C-9. Crack Propagation History Predicted by the Modified T-Criterion and the S-Criterion of the Plate with Two Holes.

fiber's axial direction. To simulate this axisymmetric problem, a two-dimensional plane strain analysis of one quarter of the model is considered. Figure III-C-10 shows the model geometry and boundary conditions. The initial finite element mesh is shown in Figure III-C-11. For fracture analysis of this problem the modified T-criterion for interface crack propagation[1] is employed, with the stress intensity factors being calculated by the crack flank displacement technique[6].

Two composite materials are considered, $E_f/E_m = 2$ (E is the Young's modulus) which is almost the case of a ceramic/ceramic composite, and $E_f/E_m = 100$ which is similar to the case of a high modulus graphite/epoxy composite. The Young's modulus of the matrix E_m is assumed to be 1 psi while the Poisson's ratio $\nu_m = \nu_f = 0.3$ is considered in the two cases.

Two loading conditions are considered, constant longitudinal strain (i.e., $\varepsilon_{matrix} = \varepsilon_{fiber}$) and uniform uniaxial load, both applied remote from the crack (see Figure III-C-12). Under the constant longitudinal remote strain condition, crack closure occurred, leading to a very high load scaling factor required for crack propagation along the interface. In the case of uniform uniaxial load, four subsequent equal propagation increments are predicted at p = 15, 11.58, 9.13 and 7.34 lb/in for the case of $E_f/E_m = 2$ and p = 2.38, 1.73, 1.32 and 1.06 lb/in for the case of $E_f/E_m = 100$. Therefore, in this model, the resistance to interface crack propagation increases as the Young's modulus of the matrix approaches that of the fiber. Although the propagation load varies substantially between the two load cases in the two composites considered,

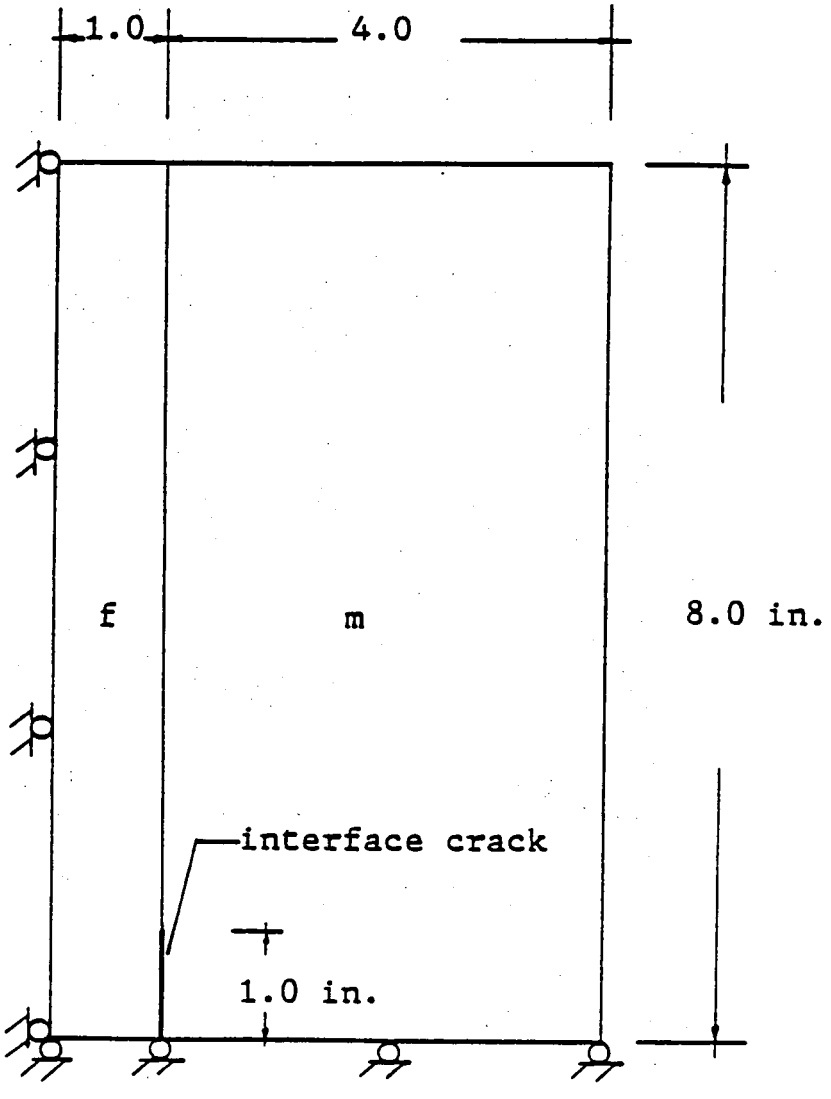

Figure III-C-10. A Single Fiber-Matrix Composite Model

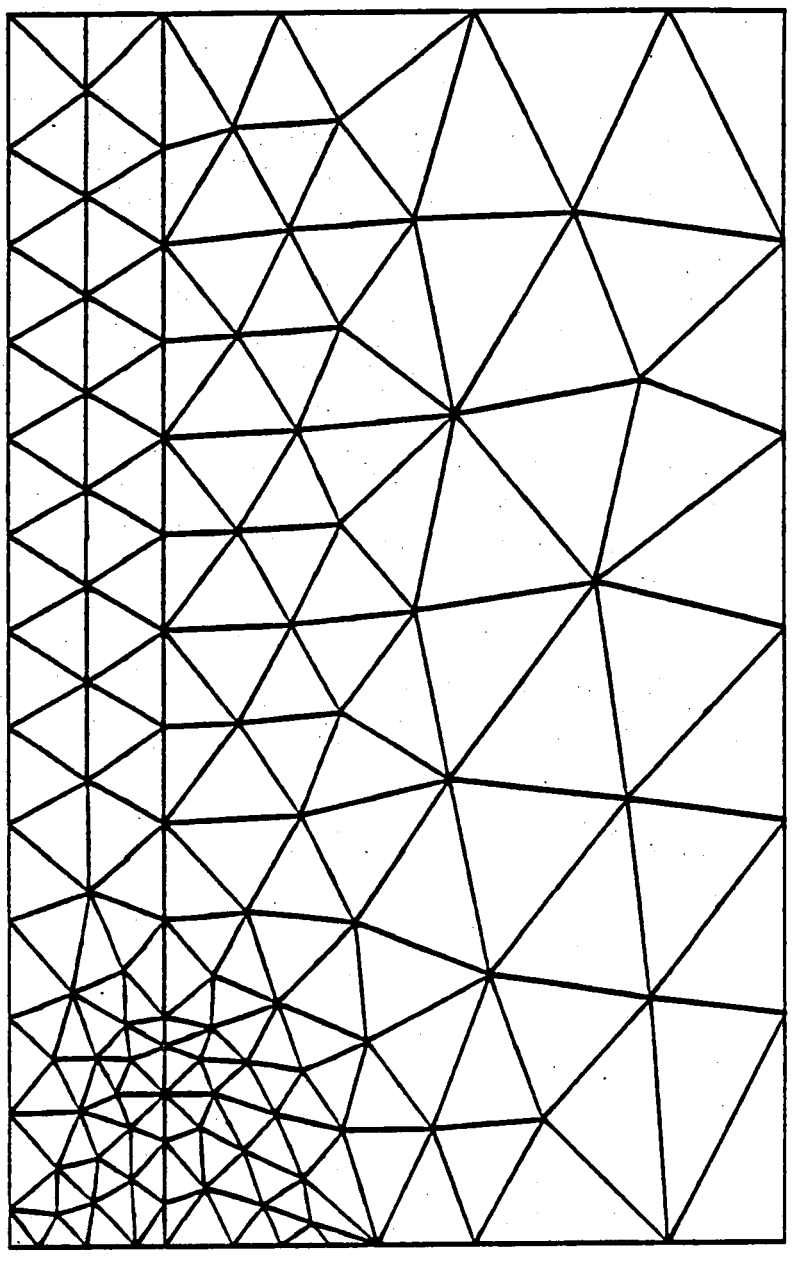

Figure III-C-11. The Initial Mesh for the Single Fiber-Matrix Composite.

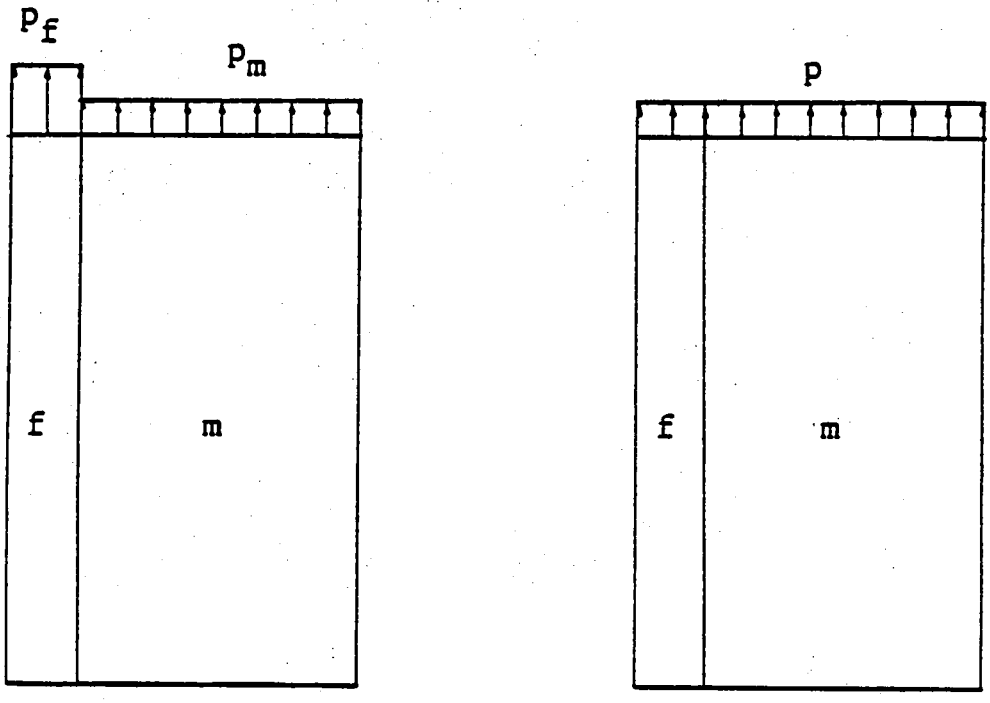

$$\varepsilon_f^{\infty} = \varepsilon_m^{\infty}$$

$$p_f = \frac{E_f}{E_m} p_m$$

$$p_f = p_m = p$$

Figure III-C-12. The Loading Conditions Applied to the Single Fiber-Matrix Model.

the propagation has been always found unstable. The meshes for the second and fourth propagation increments are shown in Figures III-C-13 and 14.

4. Plans for Upcoming Period

This progress report coincides with the completion of Nabil A. B. Yehia's Ph.D. studies. At the present time, the project is being put on hold until a new Ph.D. candidate with an appropriate background for this project can be found.

Three areas require additional effort to make this method a practical tool for micromechanical composite fracture analysis. They are:

1) adding iterative steps after each incremental solution to control drift from the true solution,

2) developing appropriate criteria to more completely represent the fiber-matrix interfaces and

3) carrying out laboratory experiments to verify analytical solutions.

5. References

1. Yehia, N. A. B., "Automatic Tracking of Micromechanical Cracking via Finite Elements", Ph.D. Thesis, Department of Civil Engineering, Rensselaer Polytechnic Institute, Troy, NY, August 1984.

2. Burd, G. S., "An Automatic Finite Element Mesh Generator and Adaptive Geometry Data Base for Tracking General Two-Dimensional Crack Growth", Master's Thesis, Department of Mechanical Engineering, Rensselaer Polytechnic Institute, Troy, NY, 1984.

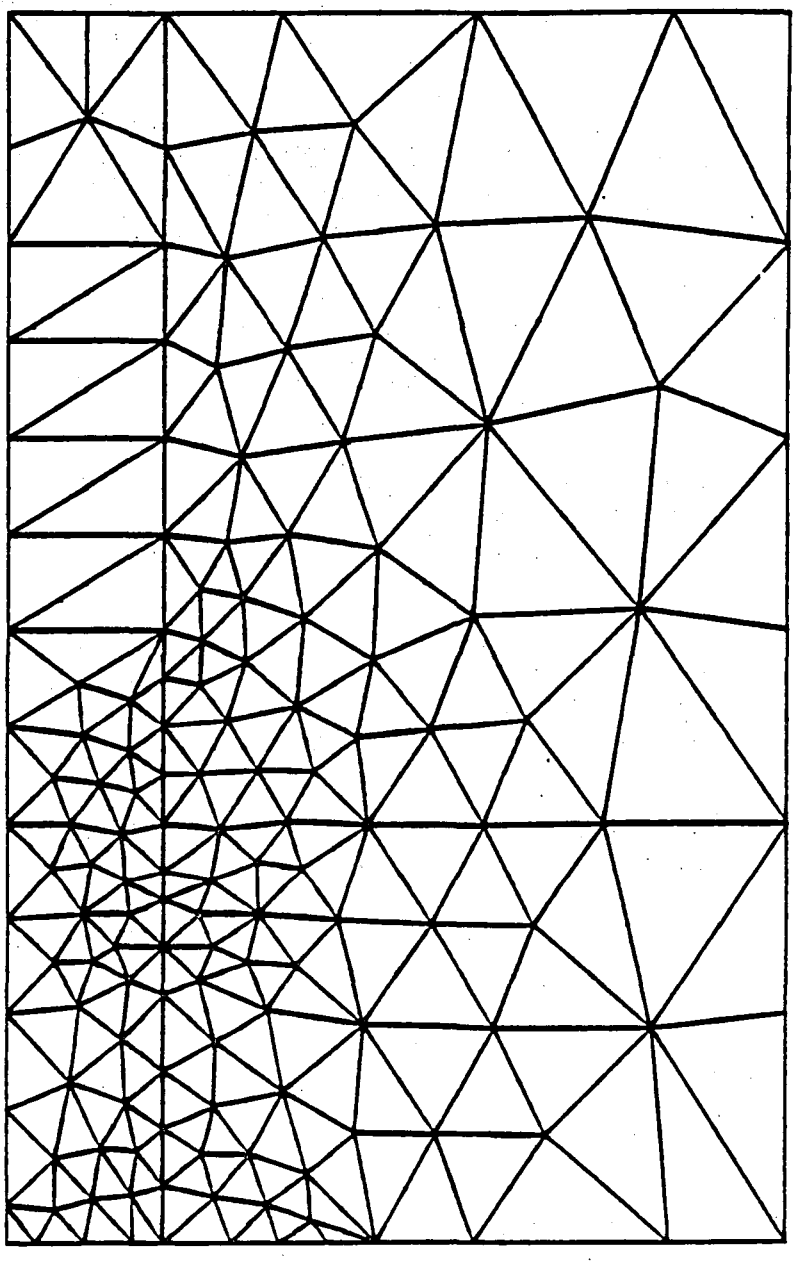

Figure III-C-13. Finite Element Mesh for the Second Propagation Increment Along the Interface of the Single Fiber-Matrix Model.

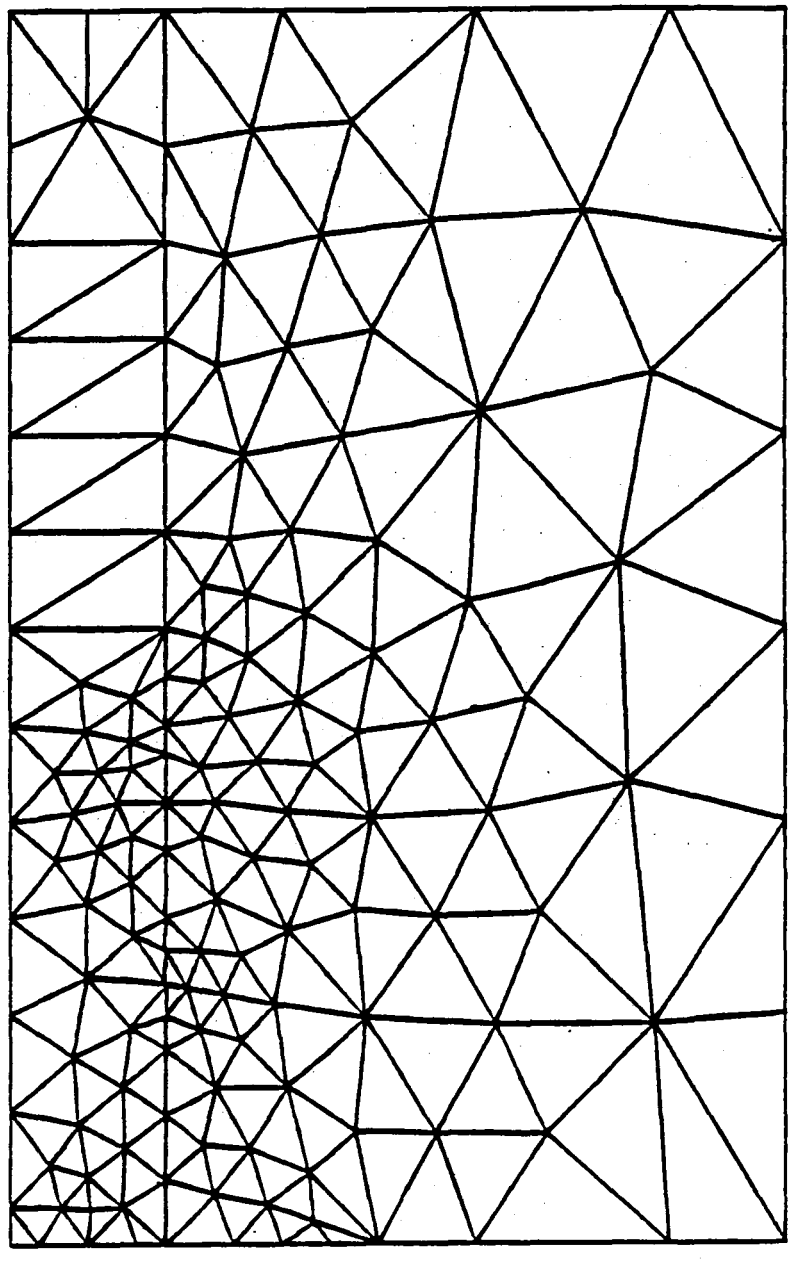

Figure III-C-14. Finite Element Mesh for the Fourth Propagation Increment Along the Interface of the Single Fiber-Matrix Model.

3. Shephard, M. S., N. A. B. Yehia, G. S. Burd and T. J. Weidner, "Automatic Crack Propagation Tracking", to appear in Computers and Structures.

4. Theocaris, P. S., G. A. Kardomateas and N. P. Anrianopoulos, "Experimental Study of the T-Criterion in Ductile Fractures", Engng. Fracture Mechanics, Vol. 17, 1982, pp. 439-447.

5. Sih, G. C., "Strain-Energy-Density Factor Applied to Mixed Mode Crack Problems", Int. Journal of Fracture, Vol. 10, 1974, pp. 305-321.

6. Smelser, R. E., "Evaluation of Stress Intensity Factors for Bimaterial Bodies Using Numerical Crack Flank Displacement Data", Int. Journal of Fracture, Vol. 15, 1979, pp. 135-143.

6. Current Publications or Presentations by Professor Shephard on this Subject

"Automated Analysis Model Generation"

Published in Computer Aided Design in Civil Engineering, C. N. Kostem and M. S. Shephard, eds., 1984, pp. 92-99.

"On the Effect of Quarter-Point Element Size", with N. A. B. Yehia.

To be published in the Int. Journal of Num. Meth. Engng.

"Automated Crack Propagation Tracking"

To be published in Computers and Structures.

To be presented at Proceedings of Symposium on Advances and Trends in Structures and Dynamics, Arlington, VA, October 22-25, 1984.

"Finite Element Model Generation"

Presented at Siggraph '84, Advanced Topics in Solid Modeling, Minneapolis, MN, July 23-27, 1984.

III-D DELAMINATION FAILURES OF COMPOSITE LAMINATES

Senior Investigator: T. L. Sham

1. Introduction

Analytical and numerical studies of the delamination failures of graphite/epoxy laminates are being investigated. The goal of this research is to provide fundamental understanding of, and characterization methodology for, the delamination failure process in composites.

2. Status

A generalized plane strain finite element program has been developed for analyzing orthotropic composite layers.

3. Progress During Report Period

In order to investigate candidate global parameters that could serve as a characterizing parameter for the initiation of free-edge delamination, an additional specialized finite element code has been incorporated into the finite element program. Trial runs on crude finite element meshes have been conducted to verify the added code, and production runs on meshes based on various lay-ups are about to begin. The particular lay-ups are chosen to coincide with those reported in the open literature on free-edge delamination experiments. Such experimental data would help us to assess the predictive capability of the candidate parameters.

The development of this finite element program also paves the way for investigating innovative approaches in calculating the energy release rate for delamination cracks. Typically, the energy release rate is computed by using either the virtual crack-closure technique or crack-tip parameters obtained directly from the singular crack-tip finite element. Preliminary analyses indicate that the global technique is promising in providing efficient and accurate means to calculate the energy release rate.

Work on applying the "homogenization theory" to composite mechanics is also underway, in an effort to clarify the effects of higher order constitutive representation of the stress and deformation states near free surfaces.

4. Plans for Upcoming Period

The tasks, which are discussed in the preceding section, will be continued.

PART IV

GENERIC STRUCTURAL ELEMENTS

IV-A EFFECT OF NOTCH SIZE ON COMPOSITE LAMINATES WITH STRESS CONCENTRATIONS

IV-B IMPROVED BEAM THEORY FOR ANISOTROPIC MATERIALS

IV-A EFFECT OF NOTCH SIZE ON COMPOSITE LAMINATES WITH STRESS CONCENTRATIONS

Senior Investigator: D. B. Goetschel

1. Introduction

Advanced composite laminates with stress concentrations show a notch size effect on failure strength. Strength is not governed solely by peak stress but also by the stress intensity in the vacinity of a peak stress. This was shown when tensile specimens with different size holes, which all should have the same peak stress concentration factor, failed at significantly different stress levels[1]*. This has been termed "notch size effect" and can not be predicted by a classical stress concentration factor.

The "average stress" criterion[2] seems to be the method for predicting this effect which is most widely accepted by industry. While this method does improve on classical peak stress concentration factors, it still has some inaccuracies and lacks generality for arbitrary stress fields. This work deals with investigating some generalizations of the average stress criteria which should make it more versatile, accurate and logical.

Three basic generalizations are being examined. First, it is not logical that the average stress calculation be a uniform average over a given length without any tapering of a weighting function. Therefore, different weighting

*Numbers in brackets in this section refer to the references which are listed on page 82.

functions will be examined to find a more reliable averaging method. Second, the failure analysis will be taken from the laminate level down to the ply level to generalize the method to irregular geometries. This has already been partially verified in previous work. Third, an area average will be investigated as opposed to the conventional line average. This is more logical, should increase accuracy and help generalize the method to irregular geometries and stress fields.

The proposed modifications to stress concentration failure prediction will primarily be investigated experimentally. An analytic investigation based on Weibull statistics will also be pursued.

2. Status

This work was initiated at the beginning of the reporting period. Work has concentrated on basic formulation of the analysis to be used and on the preparation of the experimental program.

For the analytic formulation, the following three assumptions have been made:

1) Failure mode is tensile (for now).
2) Fiber failure will dominate strength. (Static loading only is being considered at this time.)
3) Notch is free of stress singularities. (It is proposed to handle singular elastic stress fields by setting a limit on $d\sigma_x/dx$, i.e., limit on shear transfer from matrix to fiber.)

Finite element analysis will be used to find the stress fields for arbitrary geometric configurations.

3. Progress During Report Period

During the report period two tasks have been completed.

An initial finite element computer program for stress analysis has been finished in a basic form. Various post-processing capabilities still have to be added as the different proposed modifications to the average stress criteria are investigated.

The basic experimental program has been largely completed. Published experimental results are not adequate for our needs. It was decided that it was important to vary more parameters (see below) than has been consistently done so far. It was also deemed important to have statistical strength information by testing five replicates of each configuration. Published experimental programs are almost completely lacking in this respect. Additionally, most published experimental programs contain incomplete background data which makes their utilization difficult for in-depth detailed research.

The experimental program was broken down into five parts as follows:

Part I: We investigated the stacking sequence effects ($[90/\pm45/0]_s$, $[\pm45/0/90]_s$ and $[0/\pm45/90]_s$) and orthotropy effects (two groups: $[0_\alpha/\pm45]_s$, $\alpha = 1, 2, 4$ and $[0/\pm\theta]_s$, $\theta = 15°, 30°, 45°, 60°, 75°$) on failure strength. Although $[\pm45]_{2s}$

does not and [90/±30] may not satisfy the assumption that fiber failure will dominate the failure behavior, it seems worth including both in this testing program because $[90/\pm30]_s$ is a "soft" quasi-isotropic laminate, and $[\pm45]_{2s}$ is popular for the investigation of crack propagation. It is interesting to have comparisons of $[0/90]_{2s}$ and $[\pm45]_{2s}$; $[0/\pm45]_{2s}$; and $[0/\pm60]_{2s}$ and $[90/\pm30]_{2s}$, which might give some indication for application of composite structure. Also, center cracks and center slots are investigated by picking up specified orientations ([0/±45/90] and $[0_2/\pm45]$); this is for the relationship between notch type and material properties on failure strength (see Figures IV-A-1a through 1c and Table IV-A-1).

Part II: We extended the scope of notch types to include double edge crack, double edge semi-hole and shoulder (representative for general stress raiser cases) [see Figures IV-A-1d through 1f and Table IV-A-2].

Part III: We also investigated the ability to predict strength for more irregular stress distributions by cocking cracks and slots at an angle (see Figures IV-A-1g and 1h and Table IV-A-3).

Part IV: Carbide tip twist drilling for holes in composite laminates is very popular in industry. Therefore, the testing data for quasi-isotropic laminates was compared with corresponding data in Part I where diamond core drills were used. This information will be helpful in identifiying how manufacturing affects strength (see Table IV-A-4).

DESCRIPTION OF SPECIMEN:

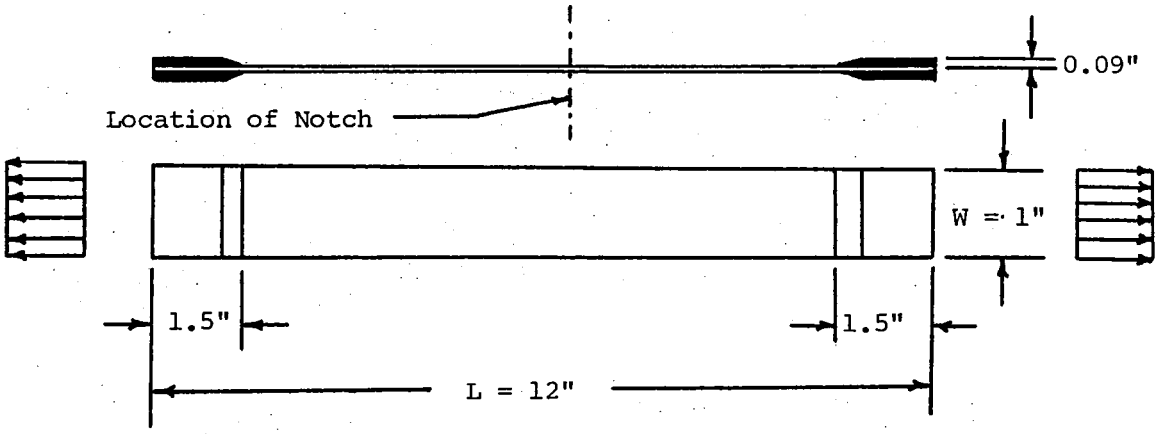

NOTCH TYPE AND SIZE:

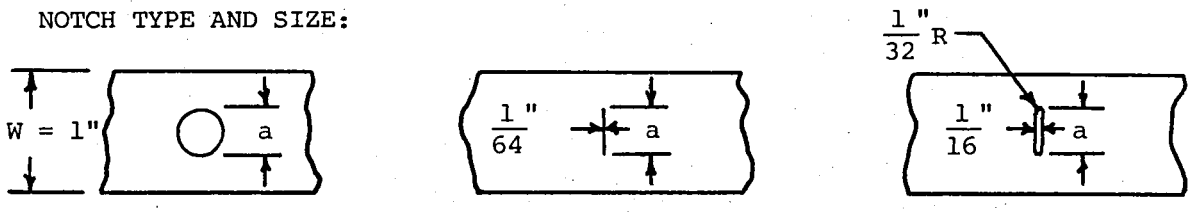

a) Center Hole b) Center Crack c) Center Slot

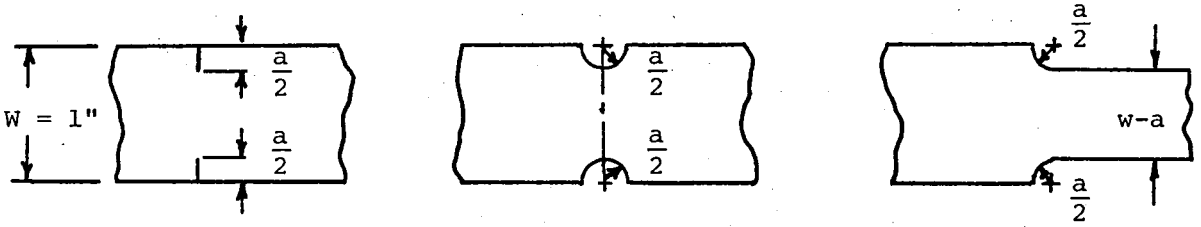

d) Double Edge Crack e) Double Edge Semiholes f) Shoulder

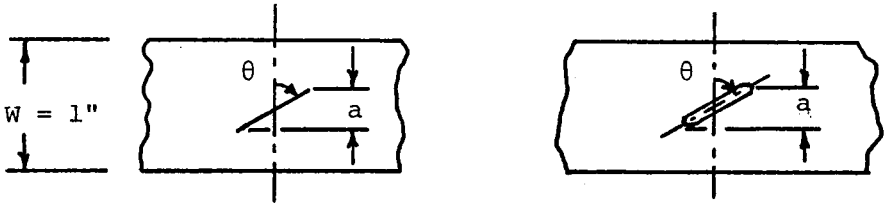

g) Center Slant Crack h) Center Slant Slot

Figure IV-A-1. Specimen Configurations

Part V: Strips of different width but equal ratio, $\frac{a}{w}$ (representing the effect of width factor on failure strength) were tested (see Table IV-A-5).

Some remarks can be made based on the experimental test results and are listed as follows:

1) Stacking sequence affects the strength of notched and unnotched specimens and in about the same proportions.
2) For center holes with large $\frac{a}{w}$, the average net cross-sectional failure stress is about equal to the failure stress of unnotched specimens (as was expected).
3) For quasi-isotropic lay-ups, different types of notches with the same nominal dimensions produced nearly equal strengths.
4) Different quasi-isotropic lay-ups, while they have the same stiffness behavior, have significantly different strengths.
5) For the unnotched specimens the Weibull distribution seemed to be a good model for failure probability, with a shape parameter around ten.
6) No significant specimen width effects were found. This indicates that, for widths of at least one inch, width is not a critical item and that edge effect coupling to stress concentration effects is not significant.

An interesting result from the finite element analysis is that the peak stress in the ±45° lay-ups occurs away from the notch boundary, in the interior of the specimen.

TABLE lV-A-1

PART ONE OF TEST PROGRAM: CENTER HOLES

Laminate	Notch Size a (in.)							
	0.0	0.030	0.065	0.125	0.250	0.375	0.500	0.750
$[90/\pm45/0]_s$	⊖[i]	NT[ii]	⊖	o[iii]	⊖	o	⊖	NT
$[\pm45/0/90]_s$	⊖	NT	⊖	o	⊖	o	⊖	NT
$[0/\pm45/90]_s$	⊖	⊖	⊖	o	⊖	o	⊖	⊖
$[0/\pm45]_s$	⊖	NT	⊖	o	⊖	o	⊖	NT
$[0_2/\pm45]_s$	⊖	⊖	⊖	o	⊖	o	⊖	⊖
$[0_4/\pm45]_s$	⊖	NT	⊖	o	⊖	o	⊖	NT
$[0/\pm15]_s$	⊖	NT	⊖	o	⊖	o	⊖	NT
$[0/\pm30]_s$	⊖	NT	⊖	o	⊖	o	⊖	NT
$[0/\pm75]_s$	⊖	NT	⊖	o	⊖	o	⊖	NT
$[0/\pm60]_s$	⊖	NT	⊖	o	⊖	o	⊖	NT
$[0/90]_{2s}$	⊖	NT	⊖	o	⊖	o	⊖	NT
$[\pm45]_{2s}$	⊖	NT	⊖	o	⊖	o	⊖	NT
$[90/\pm30]_{2s}$	⊖	NT	⊖	o	⊖	o	⊖	NT

[i] ⊖: 5 replicates already tested

[ii] NT: Not tested

[iii] o: 5 replicates scheduled for testing

TABLE IV-A-2

PART TWO OF TEST PROGRAM: ADDITIONAL SYMMETRIC NOTCH TYPES*

Notch Type	Notch Size a (in.) 0.250	0.500	0.750
Double Edge Crack	⊖[i]	⊖	⊖
Double Edge Semi-Hole	⊖	⊖	⊖
Shoulder	⊖	⊖	⊖

*Laminate: $[0/\pm45/90]_s$
$[0_2/\pm45]_s$

[i]⊖: Tested

TABLE IV-A-3

PART THREE OF TEST PROGRAM:
IRREGULAR STRESS FIELDS USING CENTER SLANT CRACKS AND SLOTS*

Slant Angle (θ)	Notch Size a (in.) 0.250	0.500	0.750
30°	⊖[i]	⊖	⊖
45°	⊖	⊖	⊖
60°	⊖	⊖	⊖
90°	⊖	⊖	⊖

*Laminate: $[0/\pm45/90]_s$
$[0_2/\pm45]_s$

[i]⊖: Tested

TABLE IV-A-4

PART FOUR OF TEST PROGRAM:
MANUFACTURING DRILL TOOL EFFECTS

	Notch Size a (in.)						
Laminate	0.030	0.060	0.125	0.250	0.375	0.500	0.750
$[0/\pm45/90]_s$	WT[i]	⊕[ii]	⊕	⊕	⊕	⊕	WT

[i] WT: Waiting to be tested

[ii] ⊕: Center hole drilled by carbide drill

TABLE IV-A-5

PART FIVE OF TEST PROGRAM: WIDTH EFFECTS

Notch Size a (in.)	0.25	0.50	0.75
Width w (in.)	0.9	1.8	2.7
Laminate: $[0/\pm45/90]_s$	⊖[i]	⊖	⊖

[i] ⊖: Tested

4. Plans for Upcoming Period

The testing program will be completed and the test results documented. Some shear test specimens may be included. Next, postprocessors for the computer analysis will be written and exercised to test the various proposed generalizations to the average stress criterion. Additionally, Weibull strength theory will be examined to see if it correlates with test results.

5. References

1. Waddoups, M. E., J. R. Eisenmann and B. E. Kaminski, "Macroscopic Fracture Mechanics of Advanced Composites Materials", Journal of Composite Materials, Vol. 5, 1971, p. 446.

2. Whitney, J. M. and R. J. Nuismer, "Stress Fracture Criteria for Laminated Composites Containing Stress Concentrations", Journal of Composite Materials, Vol. 8, 1974, p. 253.

IV-B IMPROVED BEAM THEORY FOR ANISOTROPIC MATERIALS

Senior Investigator: O. Bauchau

1. Introduction

Timoshenko beam theory is well-known by structural designers and is widely used as a first approximation in numerous structural applications. For solid cross-sectional beams made out of isotropic materials, this theory gives accurate predictions for aspect ratios $L/h \gtrsim 5$ (L is the span of the beam and h its height). Because it is based on the assumption that cross sections remain plane after deformation, the theory predicts a linear distribution of axial strains. However, additional axial strains are induced by warping incompatibilities generated either by specific loading or boundary conditions, or by the occurence of nonuniform torsion or bending.

The accuracy of Timoshenko beam theory has been shown to be rather poor in the case of thin-walled beams because of significant warping and shear lag effects and in the case of structures made out of highly anisotropic materials.

The purpose of this work is to investigate the behavior of thin-walled box beams made out of anisotropic materials.

2. Status

At the beginning of the reporting period the following tasks had been completed.

a. An analytical solution of the problem was worked out, based on the sole assumption that each cross section is infinitely rigid in its own plane but free to warp out-of-plane. This assumption has two important implications. First, the in-plane displacements of the cross sections are fully represented by three rigid body modes, and second, any applied transverse load only induces membrane stresses in the structure, namely, an axial stress flow, n, and a shear stress flow, q. For thin-walled beams, these two stress flows are uniform across the thickness of the wall, and the other stress components are assumed to be negligible.

b. A finite element solution of the problem was completed, based on the same assumptions outlined above. The results for the different approaches were found to be in close agreement.

3. Progress During Report Period

During the report period two tasks were completed. In the first task, the finite element solution was extended to allow the treatment of problems presented by structural couplings. When the axes of orthotropy of the material are not aligned with the axis of the beam, such structural couplings occur as extension-twisting, extension-bending or bending-twisting.

A specific example is described here to illustrate these results. Figure IV-B-1 depicts the thin-walled, rectangular

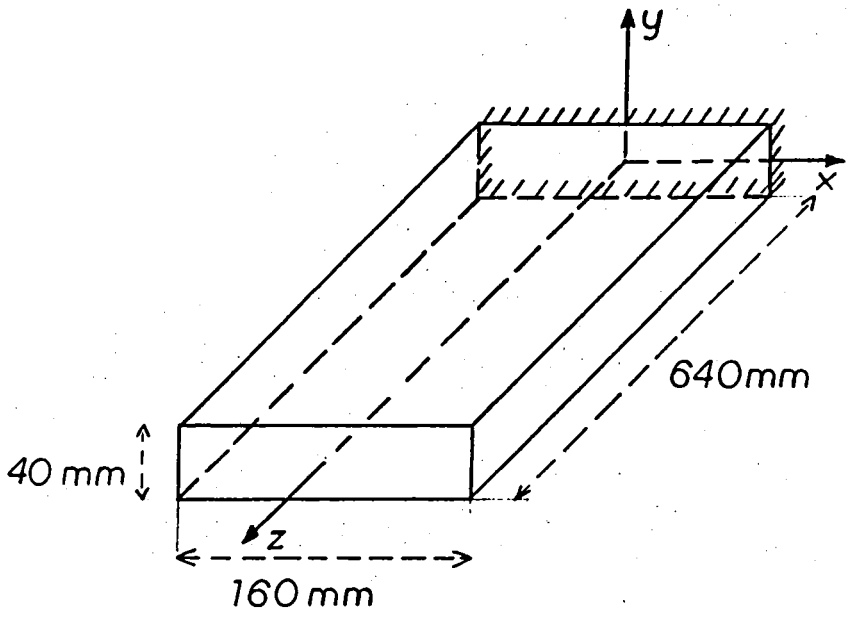

Figure IV-B-1. Geometry of the Structure.

cross-sectional beam that was analyzed. The axis of orthotropy of the upper laminate was oriented at fifteen degrees with respect to the axis of the beam, and the lower laminate's was oriented at minus fifteen degrees. The response of the structure was first analyzed under a uniform transverse load in the y direction. Figures IV-B-2 and 3 show the displacement, v, in the direction of the load and the twist, θ, respectively (note that this twist is due to the coupling effect). For each case, the results of Timoshenko beam theory (i.e., neglecting warping effects) were plotted for comparison. Due to warping deformations, the tip deflection of the beam increased by 12 percent and the tip twist increased by 78 percent.

A second case was analyzed where the structure was subjected to a uniformly distributed torque. Figures IV-B-4 and 5 show the twist, θ, and the transverse displacement, v, respectively (note that this displacement is due to the coupling effect). The Timoshenko solution was again plotted for comparison. Warping effect considerably increased the tip twist of the beam (12%) and the tip deflection (67%).

Two conclusions can be drawn from the analyses: a) an accurate modeling of the torsional behavior of anisotropic beams requires the consideration of warping effects, and b) the displacements resulting from structural coupling (i.e., twist under transverse load or transverse displacement under torque) are drastically influenced by warping deformations.

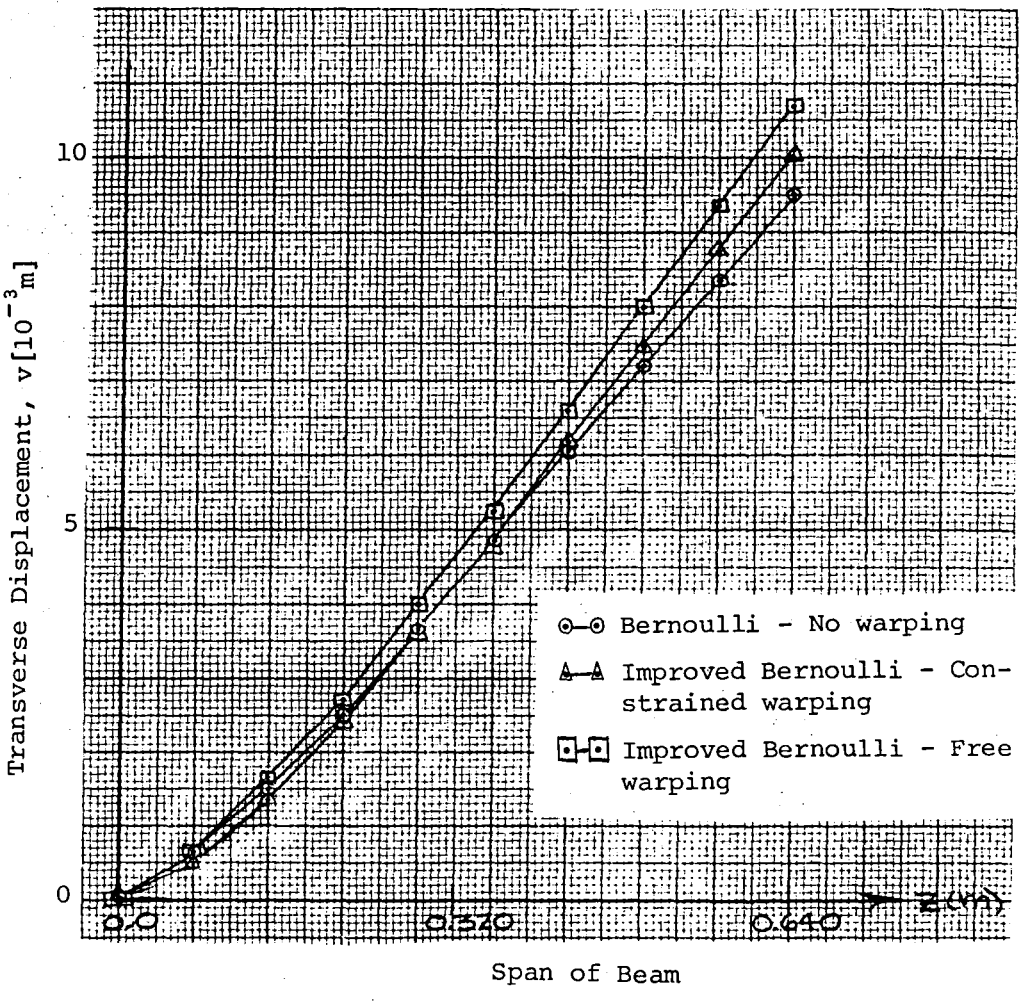

Figure IV-B-2. Transverse Displacement Along the Span of the Beam for the Uniform Load Case. (P_{oy} = 10,000 N/m)

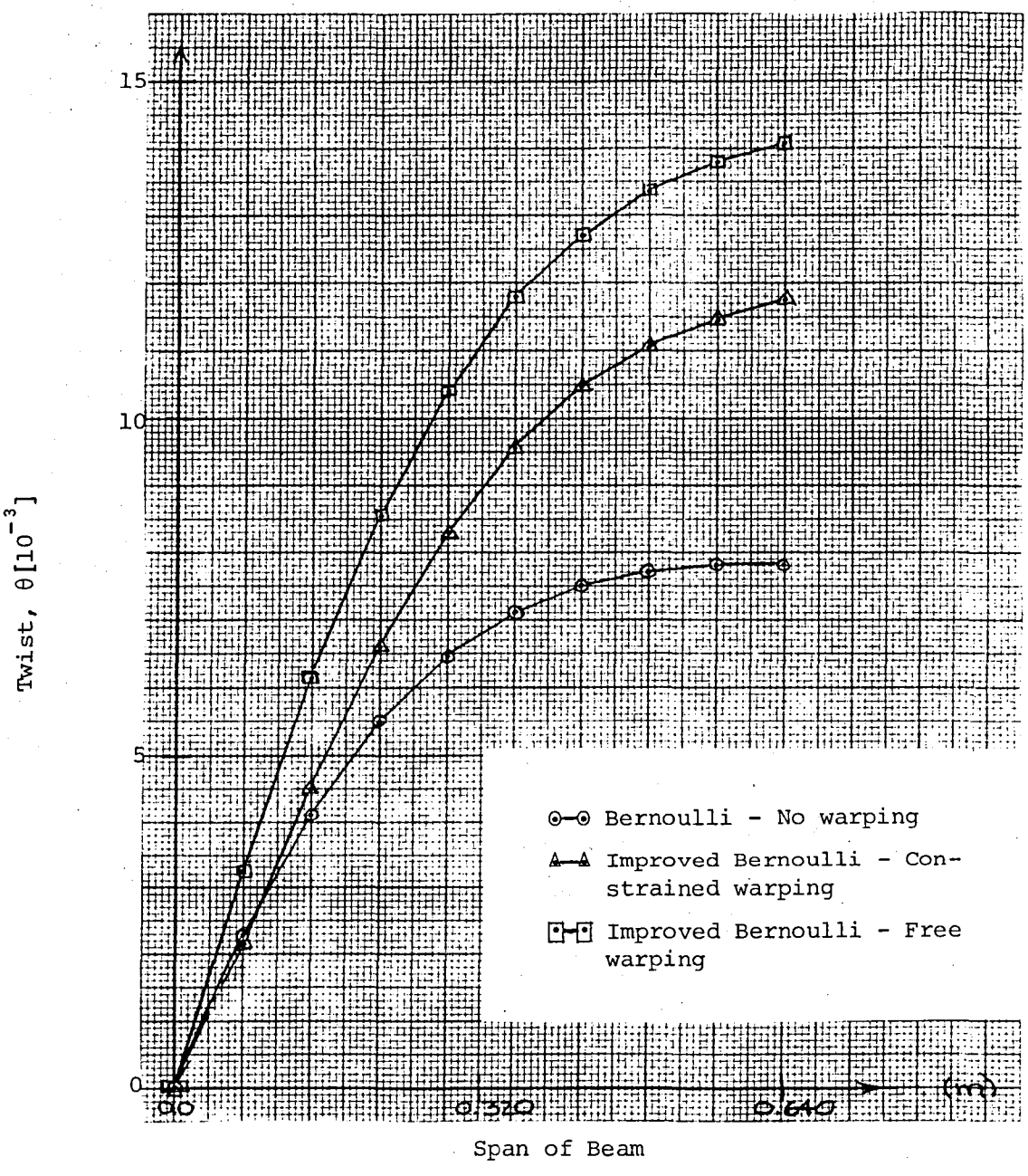

Figure IV-B-3. Twist Along the Span of the Beam for the Uniform Load Case. (P_{oy} = 10,000 N/m)

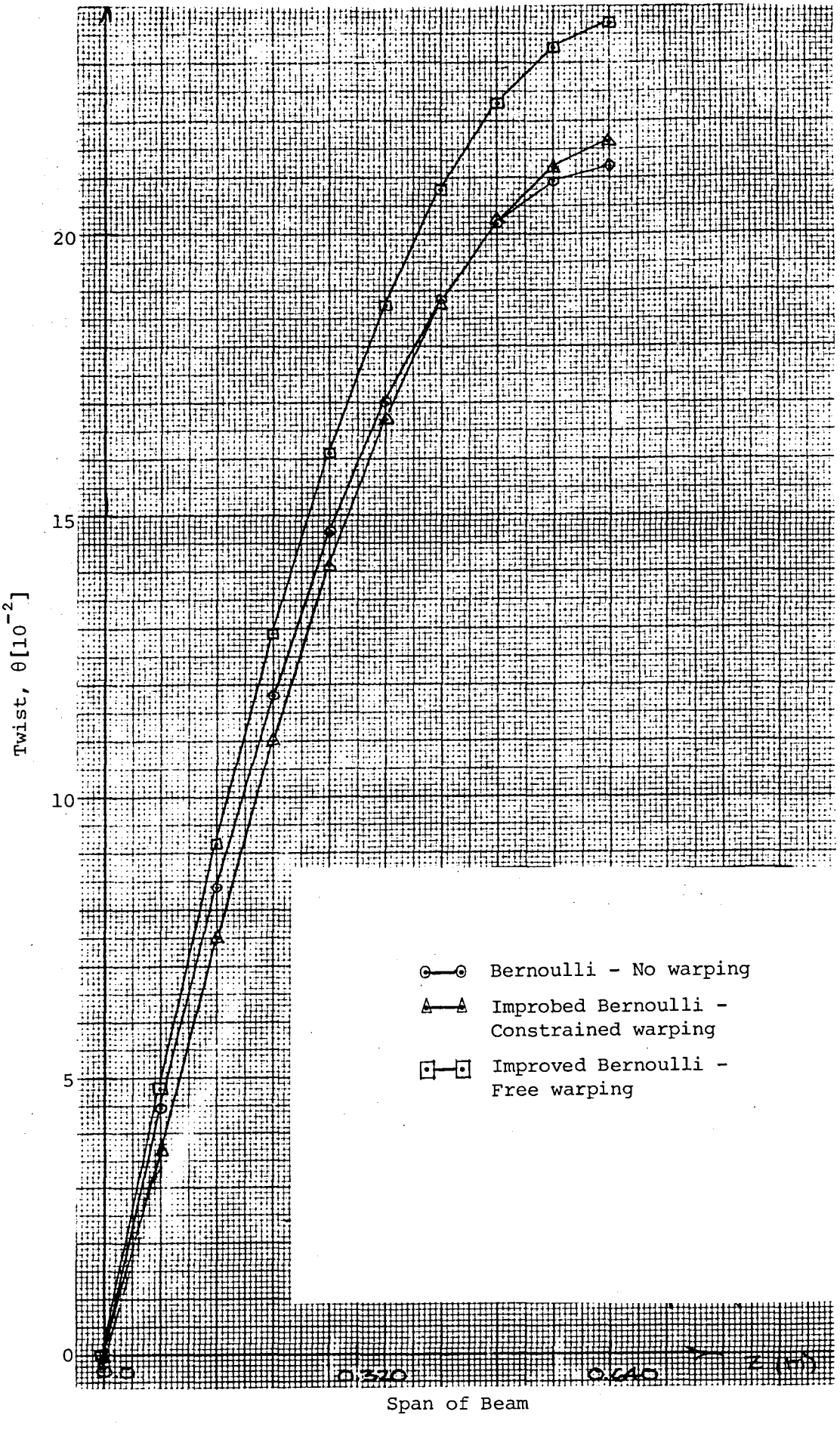

Figure IV-B-4. Twist Along the Span of the Beam for the Uniform Torsion Case. (M_o = 10,000 N)

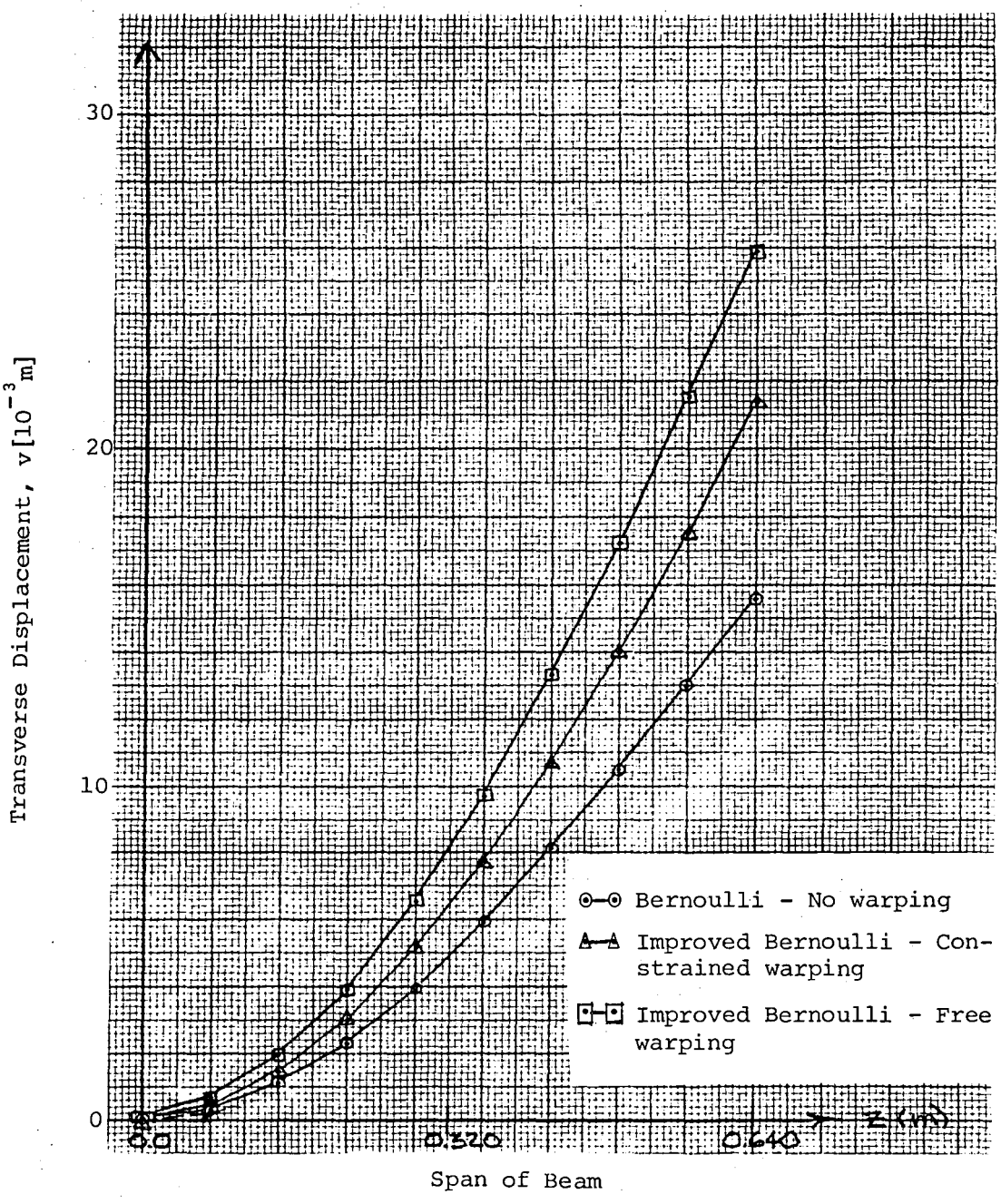

Figure IV-B-5. Transverse Displacement Along the Span of the Beam for the Uniform Torsion Case. (M_o = 10,000 N)

In the second task, an experimental program was initiated to assess the accuracy of the theory. The test specimens were thin-walled box beams with a rectangular cross section (see Figure IV-B-6). The upper and lower skins are graphite/epoxy laminates, and the webs are aluminum C-channels. The skins are bolted onto the webs to form the box beams. The beam was rigidly clamped at one end, while a concentrated transverse load or torque was applied at the other end. Two types of specimens were manufactured: First, the principal axis of orthotropy of the upper and lower skins was aligned with the axis of the beam so that no structural couplings were present, and second, the principal axis of orthotropy of the upper and lower skins was oriented at an angle with respect to the axis of the beam so that structural couplings were present.

The response of the beam was measured by means of the following instrumentation. Dial gages were used to measure the tip deflection and tip twist of the structure. Strain gages were placed near the root of the beam to measure the strain distribution across the upper skin. Axial gages, as well as rosette gages, were used so that both axial and shear strains were measured.

4. Plans for Upcoming Period

Effort will be concentrated on the completion of the testing program. First, an experimental verification of the

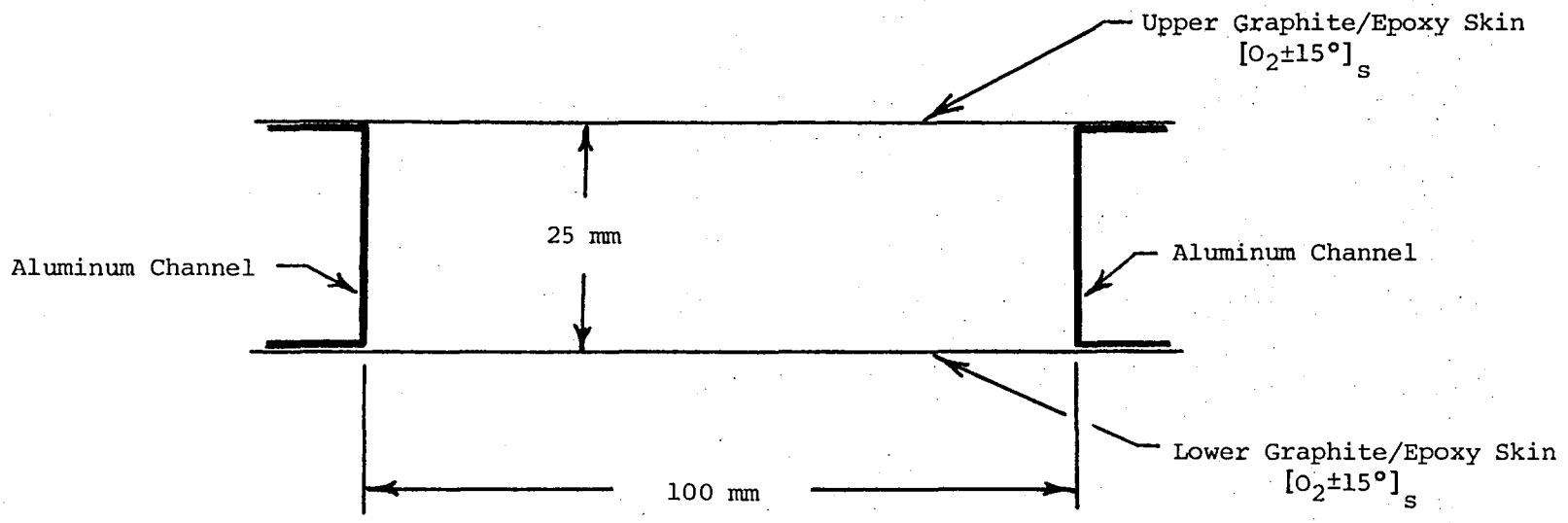

Figure IV-B-6. Cross Section of the Test Specimen.

warping theory will be sought by comparing measured deflections and strain distributions with the predicted ones.

Another point of interest will be the analysis of structural couplings. Various types (i.e., extension-twisting, and/or extension-bending and/or bending-twisting) and different strengths of structural couplings can be obtained by varying the configuration of the test specimen.

Finally, to complete the comparison between analytical approaches and experimental results, one specimen configuration will be modeled using 3-D plate finite elements.

5. Current Publications or Presentations by Professor Bauchau on this Subject

"A Beam Theory for Anisotropic Materials"
To be published in the Journal of Applied Mechanics.

PART V
PROCESSING SCIENCE AND TECHNOLOGY

V-A VARIATION OF RESIN PROPERTIES THROUGH THE THICKNESS OF CURED SAMPLES

Senior Investigator: B. Wunderlich

1. Introduction

A variation of resin properties through the thickness of a N,N,N'N'-tetraglycidyl-4,4'-diaminodiphenylmethane (TGDDM)/ 4,4'-diaminodiphenylsulfone (DDS) sample, a commonly used aerospace epoxy matrix, was initially proposed for study. The degree of cross-linking of TGDDM by DDS in a specimen was to be determined by quantitatively superposing the glass transition region (through the glass transition temperature, T_g, and the change in heat capacity at T_g, $\Delta C_p(T_g)$) of an uncharacterized material with that of a characterized reference. Different specimens of the same sample were to be analyzed to assess heterogeneity.

Curing of TGDDM/DDS systems involves two types of possible cross-linking reactions: epoxide-epoxide and epoxide-amine. Both types of cross-linking reactions proceed via a ring-opening reaction of the epoxide[1]*. For superposition to be possible, the epoxide-amine reaction should primarily determine the extent of cross-linking, in order that T_g be dependent upon the amount of hardener (DDS). Structures, descriptions and reactions of the components of the TGDDM/DDS system are given in [2].

*Numbers in brackets in this section refer to the references which are listed on page 108.

2. Status

Epoxy resins containing various amounts of hardener (DDS) were cured in a muffle furnace at 473°K for seven hours. The TGDDM manufacturer recommends this cure time[3]. T_g versus ratio-percent of hardener to epoxy resin was measured (see Figure V-A-1). A limit of approximately 475°K was rapidly reached at only two percent hardener, a 209°K increase over the uncured pure resin. Pure TGDDM was cured in a muffle furnace under the same conditions as the resin/hardener system. A T_g of 386°K was obtained, an increase of 121°K over the uncured pure resin or, approximately, half the increase seen for the samples with more than two percent hardener. In addition, Fourier Transform Infrared Spectroscopy (FT-IR) data evinces the appearance of ether groups for TGDDM/DDS systems cured at 450°K for 2.5 hours for 0 to 35 weight-percent DDS[1]. Thus, determining the extent of amine cross-linking for the TGDDM/DDS system by superposition of the glass transition temperature of a characterized reference sample under ordinary cure conditions is complicated due to a masking effect of the epoxide-epoxide curing reaction. Possible superpositon of $\Delta C_p(T_g)$ may allow differentiation between the different cures for the TGDDM/DDS system.

The glass transition region separates glassy and liquid behavior for amorphous materials. Therefore, the knowledge of the behavior and characteristics of the temperature regions below, higher and through which the glass transition

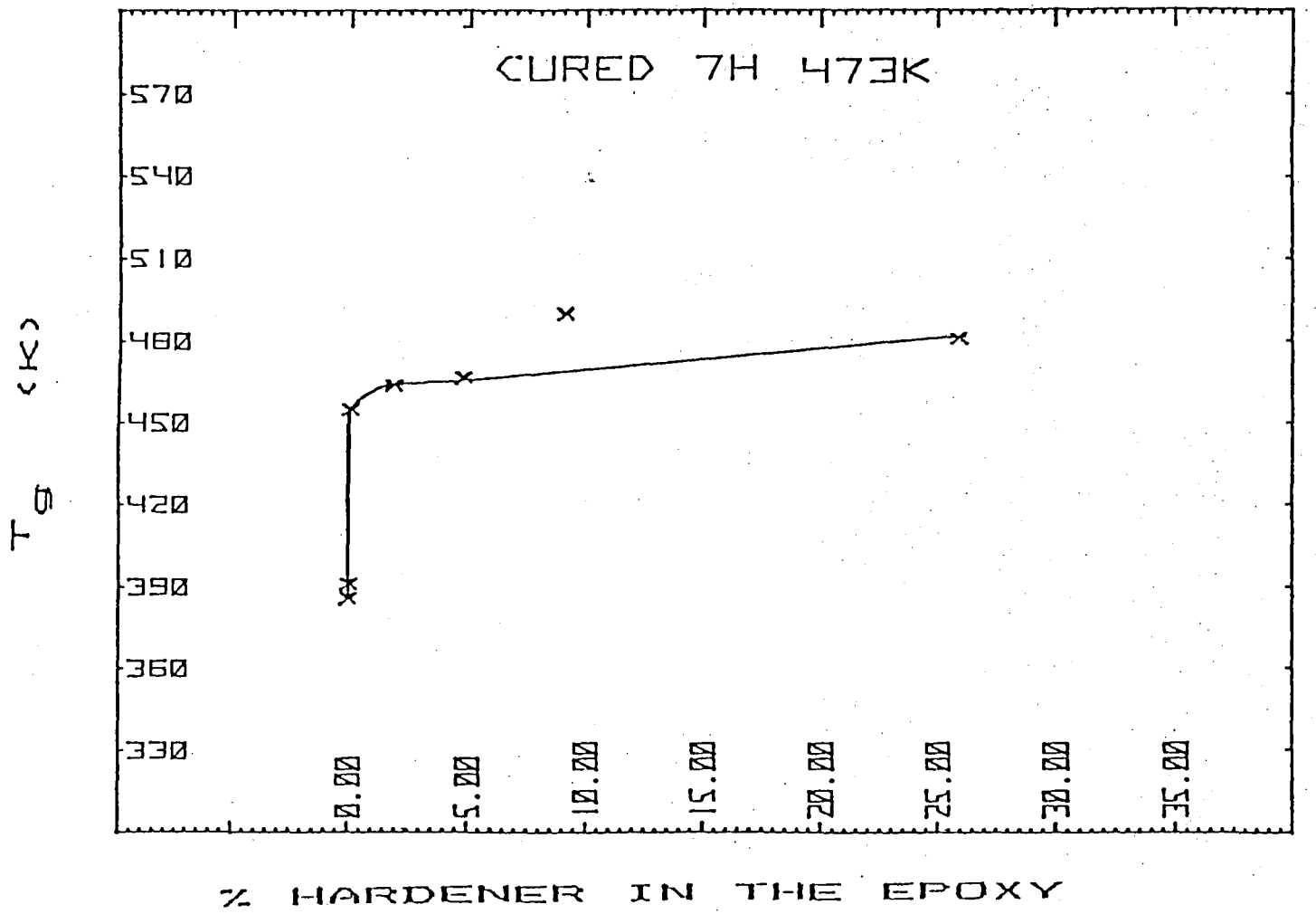

Figure V-A-1. Glass Transition Temperatures as a Function of Hardener Concentration. (Curing of TGDDM/DDS for 7 hours at 473°K in a Muffle Furnace)

occurs is critical, in the determination of application parameters for amorphous materials. Thermal properties within the glass transition region; the glass transition temperature, T_g; the change in heat capacity at T_g, $\Delta C_p(T_g)$; the heat capacity hysteresis, ΔH_h; the broadness of the inner and outer glass transition regions, ΔT_1 and ΔT_2 and, additionally, the heat capacity of the glass and melt have been studied for amorphous noncross-linked materials[4]. For amorphous, cross-linked materials few of such studies exist.

Initial work by Ueberreiter and Kanig in 1947 using volume-temperature measurements on cross-linked styrene-divinyl benzene (S-DVB) demonstrated that T_g increased with increasing cross-linking[5]. Further analysis of their data by Glans and Turner evinced a linear relationship between T_g and the cross-link density, except at low concentrations of the cross-linking agent[6]. Additionally, Glans and Turner found that ΔH_h decreases with increasing cross-linking[6]. However, very little further investigations of the interrelationships between T_g, ΔH_h and ΔT (ΔT_2 is more difficult to determine) with increasing cross-linking will be discussed in a report which is being prepared for publication. It is intended to provide the first step in a fuller understanding of thermal behavior as a function of cross-linking.

3. Progress During Report Period

a. Systems Investigated

As of this date we have investigated three cross-linked systems:

1) polysep, commercial cross-linked polystyrenes,
2) styrene, radically bulk polymerized, with divinyl benzene as cross-linking agent and
3) N, N,N',N'-tetraglycidyl-4,4"-diaminodiphenylmethane (TGDDM).

Polysep systems are commercial (Polysciences) S-DVB copolymer beads containing between 0.5 and 12 percent-by-weight DVB. The second type of S-DVB copolymer used was synthesized by bulk polymerization with 0.5 percent-by-weight of benzoyl peroxide. Finally, TGDDM, a tetrafunction epoxy, was thermally cured at 473°K, by itself, via a ring opening reaction.

b. Glass Transition Temperature

All systems were found to show an increase in T_g with an increase in cross-linking except for S-DVB samples at low concentrations of DVB (see Figures V-A-1, 2, 3). To investigate this trend at low concentrations of DVB further, various samples of bulk polymerized S-DVB, containing low concentrations of DVB, were made. A minimum two percent-by-weight of DVB was noted for both types of S-DVB samples investigated, and a lower maximum at 0.25 percent of DVB. Dissolution experiments in toluene demonstrated that the 0.25%-DVB sample was soluble, while samples with increased DVB content formed increasing amounts of insoluble gels.

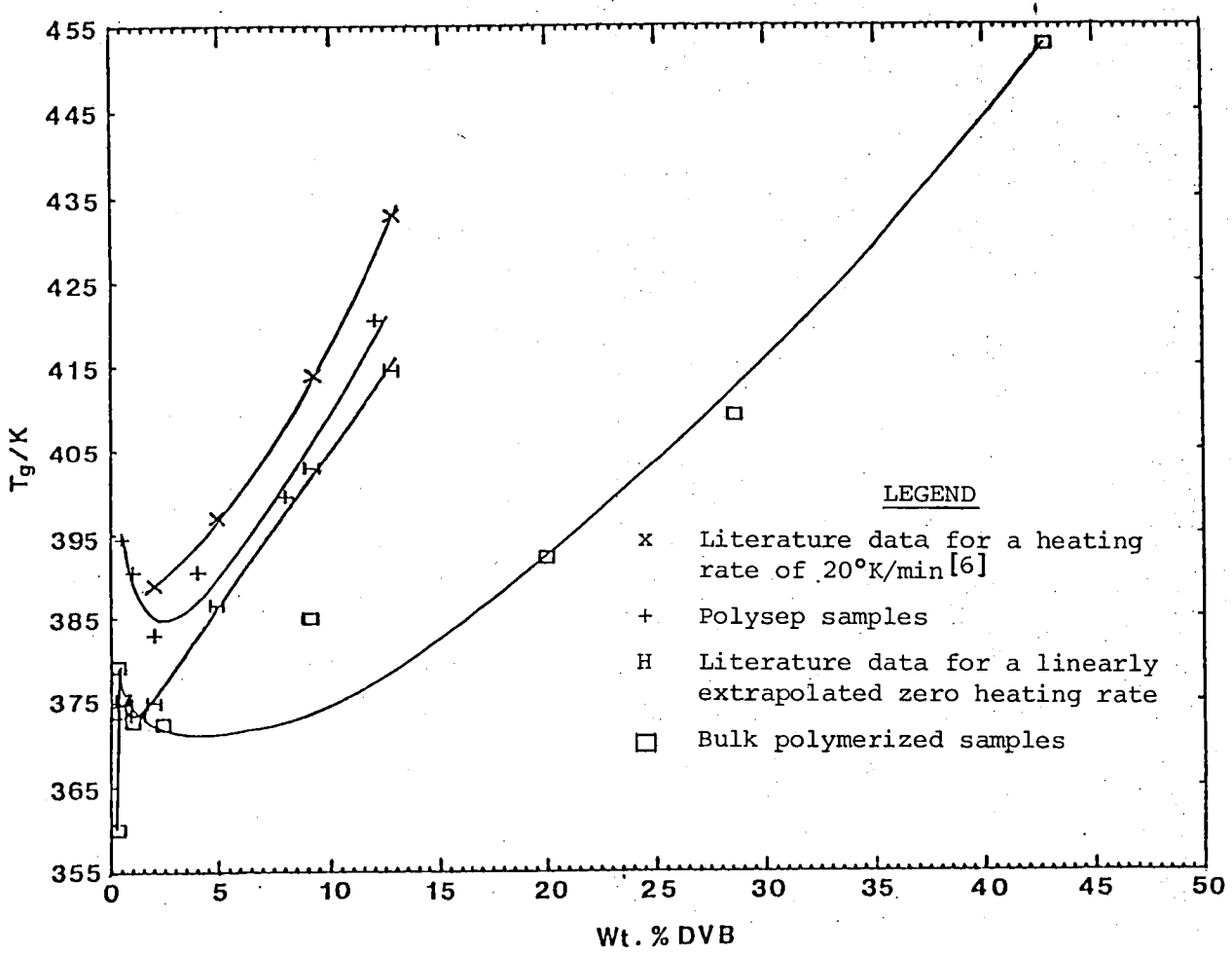

Figure V-A-2. S-DVB Glass Transition Temperatures as a Function of DVB Concentration.

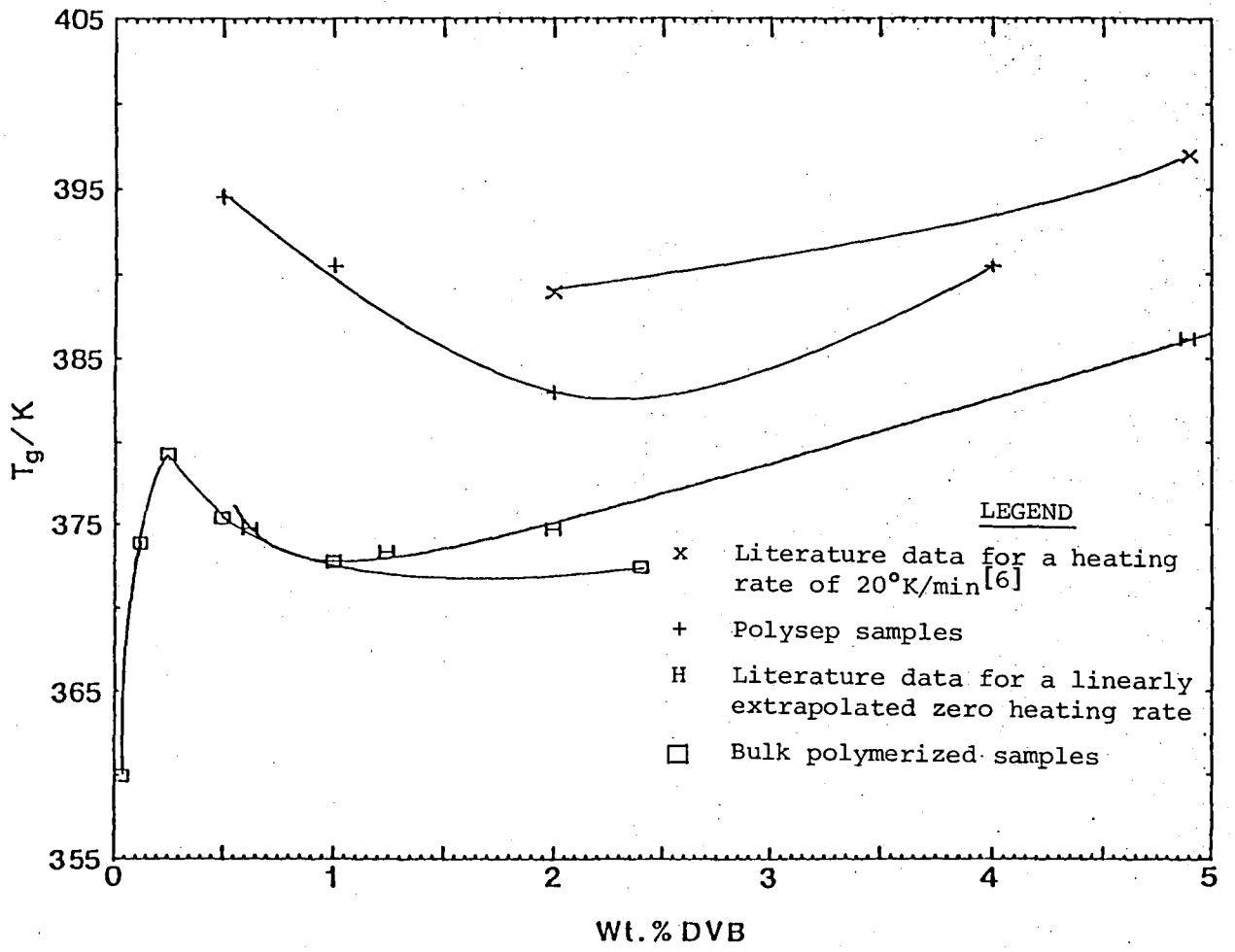

Figure V-A-3. Low Concentration Region of Figure V-A-2.

The behavior of the S-DVB samples studied may be explained in light of a heterogeneous structure. In general, many cross-linked materials are thought to consist of a heterogeneous network structure[7]. Electron microscopy studies of cross-linked materials have revealed nodular-like or colloidal-like structures of high cross-link density embedded in a matrix of lesser cross-linking[8,9,10]. Solomen et al.[11] have suggested that these "nodules" are formed early in the curing process, competing with the pure polymerization process, and then they grow. Competition between the formation of dispersed cross-link points in the matrix, nodule formation and growth may give rise to the "roller coaster" like relationship seen in Figure V-A-2. That is, highly dispersed cross-links may hold the matrix more rigidly than the more widely space "nodules" of approximately the same DVB content.

c. Heat Capacity Hysteresis Effect

The decrease of hysteresis with increasing cross-link density was investigated using S-DVB samples as a model system to obtain quantitative information on the structure of cross-linked materials. A relationship between the broadness of the glass transition region, ΔT_1, and the disappearance of the hysteresis peak, ΔH_h, was noted (see Figure V-A-4). Such relationships have been observed in block copolymers and blends, although reduction of the hysteresis has also been noted in semicrystalline and mesophase

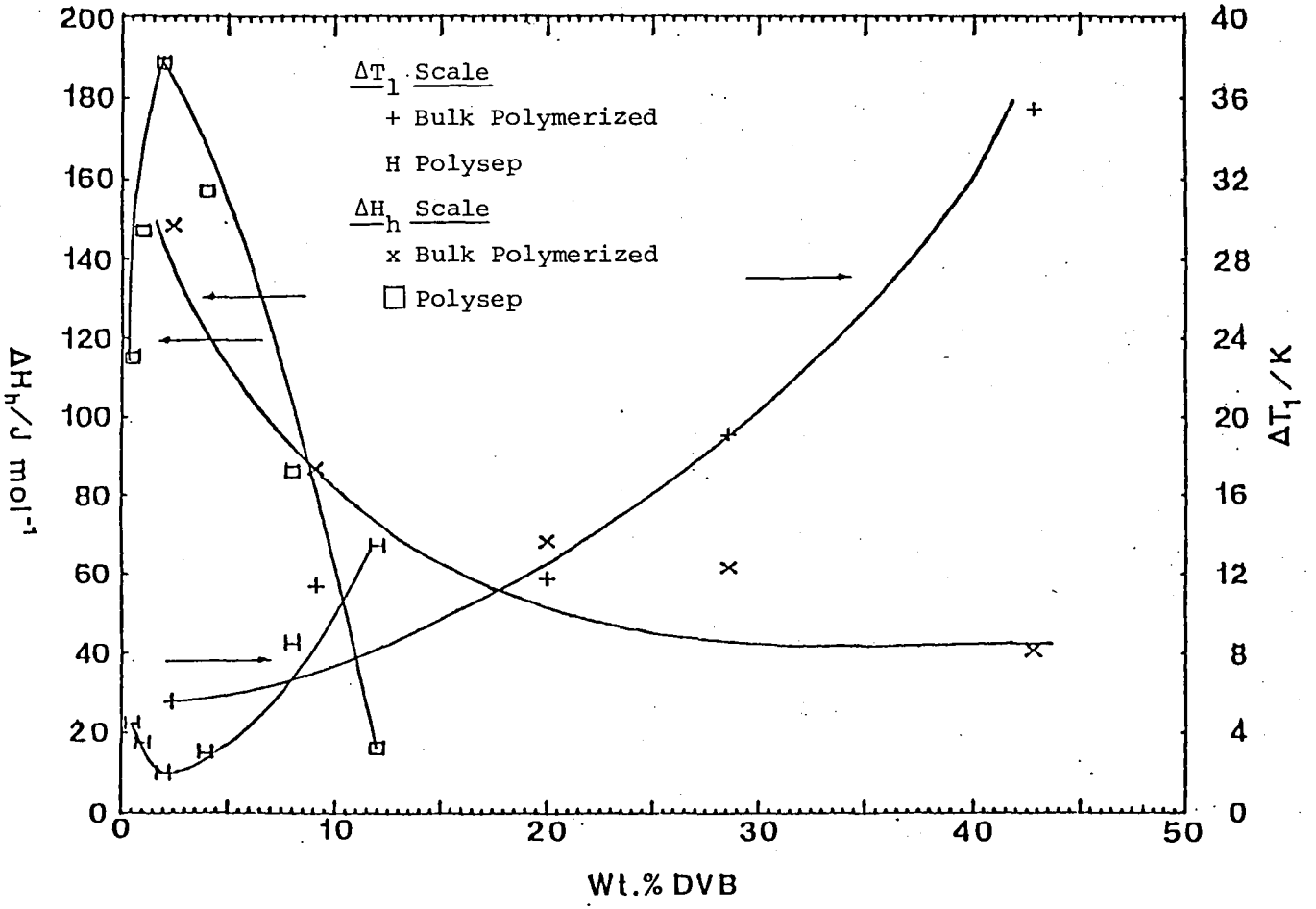

Figure V-A-4. Change of the Glass Transition Hysteresis Peak Area, ΔH_h, and the Breadth of the Glass Transition Region, ΔT_1, as a Function of Weight-Percent DVB for Cross-Linked Polystyrene. (Cooling rate 0.5 K°/min, heating rate 20°K/min, T_g determined by the $\frac{1}{2}\Delta C_p$ method from a 20°K/min cooling and heating)

materials[12,13,14,15]. A similar behavior was also found for TGDDM (see Figure V-A-5).

In general, with increasing cross-linking, T_g was found to increase, the glass transition to broaden and the hysteresis peak to be reduced. Exceptions to the previous generality occur at low concentrations of DVB (less than 2% by weight). Increasing feeds of DVB cause a decrease in T_g, and with this decrease, the glass transiton narrows and the hysteresis increases (see Figures V-A-2 and 4). Further feeds of DVB result in a reversion to the original trend. At very high degrees of cross-linking, TGDDM samples also show an exception to the previous generality. That is, with increasing cross-linking at high cross-link densities, even though T_g still increases, the glass transiton region begins to narrow, and the hysteresis peak increases again (see Figure V-A-5).

d. Broadening of the Glass Transition

The regions on both sides of the glass transition temperature were compared to assess the broadening present in cross-linked samples. Different comparisons were made on the T_1-T_B and T_E-T_2 regions and on the T_g-T_B and T_E-T_g regions. The type of broadening seen for both the S-DVB and TGDDM samples was symmetrical. That is, for the same thermal history, the differences between T_E-T_2 and T_1-T_B or T_E-T_g and T_g-T_B were approximately the same for each of the samples studied at various degrees of cross-linking.

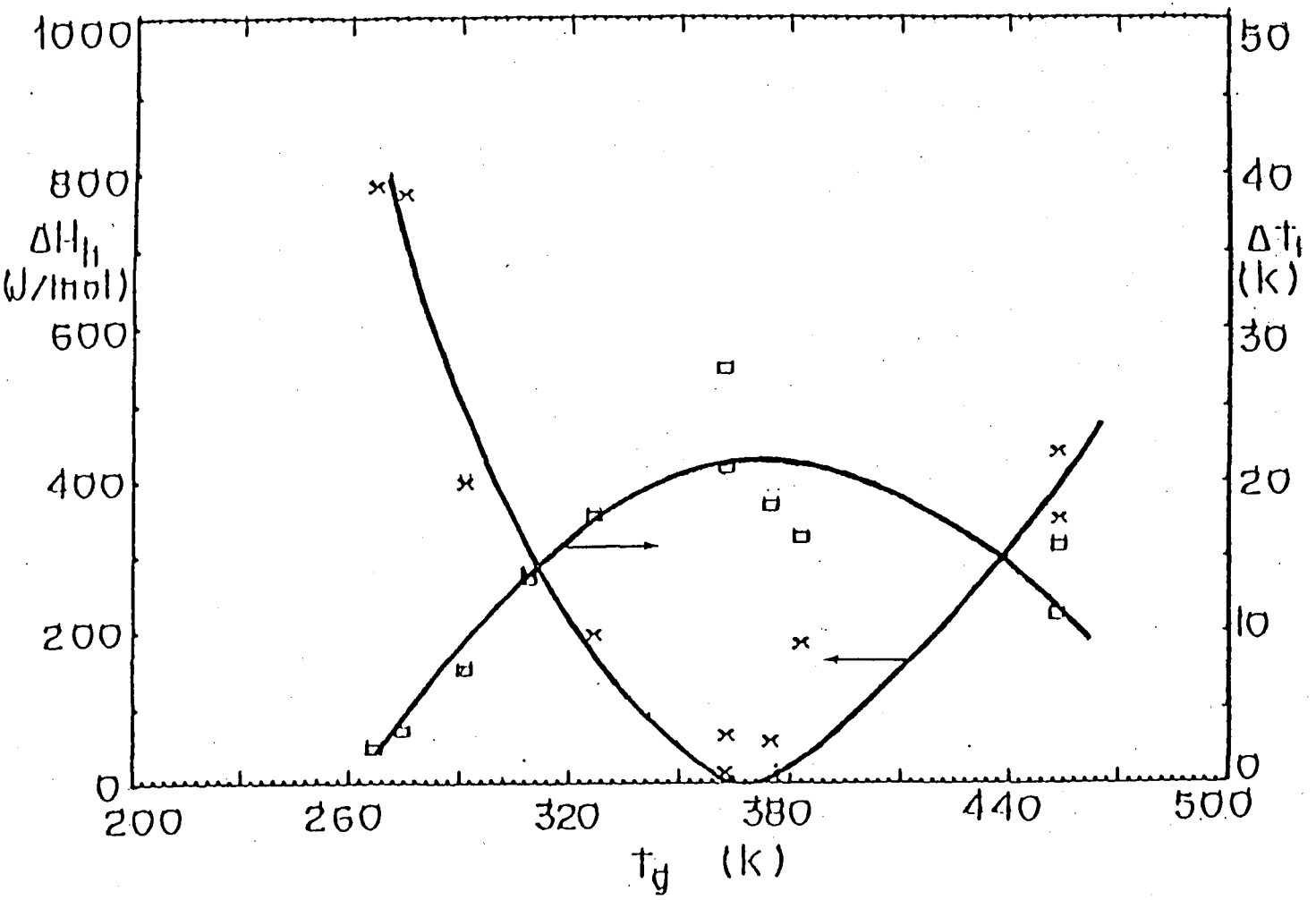

Figure V-A-5. Change of the Glass Transition Hysteresis Peak Area, ΔH_h, and the Breadth of the Glass Transition Region, ΔT_1, as a Function of Glass Transition Temperature T_g, for TGDDM Cured by Itself. (Cooling rate 0.5°K/min, heat rate 20°K/min, T_g determined by the $\frac{1}{2}\Delta C_p$ method from a 20°K/min cooling and heating)

Generally, the increasing breadth of the glass transition with increasing cross-linking may be due to the heterogeneous nature of the samples examined. Differing distances between cross-link points and "nodules" should give rise to inhomogeneities of differing rigidities. Since a more rigidly held polymeric chain has been related to increasing the T_g [16], one would expect, as the amount of cross-linking is increased, both the T_g and the distribution of inhomogeneities would increase and, hence, broaden the glass transition.

4. Plans for Upcoming Period

Heat capacity data and $\Delta C_p(T_g)$'s for cross-linked materials will be collected, evaluated and presented in our next report. Comparisons to noncross-linked materials will be made. A full interpretation of the many observed experimental facts is planned in parallel with the completion of the thesis of Mr. L. Judovits.

5. References

1. Mones, E. T. and R. J. Morgan, "The Cure Reactions, Network Structure and Mechanical Response of Diaminodiphenylsulfone Cured Tetraglycidyl-4,4'-Diaminodiphenylmethane Epoxies", Organic Coatings and Applied Polymer Science Proceedings, Vol. 51, 1984, p. 430.

2. Wunderlich, B., "Variation of Resin Properties Through the Thickness of Cured Samples", 46th Semi-Annual Progress Report, Composite Structural Materials, Rensselaer Polytechnic Institute, Troy, New York, August 1984, p. 141.

3. Ciba-Geigy, "Epoxy Resins and Hardeners", 1981.

4. Wunderlich, B., "A Computer Course on the Glass Transition", Department of Chemistry, Rensselaer Polytechnic Institute, Troy, NY, 1983.

5. Ueberreiter, K. and G. Kanig, "Second-Order Transitions and Mesh Distribution Functions of Cross-Linked Polystyrenes", J. Chem. Phys., Vol. 18, 1950, p. 399.

6. Glans, J. H. and D. T. Turner, "Glass Transition Elevation of Polystyrene by Cross-Links", Polymer, Vol. 22, 1981, p. 1540.

7. Morgan, R. J., J. E. O'Neal and D. B. Miller, "The Structure, Modes of Deformation and Failure, and Mechanical Properties of Diaminodiphenylsulfone-Cured Tetraglycidyl 4,4' Diaminodiphenylmethane Epoxy", J. Mat. Sci., Vol. 14, 1979, p. 109.

8. Racich, J. L. and H. A. Koutsky, "Nodular Structure in Epoxy Resins", J. Appl. Polym. Sci., Vol. 20, 1976, p. 211.

9. Erath, E. H. and M. Robinson, "Colloidal Particles in the Thermosetting Resins", J. Polym. Sci., C3, 1963, p. 65.

10. Doyle, M. J., A. F. Lewis and H.-M. Li, "Time-Temperature Cure Behavior of Epoxy Based Structural Adhesives", Polym. Eng. Sci., Vol. 19, 1979, p. 687.

11. Solomon, D. H., B. C. Loft and J. D. Swift, "Changes in the Reactivity of Functional Groups During Polyesterification: A New Approach to Polymerization in Fatty-Acid-Modified Polyesters (Alkyd Resins)", J. Appl. Polym. Sci., Vol. 11, 1967, p. 1593.

12. Gaur, U. and B. Wunderlich, "Study of Microphase Separation in Block Copolymers of Styrene and α-Methylstyrene in the Glass Transition Region Using Quantitative Thermal Analysis", Macromolecules, Vol. 13, 1980, p. 1618.

13. Lau, S.-f., J. Pathak and B. Wunderlich, "Study of Phase Separation in Blends of Polystyrene and Poly(α-Methylstyrene) in the Glass Transition Region Using Quantitative Thermal Analysis", Macromolecules, Vol. 15, 1982, p. 1278.

14. Menczel, J. and B. Wunderlich, "Heat Capacity Hysteresis of Semicrystalline Macromolecular Glasses", J. Polym. Sci.: Polym. Lett. Ed., Vol. 17, 1981, p. 17.

15. Menczel, J. and B. Wunderlich, "Phase Transitions in Mesophase Macromolecules, I. Novel Behavior in the Vitrification of Poly(ethylene Terephthalate-co-p-Oxybenzoate)", J. Polym. Sci.: Polym. Phys. Ed., Vol. 18, 1980, p. 1433.

16. Billmeyer, Jr., F. W., "Textbook of Polymer Science", 2nd Edition, Wiley-Interscience, NY, 1971.

V-B NUMERICAL ANALYSIS OF COMPOSITE PROCESSING

Senior Investigator: M. S. Shephard

1. Introduction

The complexities in both design and manufacture of composite materials demand the use of electronic computation to efficiently utilize these materials. Presently, the analyses performed in connection with the production of a new part are related to proper design for use in a service environment. In the future, there will be a tendency to perform more analyses associated with the manufacture of a product. The goal of this new project is to develop the appropriate analysis tools needed to describe the processing of continuous fiber resin matrix composites.

Composite properties are directly related to the quality of the lay-up that results from the fabrication process. This manufacturing process is a very complex operation that depends on many variables. An understanding of the fabrication processes will allow proper control of the manufacturing variables to obtain desirable qualities in the finished product. Numerical analysis provides a means for the solution of the complex governing differential equations that describe composite processing. The ability to solve the governing equations, coupled with the proper input data and comparison with experimental results, will lead to a better understanding of composite processing.

2. Status

The systems that are of interest for this initial work include both thermosetting and thermoplastic resins. Processing will take a slightly different general form for each of these types of matrices. However, there is a good deal of overlap in the types of numerical analyses that are required to understand the curing of thermoset composites and the processing of thermoplastic composites. For these analyses, there is a considerable amount of input data that is required, and at this point, it is assumed that the proper information will be available. A description of the processing and analyses of both thermosets and thermoplastics follows.

a. Thermosets

Springer and associates[1-4]* published several articles dealing with the analysis of the curing process for epoxy matrix composites. In their work, the curing process was examined with a series of one dimensional models for the study of heat generation and transfer, resin flow, void volume changes and thermal stresses. These analyses were carried out on a macromechanical level and are limited to a restricted geometry (infinite plate). Their work represents a good first step in the analysis of the curing process but is lacking in a few areas. However, the basic approach is valid and is described in the following paragraphs.

*Numbers in brackets in this section refer to the references which are listed on page 120.

There are several coupled processes that occur during curing that must be modelled. First, there is a thermal-chemical process that deals with heat transfer and the heat generated from the exotherm. This process is coupled to the flow process by convection heat transfer and by flow during the reaction or just flow with a nonuniform temperature distribution. The flow model is concerned with the flow of a viscous fluid through an orthotropically porous medium. In addition, a void model is necessary to account for the volatiles produced by the exotherm and the voids that are mechanically introduced. The void model is coupled to the thermo-chemical model by the temperature and the degree of completion of the reactions. Finally, there is a thermo-mechanical model to describe the thermal stress distributions that arise.

The thermal-chemical model is a heat transfer model that has terms relating to heat storage, heat generation and heat transfer. The heat stored in the material is related to the density and the heat capacity of the material. The heat generated is related to the degree of completion of the cross-linking chemical reactions. The heat transfer term accounts for heat flowing by means of conduction, convection and radiation.

The flow model requires data for the viscosity of the resin through the curing process. This model must account for flow of the resin in all directions both parallel and perpendicular to the fibers. The analysis of the flow model will result in knowledge of the resin content of the final lay-up.

The void model must account for the generation of gases during the exotherm. The volume of trapped gas has to be related to the amount of gas present, the viscosity of the resin and the pressure applied to the lay-up. Analysis of the void model will indicate the volume fraction of voids that results from the curing process.

The thermal-mechanical model relates the temperature and degree of cure to the residual thermal stresses. The model must account for the change in the resin's properties from those of a viscous fluid to those of a viscoelastic solid. This analysis must track the stresses through the change from viscous fluid to solid.

b. Thermoplastics

Similar analyses for thermoplastic composites have not been carried out. The processing of thermoplastics is more difficult because of the non-Newtonian behavior of the resin and the high temperatures and pressures required to obtain a viable engineering material. There are several methods for processing thermoplastic composites which are all characterized by the flow of the matrix material, or a solution of the matrix material, into dry fibers.

One method for forming thermoplastic composites begins by laying up alternate layers of thermoplastic film and graphite cloth[5]. Heat and pressure are then applied to complete the forming process. The lay-up is heated above the glass transition temperature of the resin in order to reduce the

viscosity. Pressure is then applied to generate the flow of the resin into dry fibers. A second processing step might be carried out from this point to form the thermoplastic composite into the desired shape with heat and pressure.

The thermal processing for thermoplastics is basically different from the curing process of a thermoset due to the absence of a chemical reaction. However, the energy equation includes a term for the heat of crystallization which is treated in the same manner during numerical analysis as the heat of reaction term. In addition, there is a possiblity for thermal expansion anisotropy in the resin and shear heating of the resin.

The flow process for thermoplastics is more complicated than the parallel process for thermosets for two reasons. The first is linked to thermal stresses caused by differences in thermal coefficients of expansion of the resin and fibers. These stresses must be tracked through the transition of the resin from a viscoelastic fluid to a viscoelastic solid. A second source of residual stresses is that associated with the dimensional change upon crystallization of the matrix.

3. Progress During Report Period

To obtain a feel for the type of numerical analyses that are going to be required for this project, a one-dimensional analysis code was implemented to solve the parabolic energy equation associated with the curing of a thermosetting

material. This analysis utilizes finite elements for the spatial domain and finite differences for the time domain.

The general macroscopic energy equation, neglecting kinetic energy, that is valid for both thermosets and thermoplastics is given by:

$$\frac{\rho D(CT)}{Dt} = \nabla \cdot [K] \nabla T + \dot{Q}(T,t)$$

where:
- ρ = the composites density
- t = time
- T = temperature
- C = the composites heat capacity
- $\dot{Q}$ = rate of heat energy due to internal sources or sinks
- $[K]$ = thermal conductivity matrix

and for cartesian coordinates

$$\frac{D(\ )}{Dt} = \frac{\partial(\ )}{\partial t} + u\frac{\partial(\ )}{\partial x} + v\frac{\partial(\ )}{\partial y} + w\frac{\partial(\ )}{\partial z}$$

$$\nabla = \left[\frac{\partial}{\partial x} \frac{\partial}{\partial y} \frac{\partial}{\partial z}\right]^T$$

$$\nabla T = \left[\frac{\partial T}{\partial x} \frac{\partial T}{\partial y} \frac{\partial T}{\partial z}\right]^T$$

The $\dot{Q}$ term is used to represent the heat of reaction, heat of crystallization or viscous heating.

Several assumptions are made in the solution of the energy equation for the curing of a thermoset composite; the composite being cured is a thin infinite plate, convected heat transfer terms are negligible, and there are no viscous losses. For this initial analysis, the coefficients in the

equation are taken to be constant for position, time and temperature. With these assumptions, the energy equation reduces to the nonlinear parabolic equation given by:

$$\rho C\frac{\partial T}{\partial t} = k\frac{\partial^2 T}{\partial z^2} + Q(T,t)$$

The analysis code was written using linear finite elements to discretize the thickness of the laminate. A forward difference scheme is used for time integration. This scheme was chosen due to its simplicity in handling the nonlinearity associated with the heat of reaction term and its ease of implementation. The program accepts Dirichlet boundary conditions that are functions of time.

The program was tested in two ways. First, with an example that did not contain any internal heat sources and thus had an exact analytic solution, and second, with an example that included an expression for the heat of reaction and did not have an exact solution. For the purposes of testing, the heat of reaction term was represented by two uncoupled Arrhenius rate equations. Two equations were used to represent the two major reactions that occur when curing Hercules 3501-6 resin[2]. The coefficients of the rate equations were chosen such that good agreement was obtained with the data of Reference [2]. The boundary conditions used for this problem are the same as those used in References [3] and [4] and consist of a ramp temperature increase from room temperature to 177°C

in 60 minutes. The analysis for this problem yielded solutions for the temperature and degree of completion of the reactions as functions of position and time. Figure V-B-1 shows the temperature as a function of the thickness at a particular instant of time. The temperature in the center of the laminate is higher than that at the boundaries due to the exotherm. This example was used to demonstrate that the code was working properly and not necessarily to depict reality. In order to obtain realistic results, a more accurate description of the kinetics of the reaction is required. Inclusion of an improved reaction model will only require minor code modifications.

4. Plans for Upcoming Period

The one dimensional solution of the energy equation for thermosets will be expanded to incorporate all sources of nonlinearity. The coefficients will be allowed to vary with position in the laminate, degree of cure and temperature. The literature will be examined for experimental results that can be used to test this model and determine the importance of these terms.

The finite element code ABAQUS can be used to test the need for analysis of the energy equation with constant coefficients in more than one dimension. ABAQUS has solid and shell heat transfer elements that can handle the heat of reaction with user supplied subroutines.

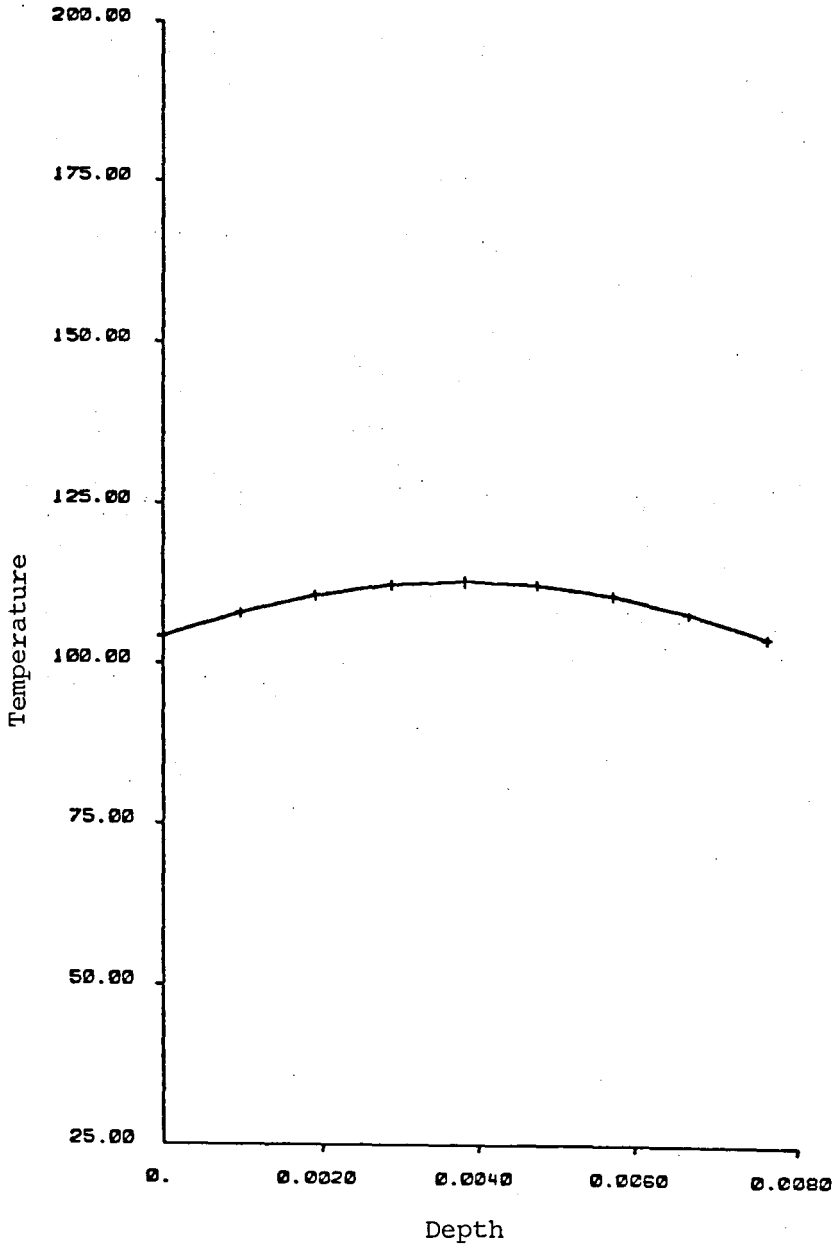

Figure V-B-1. Temperature Profile Through Thickness.

Solution of the flow equation will begin by finding the constitutive relations necessary to capture the important features of the non-Newtonian behavior of the candidate polymeric matrices.

5. References

1. Springer, G. S., "Resin Flow During the Cure of Fiber Reinforced Composites", Journal of Composite Materials, Vol. 16, September 1982, p. 400.

2. Lee, W. I., A. C. Loos and G. S. Springer, "Heat of Reaction, Degree of Cure and Viscosity of Hercules 3501-6 Resin", Journal of Composite Materials, Vol. 16, November 1982, p. 510.

3. Loos, A. C. and G. S. Springer, "Curing of Epoxy Matrix Composites", Journal of Composite Materials, Vol. 17, March 1983, p. 135.

4. Loos, A. C., "Curing of Graphite/Epoxy Composites", Ph.D. Thesis, University of Michigan, 1982.

5. Kim, R., W. Click, J. Hartness, M. Koenig, M. Rich and S. Soni, "Improved Materials for Composite and Adhesive Joints", AFWAL-TR-82-4182.

V-C HEAT TREATMENT OF METAL MATRIX COMPOSITES

Senior Investigator: N. S. Stoloff

1. Introduction

During this report period a new program on metal matrix composites produced by directional solidification was begun. The objective of this work is to utilize postsolidification heat treatments to improve the mechanical properties of carbide-reinforced eutectic composites. The alloy system chosen for study is Fe-Mn-Cr-C, which can be directionally solidified at unusually high rates (to 25 cm/hr) and still maintain its composite structure. A further advantage of this system is that in the as-solidified condition it is one of the strongest iron-base alloys known; its strength at elevated temperatures is comparable to that of iron-nickel and cobalt-base superalloys* (see Figure IV-C-1). As such it is a face centered cubic Fe-Mn-Cr solid solution, and the fibers are Cr_7C_3.

The specific properties to be measured as a function of postsolidification heat treatment are tensile strength and fatigue resistance, in both longitudinal and transverse orientations.

---

*Lemkey, F. D., E. R. Thompson, J. C. Schuster and H. Nowotny, "In Situ Composites IV", F. D. Lemkey, H. E. Cline, M. McLean, eds., North Holland, NY, 1982, p. 31.

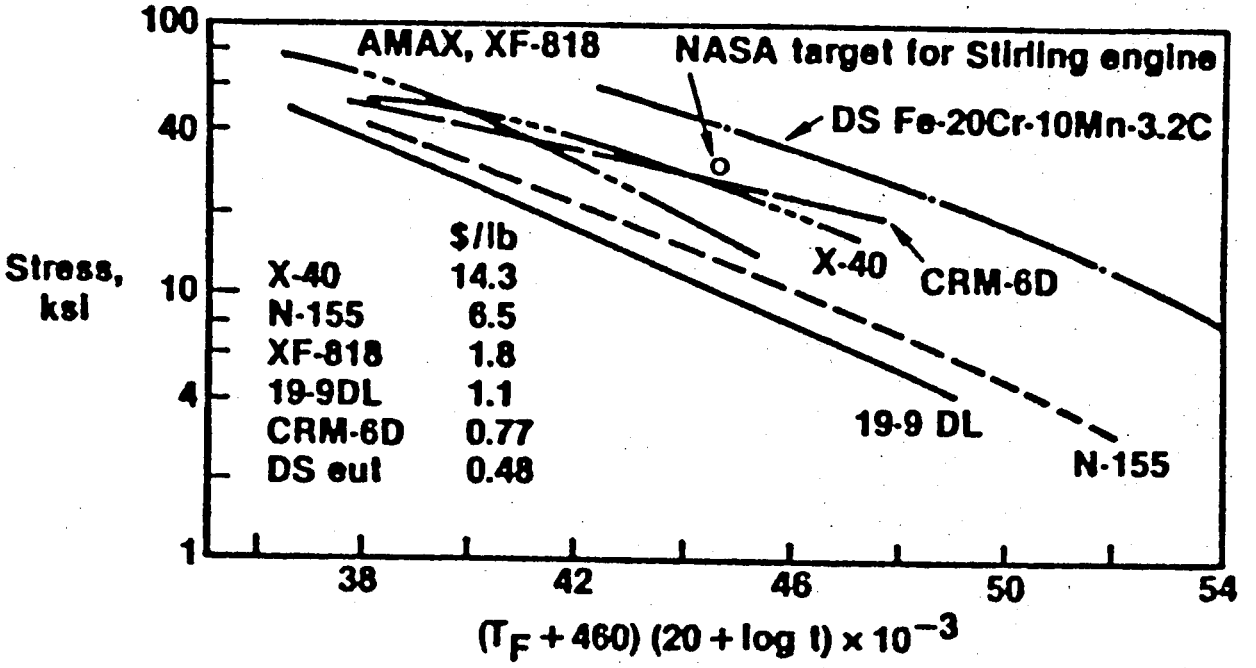

Figure V-C-1. Fe and Co Alloys Designed for High Temperature Usage.[1]

2. Progress During Report Period

Immediately upon commencing this work, a directionally solidified ingot of Fe-20%Cr-10Mn-3.4C was obtained from Dr. Frank Lemkey of United Technologies Research Center. This material had been solidified at 25 cm/hr.

Exploratory heat treatments to develop increased strength and hardness were carried out. All treatments consisted of a high temperature solution anneal, followed by a low temperature age. Hardness versus aging time was measured for each heat treatment. Optimum hardness was obtained by solutioning the alloy at 1170C°, followed by again at 850°C for eight hours. The results of that experiment are shown in Figure V-C-2. The microstructures before and after aging are shown in Figures V-C-3a and 3b, respectively. Aging appears to have developed relatively fine carbides dispersed in the matrix between the massive carbide fibers.

Subsequently, small compression specimens, 3/16-inch diameter by 3/8-inch height were machined from the as-DS rod; half of these were heat treated to peak hardness. Initial testing of the as-DS material revealed a yield strength near 270 ksi. The load required to deform this sample was so high that new samples of smaller diameter need to be machined in order to measure tensile properties of aged material.

A second alloy, Fe-30Cr-3C, solified at 25 cm/hr, has recently been received from Dr. Lemkey.

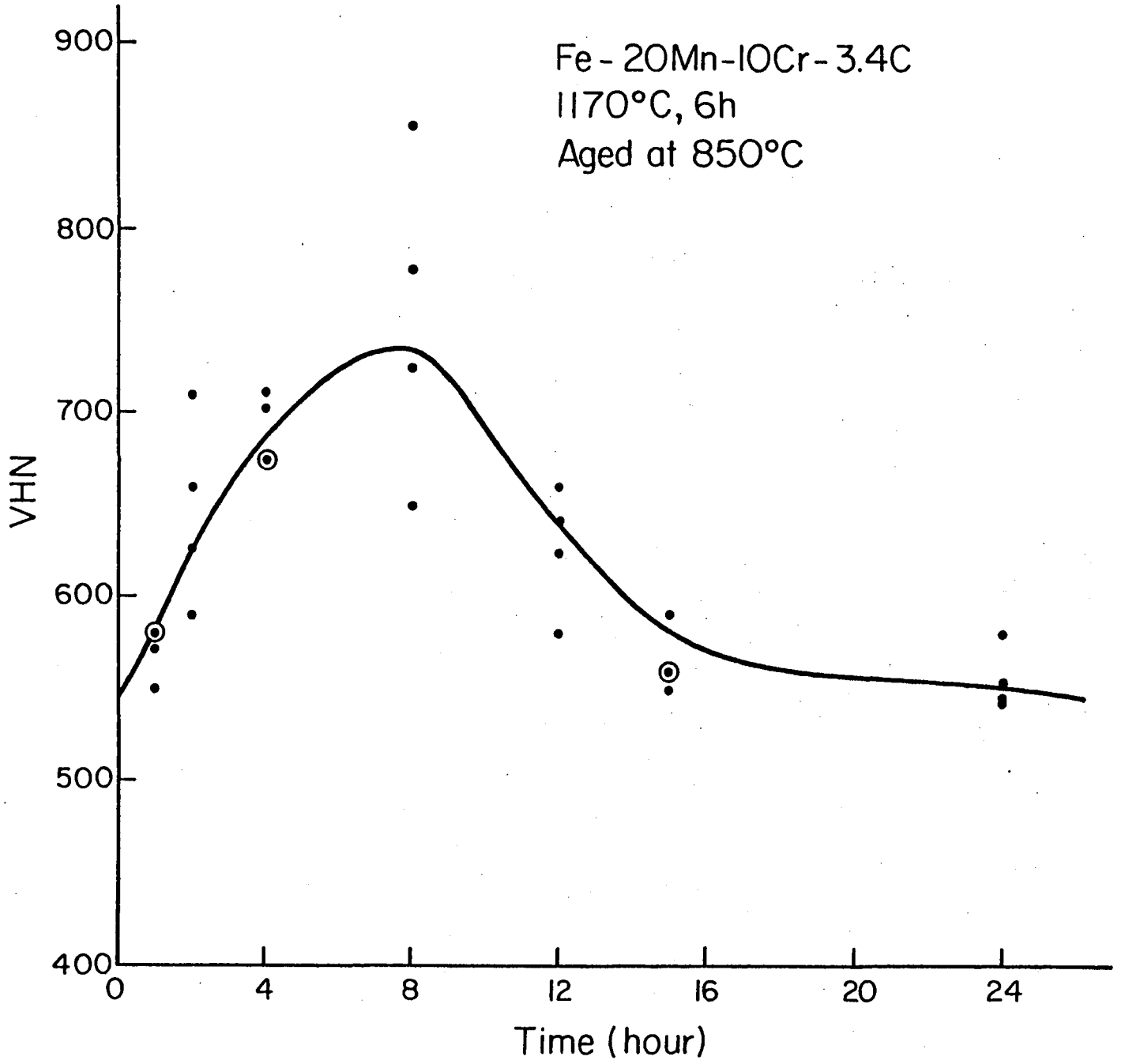

Figure V-C-2. Hardness as a Function of Aging Time for the Test Specimen.

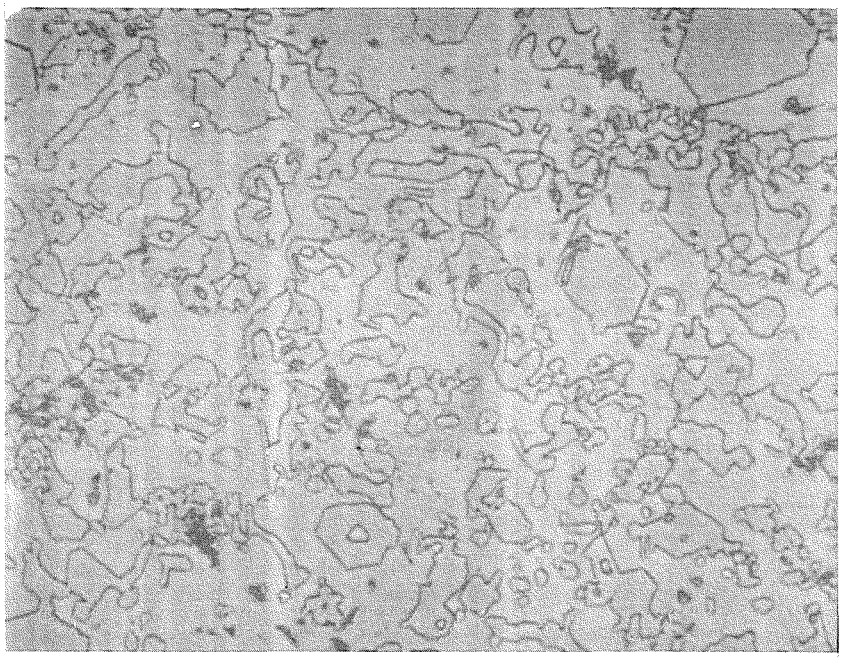

a) As-Received, x 500

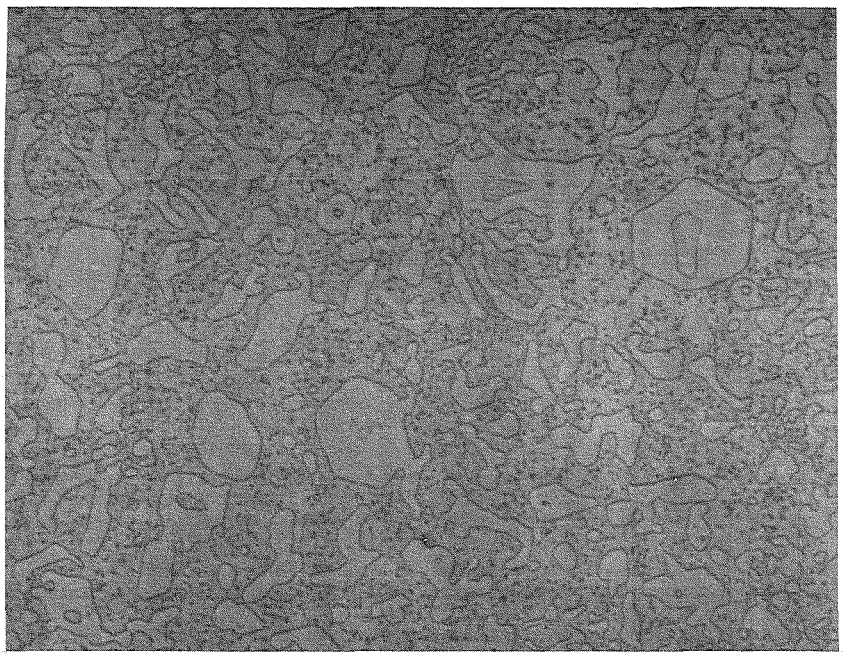

b) 1170°C for 6h, Aged 850°C for 24h, x 1000

Fe-20Mn-10Cr-3.4C

Figure V-C-3. Microstructure of Test Specimen Before and After Aging.

3. Plans for Upcoming Period

New compression samples are to be machined so that tests at both 25°C and at temperatures to 850°C can be conducted. These tests will serve as the basis for later tensile and fatigue studies on larger ingots of this alloy.

The second ingot, Fe-30Cr-3C, will be examined for optimum heat treatment response and then prepared for compression testing as described above.

4. Current Publications or Presentations by Professor Stoloff on this Subject

"Eutectic Composites for High Temperature Applications"

To be presented at the Joint U.S./Japan Seminar on Superalloys, Mt. Fuji, Japan, December 7-11, 1984.

"Current Status and Prospects of Eutectic Composite Superalloys"

To be presented at the Superalloy Seminar, Chung Shan Institute of Science and Technology, Lung-Tan, Taiwan, December 17-18, 1984,

V-D INITIAL SAILPLANE PROJECT: THE RP-1

Senior Investigators: F. P. Bundy
R. J. Diefendorf
H. Hagerup

During this reporting period the RP-1 glider has been stored on the balcony of the Composite Materials Shop Area in the Jonsson Engineering Center under ambient conditions of temperature and humidity.

The glider was assembled inverted and given its "annual" static strength test on November 15, 1984 as a simple bending wing loading up to over 4 G's, in the same manner as in previous years. The deflections at the wing tips due to the staged wing loadings are compared, for the four years of testing, in Table V-D-1.

TABLE V-D-1
ANNUAL STATIC STRENGTH TESTS FOR THE RP-1

Load (lbs/wing)	Wing Tip Deflection (cm) 1984	1983	1982	1981
0	0	0	0	0
150	5.72	5.48	5.8	5.7
300	11.45	10.87	11.7	11.3
430	15.17	14.50	15.4	15.5
550	18.15	17.26	18.4	18.1
590	18.56	17.72	--	--
550	18.22	17.40		
430	15.49	14.72		
300	11.83	11.20		
150	6.18	5.80		
0	.40	.25		

Although an attempt was made to make the test setup the same for each year, there were some minor differences in the supporting system which could account for the variations noted in the table for the same wing loadings. The overall conclusion is that the airframe strength and rigidity are not degrading with time, and that the structure is airworthy.

V-E SECOND SAILPLANE PROJECT: THE RP-2

Senior Investigators: F. P. Bundy
R. J. Diefendorf
H. Hagerup

1. Status

At the last report period the air frame with the rebuilt wings and redesigned and rebuilt wing beam linkage had been tested to over +6 G's in simple bending and to a negative torque of 7000 pounds with completely acceptable results, except for some forward bending of the wing which caused about a 3/16-inch pullout of the aft wing pins from the sockets in the fuselage. Also, it was reported that a design had been developed which would provide tension linkage between the aft pin areas of the wings and prevent pullout of the aft pins during heavy loading, and that a full size model of this tension linkage had been constructed and force-tested.

2. Progress During Report Period

During the current report period the aft wing tension linkage system was built into the wings and fuselage. After the installation, the air frame was assembled inverted and put through the regular +6-G sand bag loading test, as before. This was the third +6-G loading test to which the rebuilt wings and wing beam linkage had been subjected. It behaved very satisfactorily, including negligible pull out of the aft wing pins. On the basis of the static strength

and deflection tests, the wing/fuselage assembly is capable of any aerodynamic loading within conditions of the flight envelope for the aircraft.

The towhook/fuselage structure was force-tested to the FAA standards of 2 G's in directions ranging from 30-degrees up, 75-degrees down and 30-degrees sidewards. The RP-2 structure held up satisfactorily, and the towhook release worked under those specified conditions of loading.

The FAA-specified static strength tests of the empennage/fuselage structure were done and passed satisfactorily; likewise for the landing gear/fuselage structure.

After all the above-mentioned major strength tests were accomplished, work proceeded on fabrication of the foredeck and rudder pedal assembly, fitting and mounting arrangements for the fuselage skins and a control stick trim lever assembly.

3. Plans for Upcoming Period

During the next two reporting periods it appears that the glider can be completed and made ready for flight testing. The work remaining is mainly the finishing of the fuselage shell, cockpit rim, canopy rim frame instrument panel and painting.

4. Current Publications or Presentations by Professor Bundy on this Subject

"Composite Materials, Engineering and Gliders at RPI"
Published in 1983-1984 Hangar Flying, by invitation of the editor of the Flying Engineers

PART VI
TECHNICAL INTERCHANGE

Technical meetings, both on- and off-campus, provide for the interchange of technical information. In order to assure that a Rensselaer faculty/staff member can participate, a central listing of upcoming meetings is compiled, maintained and distributed on a quarterly basis. The calender for this reporting period is shown in Table VI-1. Table VI-2 shows the meetings attended by RPI composites program faculty/staff/students during the reporting period. Some on-campus meetings, with special speakers particularly relevant to composites, are listed in Table VI-3. A list of composites-related visits to relevant organizations, attended by RPI faculty/staff/students, along with the purpose of each visit is presented in Table VI-4.

The diversity of the research conducted within this program has increased over the last several years. To insure information transfer, once-a-week luncheon programs have been held among the faculty and graduate students involved (listed in Part VII. Personnel - of this report). These meetings are held during the academic year and are known as "Brown Bag Lunches" (BBL's), since attendees bring their own. Each BBL allows an opportunity for graduate students and faculty to briefly present plans for, problems encountered in and recent results from their individual projects. These seminars also are occasions for short reports on the content of off-campus meetings attended by any of the faculty/staff participants (see Tables VI-2 and VI-4) and for brief administrative

TABLE VI-1

CALENDAR OF COMPOSITES-RELATED MEETINGS

(April 30, 1984 through September 30, 1984)

5/1-4	AIAA Annual Meeting and Technology Display, Washington, DC. Sponsored by AIAA.
5/14-16	25th Structures, Structural Dynamics and Materials Conference, Palm Springs, CA. Sponsored by AIAA/ASME/SAE.
5/16-18	AHS Annual Forum and Technology Display, Washington, DC. Sponsored by AHS.
5/29-30	USAF Aeronautical Systems Division Advisory Group Meeting, Dayton, OH. Sponsored by USAF.
6/10-15	5th International Conference on Experimental Mechanics, Montreal, Canada. Sponsored by SESA/BSSM.
6/25-29	Composites and Paper Physics Technology Interchange, Stockholm, Sweden. Sponsored by NSF.
7/2-6	Carbon 84 Conference, Bordeaux, France. Sponsored by the University of Bordeaux.
7/4-5	Conference on Materials in Engineering, Solihull, England. Sponsored by PRI.
7/8-14	1st Gordon Conference on Liquid Crystals, New London, NH. Sponsored by Gordon Conferences.
7/11-13	JSPE International Symposium on Design and Synthesis, Tokyo, Japan. Sponsored by JSPE.
7/16-20	10th International Liquid Crystal Conference, York, England. Sponsored by the University of York.
7/19-20	Materials Research Council Meeting, La Jolla, CA. Sponsored by DARPA and MRC.
7/23-27	Siggraph '84, Advanced Topics in Solid Modeling, Minneapolis, MN. Sponsored by Siggraph.
7/28-8/4	Experimental Aircraft Association Annual Meeting, Oshkosh, WI. Sponsored by EAA.
8/2	IUPAC Working Party on Polymer Characterization and Rheology Meeting, Wilmington, DE. Sponsored by IUPAC.
8/7-9	17th ASTM National Symposium on Fracture Mechanics, Albany, NY. Sponsored by ASTM.
8/13-16	ACEE Composite Structures Technical Conference, Seattle, WA. Sponsored by ACEE.

TABLE IV-1 continued

8/13-17	Army Sagamore Conference, Lake Lucerne, NY. Sponsored by the United States Army.
8/19-25	16th International Congress of Theoretical and Applied Mechanics, Copenhagen, Denmark. Sponsored by AIAA/IUTAM.
8/20-22	Experimental Mechanics of Fiber Reinforced Composite Materials, Dayton, OH. Sponsored by SESA.
8/20-22	Atmospheric Flight Mechanics Conference, Seattle, WA. Sponsored by AIAA.
8/21-23	Triservice Workshop on Dynamics, Mechanical Properties, Characteristics and Processes of Lightweight Metal Matrix Composites, Leesburg, VA. Sponsored by ARO/ONR.
8/26-31	ACS 188th National Meeting, Philadelphia, PA. Sponsored by ACS.
8/29-31	Colloqium on Mechanical Characteristics of Load-Bearing Fiber Composite Laminates, Brussels, Belgium. Sponsored by EUROMECH.
9/2	IUPAC Working Party on Polymer Characterization and Rheology Meeting, Wilmington, DE. Sponsored by IUPAC.
9/4-7	Advanced Research Workshop on Applications of Fracture Mechanics to Cementitous Composites, Evanston, IL. Sponsored by Northwestern/ARO.
9/9-11	2nd Workshop on Advanced Materials: Recent Advances in Nondestructuve Evaluation of Materials, Traverse City, MI. Sponsored by AIAA.
9/17-21	Colloqium on Mathematical Programming Methods for the Plastic Analysis of Structures, London, England. Sponsored by EUROMECH.
9/17-21	Composite Materials: Processing, Quality Assurance and Repair, Los Angles, CA. Sponsored by UCLA.
9/17-21	Failure Modes in Composites VII: Deformation Associated with Fracture, Fall Meeting, Warrendale, PA. Sponsored by TMS/AIME.
9/18-20	International Conference on Specialty Polymers: Present and Future, Birmingham, England. Sponsored by BS.
9/23-26	13th NATAS Meeting, Philadelphia, PA. Sponsored by NATAS.
9/24-28	International Symposium in Composites: Materials and Engineering, Newark, DE. Sponsored by the University of Delaware.

TABLE VI-2

COMPOSITES-RELATED TECHNICAL MEETINGS ATTENDED OFF-CAMPUS

(April 30, 1984 through September 30, 1984)

5/16-18 AHS Annual Forum and Technology Display (Prof. Diefendorf), Washington, DC.

6/25-29 Composites and Paper Physics Technology Interchange (Prof. Sternstein), Stockholm, Sweden.

Professor Sternstein presented the invited lecture: "Mechanical Characterization of Composites".

7/2-6 Carbon '84 Conference (Prof. Diefendorf), Bordeaux, France.

Professor Diefendorf presented the invited lecture: "Chemical Vapor Disposition of Carbon" and the papers: "Characterization of Isotropic Phase and Mesophase Pitch Fractions", Effects of Lithium Radiation Techniques on the Determination of Pitch Molecular Weight" and "Pitch Solvent Interactions and Their Effects on Mesophase Formation".

7/8-14 1st Gordon Conference on Liquid Crystals (Prof. Wunderlich), New London, NH.

Professor Wunderlich presented the invited lecture: "Condis Crystals" and the paper: "Condis Crystals of Linear Macromolecules".

7/16-20 10th International Liquid Crystal Conference (Prof. Diefendorf), York, England.

Professor Diefendorf presented the paper: "Mesophase Formation in Polynuclear Aromatic Compounds".

7/19-20 Materials Research Council Meeting (Prof. Sternstein), La Jolla, CA.

Professor Sternstein presented the invited lecture: "Mechanical Characterization and Failure of Composites".

7/23-27 Siggraph '84, Advanced Topics in Solid Modeling (Prof. Shephard), Minneapolis, MN.

Professor Shephard presented the paper: "Finite Element Model Generation".

TABLE VI-2 continued

7/28-8/4	Experimental Aircraft Association Annual Meeting (Prof. Diefendorf), Oshkosh, WI. Professor Diefendorf presented the paper: "Fabrication of Composite Materials at RPI".
8/13-16	ACEE Composite Structures Technical Conference (Prof. Loewy), Seattle, WA.
8/13-17	Army Sagamore Conference (Prof. Diefendorf), Lake Lucerne, NY. Professor Diefendorf presented the paper: "Materials Characterization of Carbon Fibers".
8/26-31	ACS 188th National Meeting (Prof. Sternstein), Philadelphia, PA. Professor Sternstein presented the paper: "Viscoelastic Characterization of Composites".
9/2	IUPAC Working Party on Polymer Characterization and Rheology Meeting (Prof. Sternstein), Wilmington, DE.
9/23-26	13th NATAS Meeting (Prof. Wunderlich), Philadelphia, PA. Professor Wunderlich gave the lecture: "The Glass Transition of Poly(ethylene terephthalate)".
9/24-28	International Symposium in Composites: Materials and Engineering (Prof. Diefendorf), Newark, DE.

TABLE VI-3

COMPOSITES-RELATED MEETINGS/TALKS HELD AT RPI

(April 30, 1984 through September 30, 1984)

Topic	Date	Speaker(s)
"Geometric Modeling for Mechanical Analysis and Synthesis"	5/1	Dr. M. Y. Zarrugh University of Michigan
"Structural Optimization: Toward a Reliable CAD Tool"	5/31	Dr. C. Fleury and Mr. V. Braibant University of Liege Belgium
"Coalescence of Surface Fatigue Cracks"	7/23	Prof. K. Iida University of Tokyo Japan
"Ductile Fracture"	8/8	Dr. J. W. Hancock University of Glasgow Scotland
"An Implicit Time Integration Scheme for Inelastic Constitutive Equations with Internal State Variables"	9/11	Prof. F. G. Kollman Technishe Hochschule Darmstadt West Germany

TABLE VI-4

COMPOSITES-RELATED VISITS TO RELEVANT ORGANIZATIONS

by RPI Faculty/Staff/Students

(April 30, 1984 through September 30, 1984)

Visited	Date	By	Purpose
East China Institute of Textile Science and Technology, Shanghai, China	5/12-23	Prof. B. Wunderlich	Attended series of ten lectures
Jiao Tong University, Shanghai, China	5/17	Prof. B. Wunderlich	Attended seminar
Fudan University Shanghai, China	5/22	Prof. B. Wunderlich	Attended lecture
Aerospace Corporation, El Segundo, CA	5/22-23	Prof. R. J. Diefendorf	Attended Rocket Propulsion Laboratory Workshop on "Carbon/Carbon Exit Cones"
Jing-shan Chemical Complex, Shanghai, China	5/24	Prof. B. Wunderlich	Attended seminar
Goodrich Research and Development Center, Breckville, OH	5/25	Prof. R. J. Diefendorf	Attended seminar
University of Science and Technology of China, Hefei, China	5/26-27	Prof. B. Wunderlich	Attended two lectures and seminar
AVCO Corporation Specialty Materials Division, Lowell, MA	5/30	Prof. N. S. Stoloff	Attended lecture
Beijing Institute of Technology, Beijing, China	6/2-5	Prof. B. Wunderlich	Attended three lectures
General Motors Technology Center, Warren, MI	7/25	Prof. R. J. Diefendorf	Attended seminar
Lord Corporation, Erie, PA	8/28	Prof. R. J. Diefendorf	Attended seminar

TABLE VI-4 continued

Visited	Date	By	Purpose
General Electric Company, Waterford, NY	9/13	Prof. R. J. Diefendorf	Attended seminar
General Motors Technology Center, Warren, MI	9/28	Prof. R. J. Diefendorf	Attended seminar

reports, usually on the part of one of the Co-Principal Investigators. Off-campus visitors, at RPI during a BBL day, are often invited to "sit in". Table VI-5 lists a calender of internal, oral progress reports as they were given at BBL's during this reporting period.

As indicated in the Introduction of this progress report, an initiative has been implemented which is intended to bring about increased communication between NASA researchers and their RPI counterparts. A first step in that direction has been taken by the planning of a series of Research Coordination Meetings. The first of such meetings was held at RPI on August 27, 1984, and fourteen members of RPI's Composite Materials and Structures Program along with seven members of NASA Langley Research Center's Materials Division were present. The day-long meeting began with a welcoming statement by Dr. R. Loewy, RPI's Composite Program Co-Principal Investigator, followed by introductory remarks by Dr. L. Vosteen of NASA Langley Research Center. The meeting was then split into groups of participants with parallel research interests. Participants were free to move from group to group as they so desired. A final session with all participants provided an opportunity for individuals to make comments or suggestions with regard to furthering cooperation between organizations. The agenda for this meeting is shown in Table VI-7. A second of such meetings with researchers from NASA Lewis Research Center is in the planning stage.

TABLE VI-5

COMPOSITE MATERIALS AND STRUCTURES PROGRAM

BROWN BAG LUNCH (BBL) SCHEDULE

(April 30, 1984 through September 30, 1984)

Date	Topic	Responsible Faculty
5/4	Administrative Report	R. Loewy
	Matrix Characterization and Environmental Effects	S. Sternstein
	Fabrication Technology Experiments	F. Bundy H. Hagerup V. Paedelt
9/7	Administrative Report	R. Loewy
	Report on NASA Langley Visit	R. Loewy
9/14	Administrative Report	R. Loewy
	Edge Failures	S. Sham
	Beams and Warping	O. Bauchau
9/28	Administrative Report	J. Diefendorf
	Eutectucs	N. Stoloff
	Fabrication Technology Experiments	F. Bundy H. Hagerup V. Paedelt

TABLE VI-6

COMPOSITE MATERIALS AND STRUCTURES PROGRAM

RESEARCH COORDINATION MEETING

NASA Langley Research Center and Rensselaer Polytechnic Institute

August 27, 1984: AGENDA

1st Plenary Session

10:45	Welcome	Dr. R. Loewy Rensselaer Polytechnic Institute
11:00	Introductory Remarks	Dr. L. Vosteen NASA Langley Research Center

Individual Meetings (flexible)

11:30-12:30	Groups A, B, C
12:30-1:30	Lunch
1:30-4:00	Groups A, B, C, D

2nd Plenary Session

4:00	General Discussion
5:00	Adjourn

TABLE VI-7

COMPOSITE MATERIALS AND STRUCTURES PROGRAM

RESEARCH COORDINATION MEETING

NASA Langley Research Center and Rensselaer Polytechnic Institute

August 27, 1984: ATTENDEES

Dr. R. Loewy, Rensselaer Polytechnic Institute

Dr. L. Vosteen, NASA Langley Research Center

Group A: Fiber and Matrix Development and Laminate Processing

NASA - J. Maas
J. Hinkley

RPI - J. Diefendorf
M. Shephard
S. Sternstein
B. Wunderlich
N. Stoloff

Group B: Fracture and Fatigue

NASA - W. Elber
K. O'Brien

RPI - E. Krempl
M. Shephard
S. Sham

Group C: Mechanics and Structural Analysis

NASA - M. Shuart
M. Nemith

RPI - D. Goetschel
M. Shephard
O. Bauchau

Group D: Innovative Fabrication Techniques (Sailplane Projects)

NASA - M. Shuart
M. Nemith
E. Elber

RPI - D. Goetschel
V. Paedelt
O. Bauchau
F. Bundy

PART VII

PERSONNEL

AUTHOR INDEX

PERSONNEL

Co-Principal Investigators

Ansell, George S., Ph.D.	Dean, School of Engineering
Loewy, Robert G., Ph.D.	Institute Professor
Wiberley, Stephen E., Ph.D.	Professor of Chemistry

Senior Investigators

Bauchau, O., Ph.D. (Structural dynamics, advanced composites)*	Assistant Professor of Aeronautical Engineering
Bundy, F. P., Ph.D. (Physical chemistry and structures testing)*	Research Professor of Materials Engineering
Diefendorf[i], R. J., Ph.D. (Fabrication, resin matrix, fiber behavior, interfaces)*	Professor of Materials Engineering
Feeser[i], L. J., Ph.D. (Computer applications and graphics, computer-aided design, optimization)*	Professor of Civil Engineering Associate Dean, School of Engineering
Goetschel, D. B., Ph.D. (Structural analysis design and testing)*	Assistant Professor of Mechanical Engineering
Hagerup, H. J., Ph.D. (Aerodynamics, configuration, pilot accomodation, flight testing)*	Associate Professor of Aeroneering Engineering
Krempl, E., Dr.Ing. (Fatigue studies, failure criteria)*	Professor of Mechanics and Director of Cyclic Strain Laboratory
Sham, T-L., Ph.D. (Fracture mechanics, composites)*	Assistant Professor of Mechanical Engineering

*Fields of Speciality

[i]Member of Budget Committee together with Co-Principal Investigators

Shephard, M.S., Ph.D. (Computer graphics, finite element methods)*	Associate Director, Center for Interactive Computer Graphics and Assistant Professor of Civil Engineering
Sternstein[i], S. S., Ph.D. (Failure analysis, matrix behavior, moisture effects)*	William Weightman Walker Professor of Polymer Engineering
Stoloff, N. S. Ph.D. (Mechanical behavior of crystals, order-disorder reactions, fracture and stress (corrosion)*	Professor of Materials Engineering
Wunderlich, B., Ph.D. (Processing science, constituent material characteristics)*	Professor of Chemistry

Research Staff

Manager & Master Technician, Composites Laboratory

Paedelt, Volker

Research Associates

Grebowicz, Janusz, Ph.D.

Research Administrator

Trainer, Asa, M.S.

Graduate Assistants

An Duek, M.S.	Singh, Sachchida, M.S.
Burd, Gary, M.S.	Srinivasan, Krishna, B.Tech.
Chen, Kuong-jung, M.S.	Szewczyk, Christine, B.S.
Coffenberry, Brian, B.S.	Uzoh, Cyprian, B.S.
Gjaja, Niko, M.S.	Weidner, Theodore, B.S.
Hu, Tsay-hsin, M.E.	Yang, Chung-Ming (Philip), M.S.
Judovits, Lawrence, M.S.	Yehia, Nabil, M.S.
Liu, Shiann-hsing, M.S.	Yerry, Mark, M.E.
Shick, Douglas, M.S.	Yurgartis, Steven, M.S.

*Fields of Speciality

[i]Member of Budget Committee together with Co-Principal Investigators

Undergraduate Assistants - Seniors

Basel, Roger
Cimino, Paul
Di Lello, Frank
Father, Richard
Hubner, Angela
Karkow, Jon
Kim, S. Kwong
Kirker, Philip
Krupp, Alan
Lowy, Robert
Mao, Marlon
Williams, Thomas

Undergraduate Assistants - Juniors

Bell, Joseph
Burdick, Mark
Douskay, Eugene
Egbert, Mark
Hill, Stephen
Kashynski, Stephen
O'Connell, James
Ragczewski, David
Young, Richard

Undergraduate Assistants - Sophmores

Baldwin, Reid
Meyer, John
Park, Brian
Rosario, Estrella

AUTHOR INDEX

End of Document